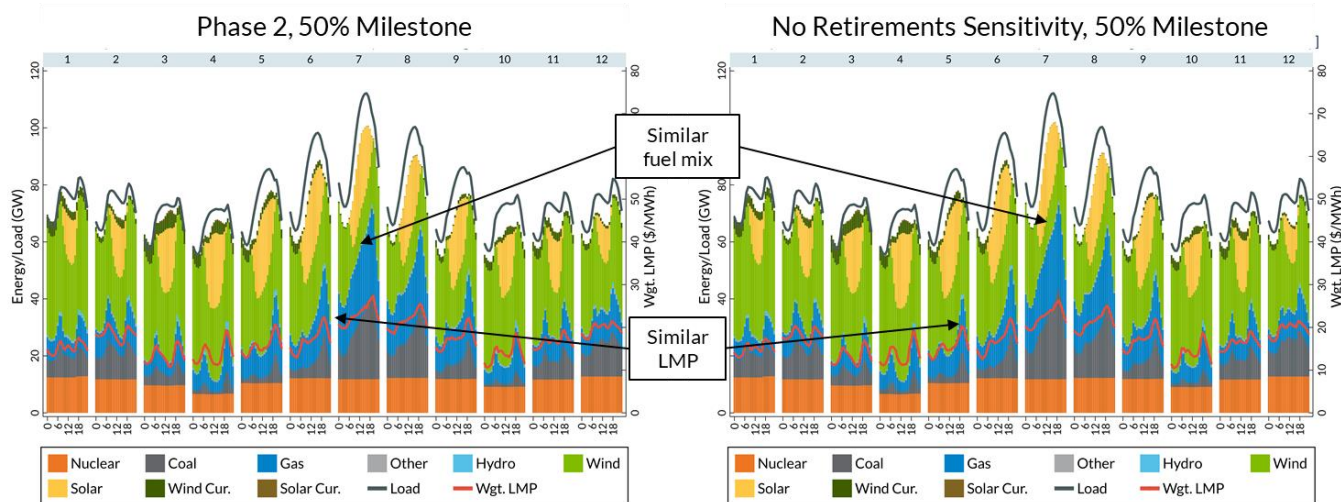


**Figure EA-47: Thermal units retirement assumptions in the no retirements (left) and high retirements (right) sensitivities, compared to the original work (Phase II-Final, center of clustered bars)**

Despite having an additional 17.4 GW of thermal generating capacity available in the model, the simulation results of the no retirements sensitivity did not differ notably from the Phase II-Final model. This holds true whether examining the annual renewable production and penetration (Table EA-4), fuel mix and LMPs (Figure EA-48 and Figure EA-49), or thermal unit ramping (Figure EA-50). These results provide additional evidence supporting the previous conclusion that transmission constraints are the primary factor preventing increases in renewable penetration, rather than lack of thermal unit support for ramping needs or flexibility, based on the current model assumptions.



**Figure EA-48: Monthly diurnal average of fuel mix and LMP in the no retirements sensitivity**

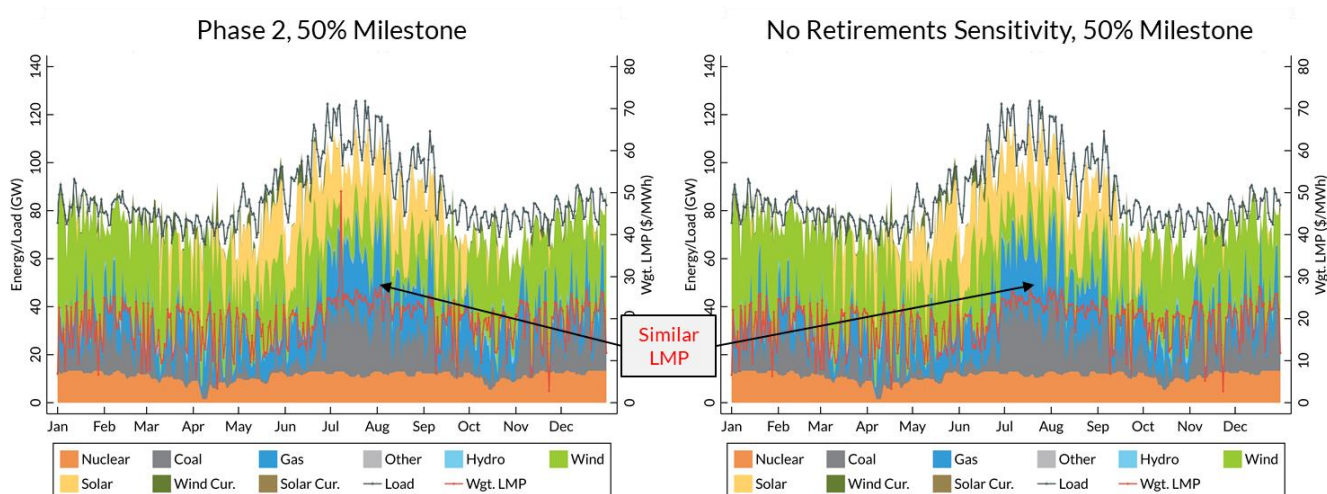
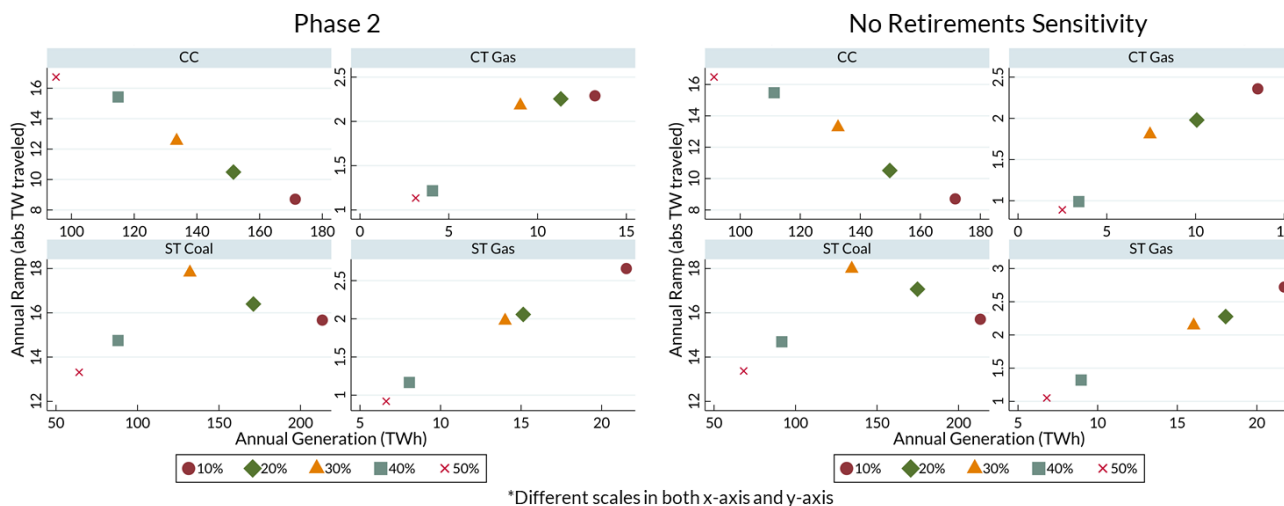


Figure EA-49: Daily peak hour of fuel mix and LMP in the no retirements sensitivity



\*Different scales in both x-axis and y-axis

Figure EA-50: Thermal unit ramping in the no retirements sensitivity

On the other hand, when an accelerated pace of thermal unit retirement (as in the high retirements sensitivity), the lack of thermal unit support for system ramping becomes an issue. In Table EA-4, the high retirements sensitivity has the lowest penetration and annual renewable production compared to the Phase II-Final model and other sensitivities. Despite the fact that the fuel mix does not change significantly, the system average LMPs spike during evening hours (Figure EA-51) and during daily peak-load hours (Figure EA-52). This illustrates the reduced thermal capacity available in the system to support ramping.

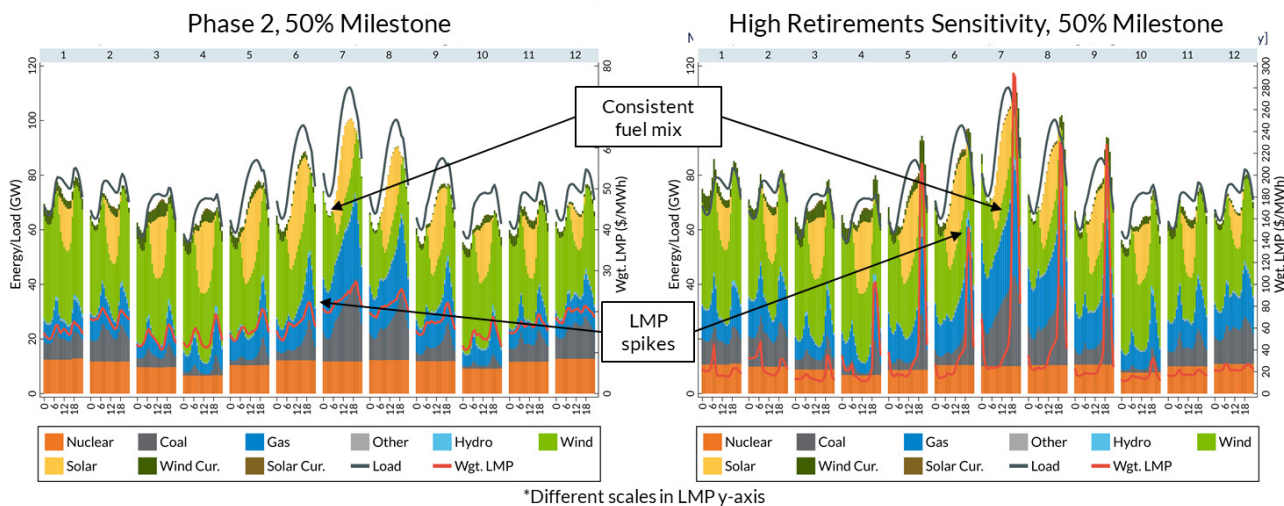


Figure EA-51: Monthly diurnal average of fuel mix and LMP in the high retirements sensitivity

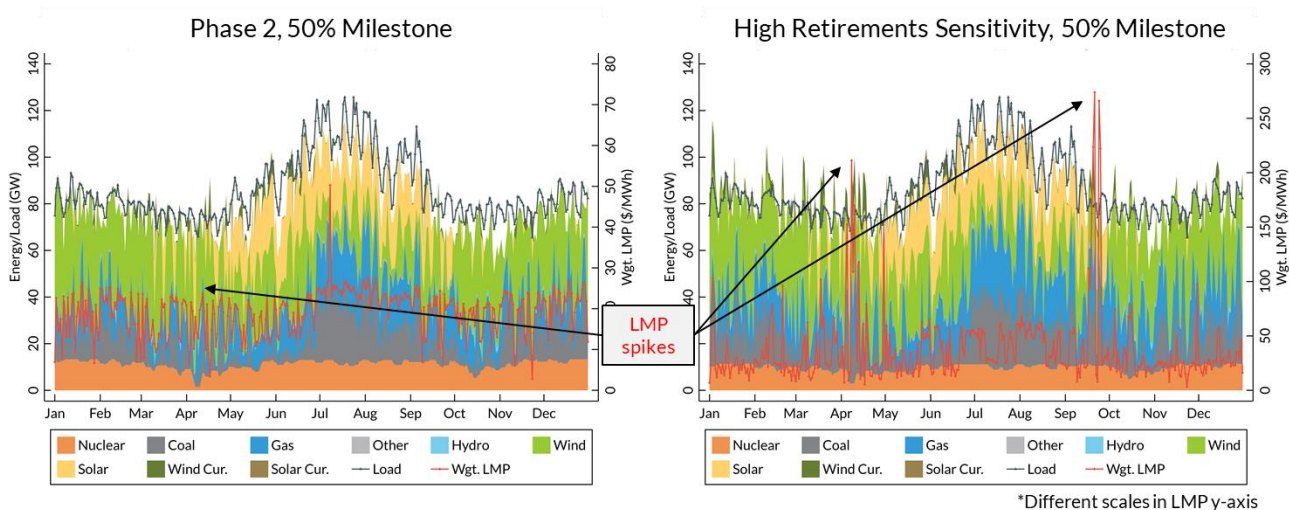


Figure EA-52: Daily peak hour of fuel mix and LMP in the high retirements sensitivity

Figure EA-53 shows the contribution of different technologies and fuels to ramping. Because less thermal capacity is available in the system for the high retirements sensitivity, the remaining coal and CT gas units need to provide more ramping between the 40% and 50% milestones to accommodate the increased variability of renewable energy production.

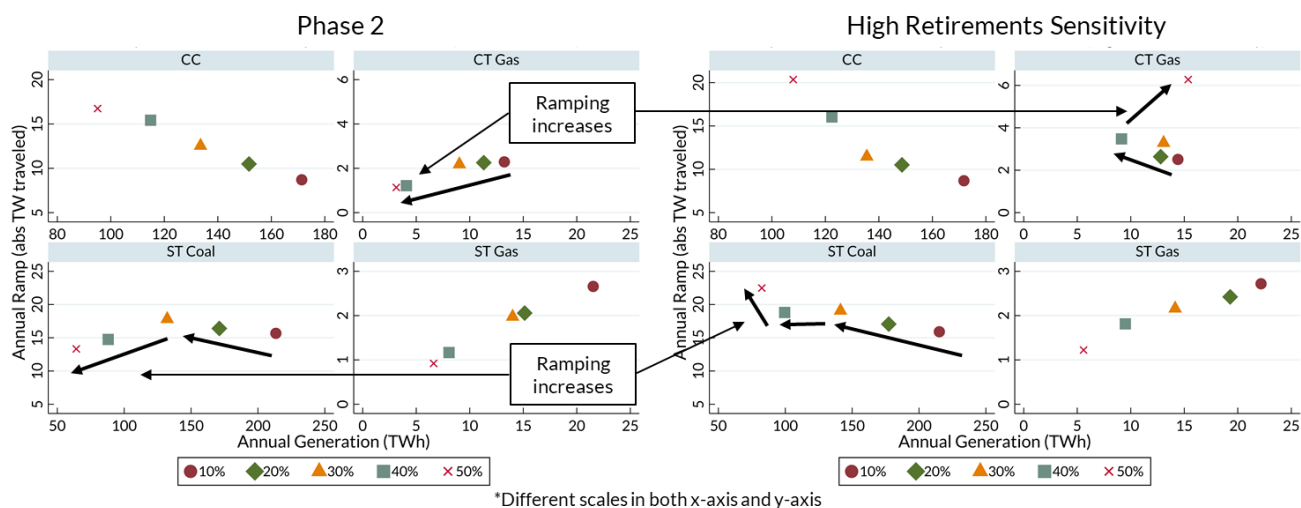


Figure EA-53: Thermal unit ramping in the high retirements sensitivity

### (D) Siting sensitivity

In years since the RIIA study began, the MISO Interconnection Queue has begun to shift to include more and more solar units, evaluating the impacts of renewable mix and siting locations through sensitivity analysis sheds light into an alternative path of renewable development. For the siting sensitivities, the renewable capacity expansion included more solar capacity relative to wind. Because wind comprises the majority of installed renewable generating capacity in the current MISO system, the siting] sensitivity gradually increased the installed solar capacity across milestones, such that the available energy production from wind and solar resources approached an even split by the 50% penetration milestone, compared to the 75:25 split in the Phase II-Final model (Figure EA-54). Furthermore, a localized renewable capacity expansion was used to choose sites at each Local Resource Zone. As a result, more solar is sited in the Central and South regions, while less wind capacity is added to the North (Figure EA-55).

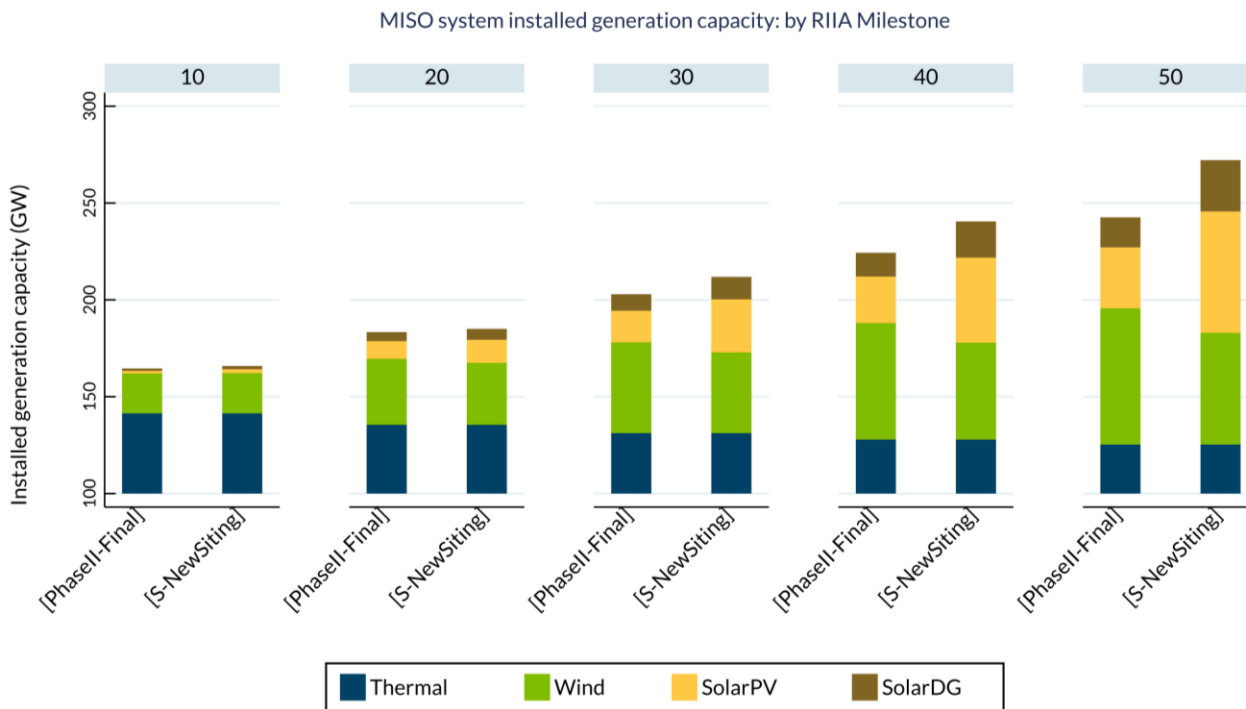


Figure EA-54: Wind and solar capacity expansion assumptions for the siting sensitivity

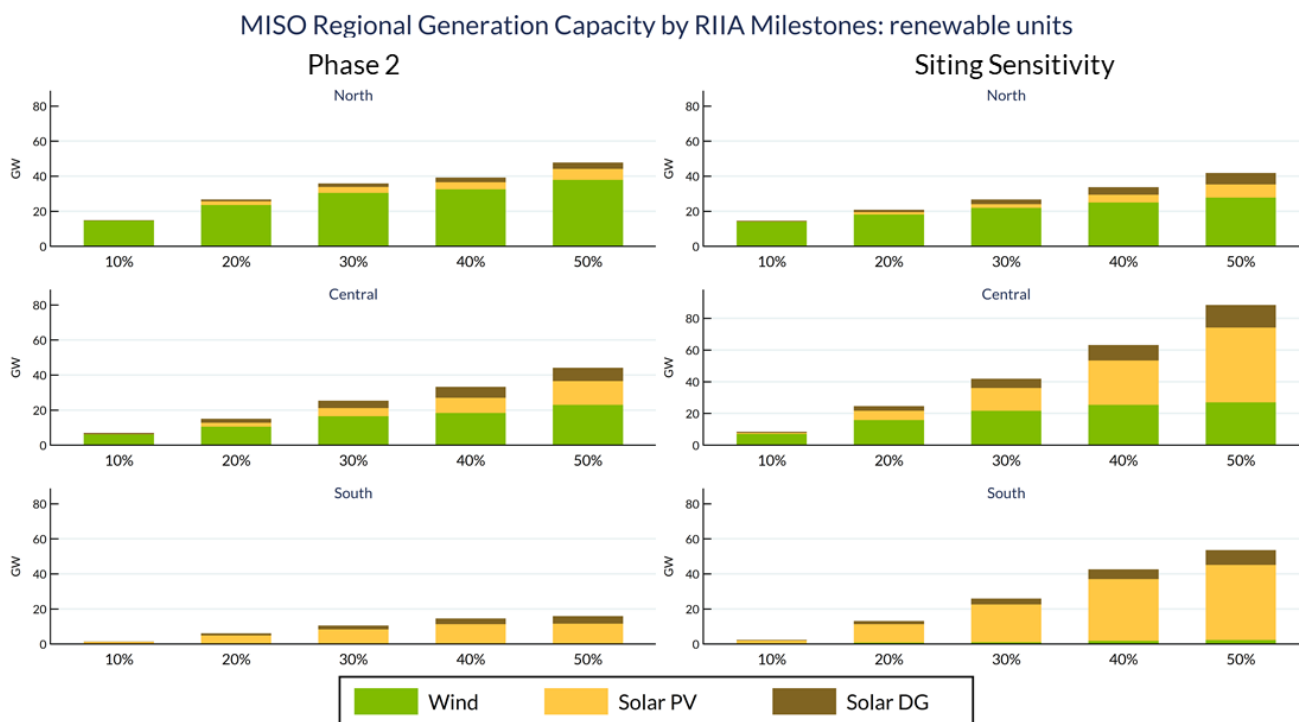


Figure EA-55: Regional breakdown of assumed wind and solar capacity expansion for the siting sensitivity



Because more solar capacity was assumed in the siting sensitivity, the middle of the day shows increased solar generation and reduced average LMPs and price volatility during peak-load hours (Figure EA-56 and Figure EA-57). Interestingly, curtailment of solar energy showed up in shoulder months, usually around midday. Since the original transmission solutions were developed to mostly facilitate wind energy delivery, it is not expected that they would have a large impact on reducing solar curtailment. The new siting of solar capacity for this sensitivity may have created new local congestion, however no new solutions were developed as a part of the sensitivity analysis. Regardless of the solar curtailment, the penetration target is achieved in the siting sensitivity.

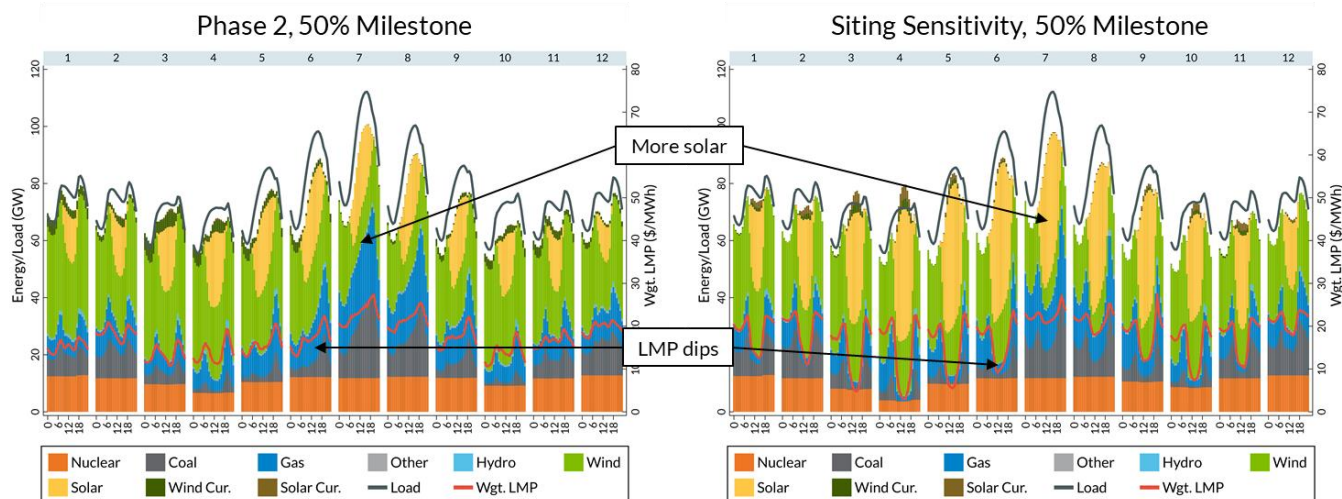


Figure EA-56: Monthly diurnal average of fuel mix and LMP in the siting sensitivity

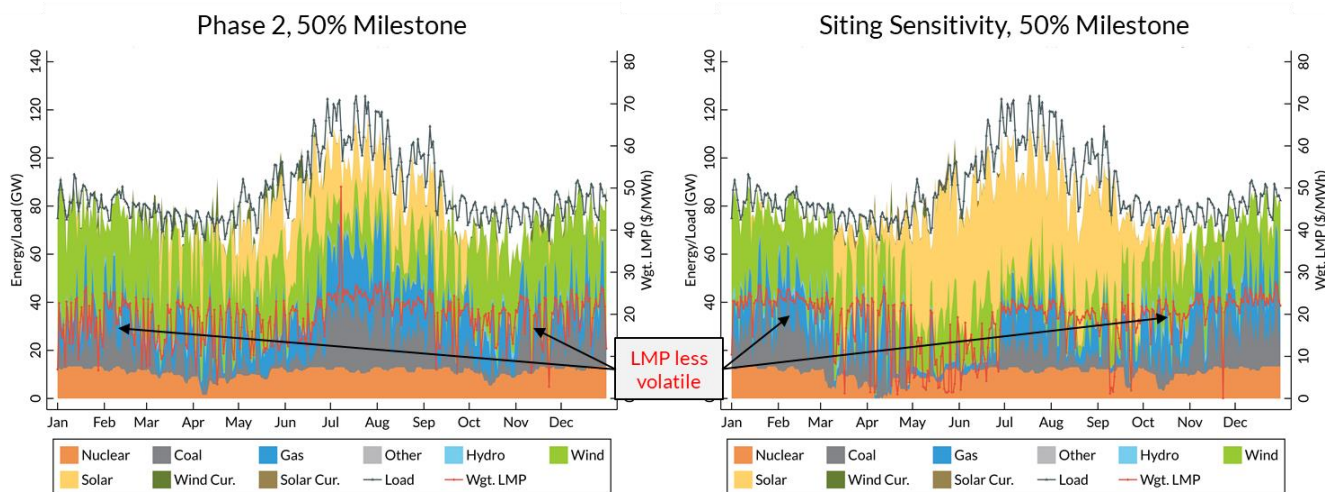


Figure EA-57: Daily peak hour of fuel mix and LMP in the siting sensitivity

Due to the increased solar production, more system ramping is needed from thermal units in the morning hours when the sun rises and during the evening hours when the sun sets. As a result, coal and CT gas units are needed to provide more ramping in the 40% and 50% milestones (Figure EA-58) to accommodate the “duck curve” induced by



the solar production profile in the siting sensitivity. In particular, North coal units and Central CT gas units increase their ramping between the 40% and 50% milestones.

The increased solar production also affects the diurnal flow pattern on transmission lines. The percentage of lines with changing flow direction increases to accommodate solar production profiles. Such power flow flips are particularly notable among higher voltage lines (Figure EA-59).

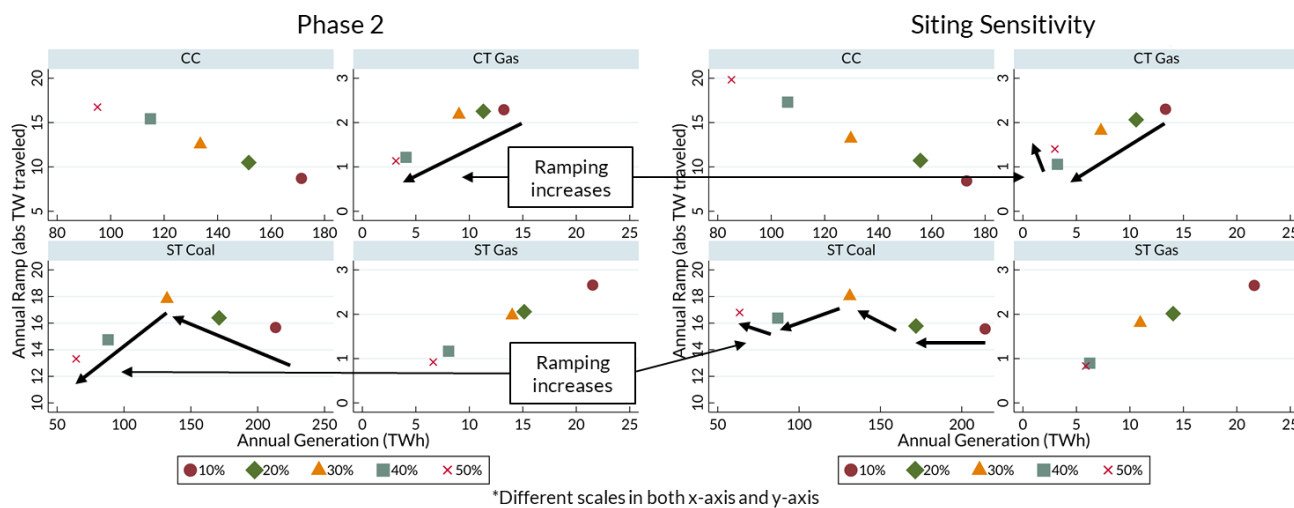


**Figure EA-58: Thermal unit ramping for the siting sensitivity**

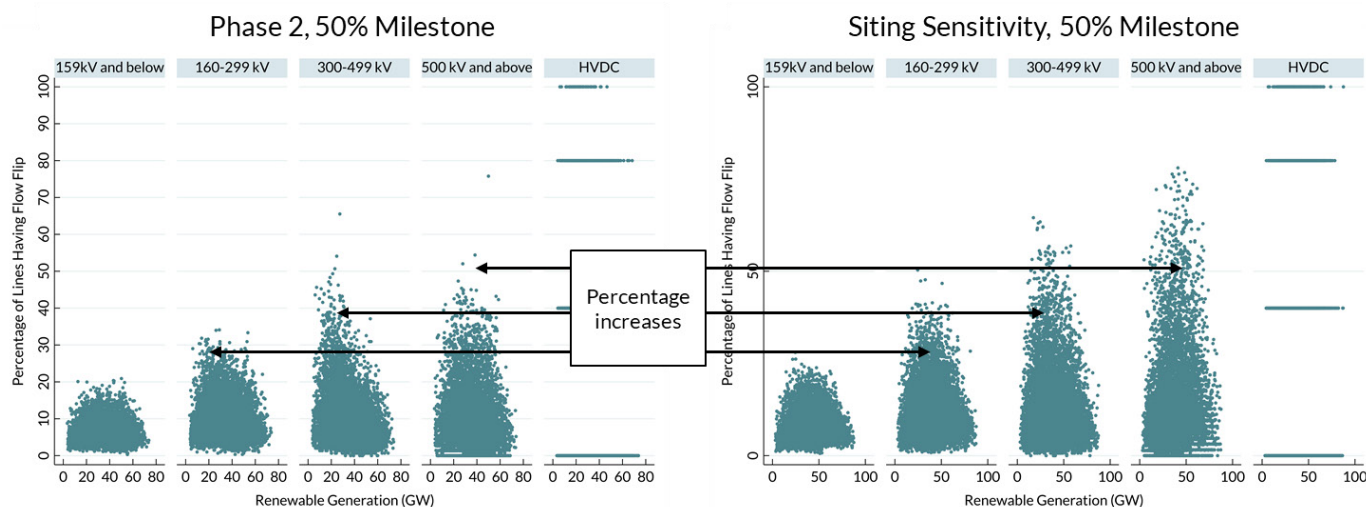


**Figure EA-59: Percentage of transmission lines where the flow changes direction for the siting sensitivity (right), compared to the original work (left)**

**Finding:** Increased solar capacity in the siting sensitivity creates a new stressed operating point during the shoulder load periods, which may need further review in Operating Reliability.

The last metric examined in the sensitivity analysis was system operating points. The analysis investigated whether there were any changes that might warrant further analysis. A new potential stress point was found in the siting sensitivity at the 50% milestone, called here “shoulder load, high renewable (SLHR)” (Figure EA-60). This new



potential stress point appears in June (darker points in Figure EA-61). In June, load is increasing but remains less than the annual peak load, yet a notable amount of solar generation shows up in the system. Figure EA-61 illustrates this SLHR zone, which may need further review under the focus area of Operating Reliability.

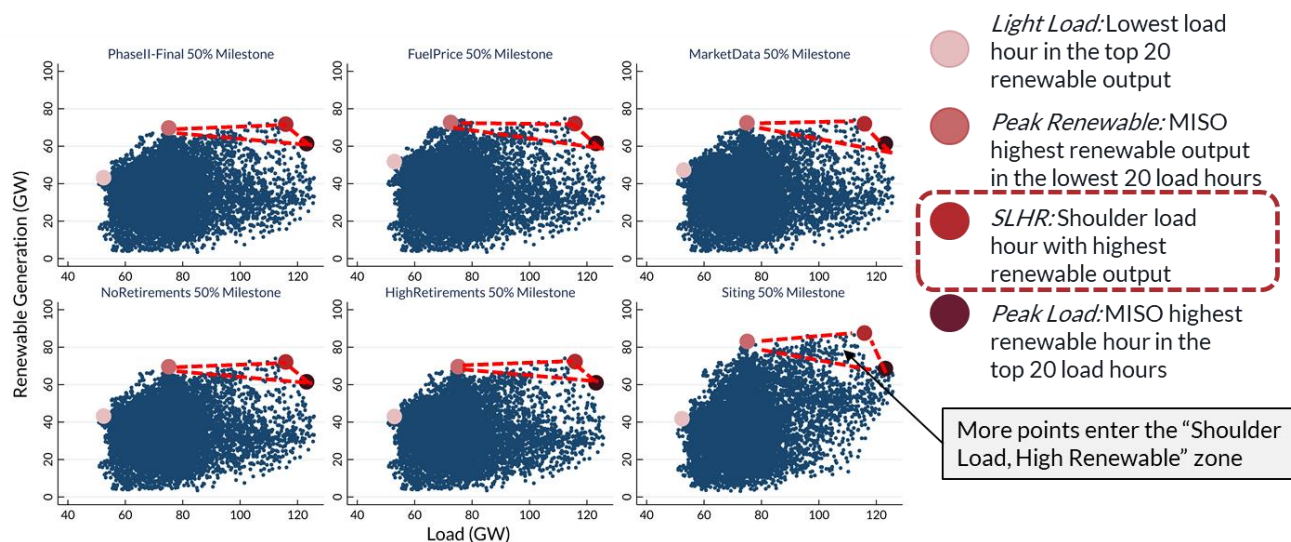


Figure EA-60: System stress points for the fuel price, market data, no retirements, high retirements, and siting sensitivities

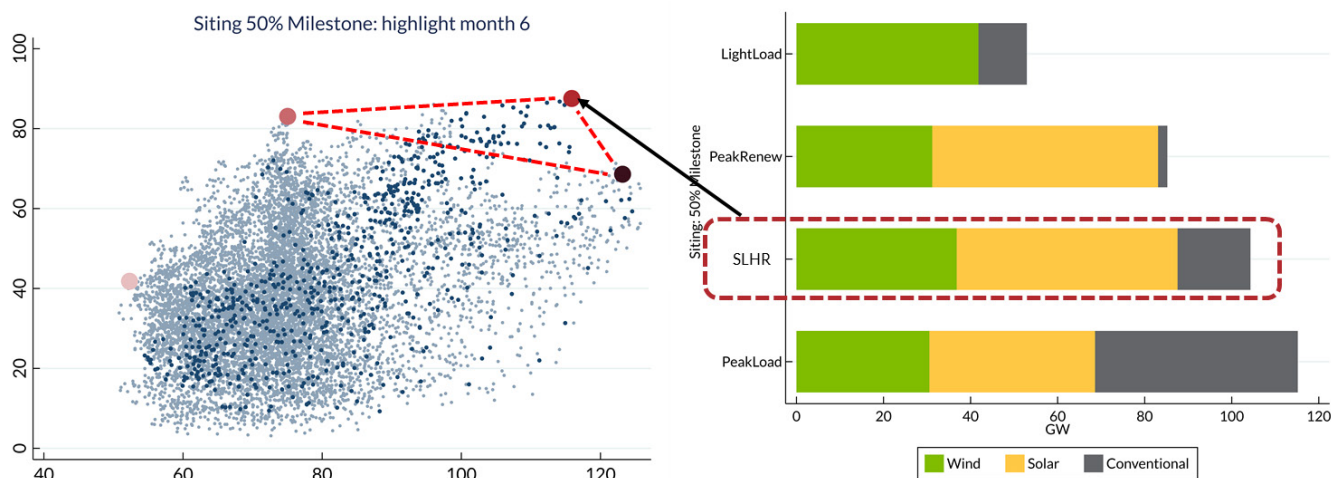


Figure EA-61: The shoulder load, high renewable (SLHR) zone appears for the siting sensitivity

### (E) Energy Storage Sensitivity

The objective of the energy storage sensitivity is to explore how energy storage can contribute to renewable integration. Simulations were performed to discover whether energy storage can be used to facilitate meeting the renewable penetration target by maximizing renewable energy delivery. Analysis was focused on the Phase II-Final model at the 40% penetration milestone, with 60 GW of installed wind capacity, 24 GW of utility-scale solar PV, and 12 GW of distributed solar.



Please note that the scope of the energy storage sensitivity does not include the following:

- a. Evaluating storage at every penetration milestone
- b. Determining optimal mode of operation for energy storage
- c. Studying detailed financial feasibility of individual storage locations
- d. Studying stacked-benefit of storage
- e. Studying storage under the existing MISO Storage Aa Transmission Only Asset (SATO) construct

Table EA-5 lists the scenarios and assumptions of the energy storage sensitivity. In the first scenario, “heuristic”, a total of 30 GW of energy storage was included in the model. This 30 GW of energy storage capacity was sourced from a separate MISO storage study, which utilized a multi-step approach to determine the location and quantity of energy storage by Local Resource Zone (LRZ) in the MISO footprint. In the heuristic scenario, most of the energy storage capacity is sited near load centers (left panel, Figure EA-62).

In the second scenario, “co-location or hybrid”, 6 GW and 12.1 GW of battery storage were assumed to be located at the same node as solar generation resources and wind resources, respectively (central panel, Figure EA-62).

Detailed assumptions of these co-located batteries are described in Table EA-6.

The third scenario is “MISO-developed optimization,” where storage was included as a solution candidate. When both storage and transmission are solution candidates, the optimization process selects only 0.5 GW of battery storage (Run 1). However, if storage is the only solution candidate, the optimization process selects 16 GW of storage (Run 2), and the locations of that 16 GW (right panel, Figure EA-62).

Scenario	Assumption	Total Storage (GW)
Heuristic	<ul style="list-style-type: none"> <li>• Storage capacity sourced from another MISO storage study</li> <li>• Phase 2 solutions are NOT included</li> </ul>	30
Co-location or hybrid	Assume batteries co-located with wind and solar resources	
	Solar sites: batteries with fixed charging and discharging profiles	6
	Wind sites: batteries are price responsive	12.1
	Phase 2 solutions up to 30% milestone are included	
MISO-developed optimization	Storage as solution candidate in optimized solution development	
	Run 1: Both transmission and storage as solution candidates	0.5
	Run 2: Only storage as solution candidate	16
	Phase 2 solutions up to 30% milestone are included	

**Table EA-5: Scenarios and assumptions of the energy storage sensitivity**



Charging-Discharging Philosophy	Primary Purposes	Locations	Size Details
<p>Pre-programmed, fixed profile: Utility-scale photovoltaic (PV)</p> <ul style="list-style-type: none"> <li>Storing 10% of available solar energy (every day) from hour 10:00 to 15:00;</li> <li>Discharge energy stored equally from hour 17:00 to 19:00; maintain 85% or 80% efficiency</li> </ul> <p>Distributed PV</p> <ul style="list-style-type: none"> <li>Storing 25% of available solar energy (every day) from hour 10:00 to 15:00</li> <li>Discharge energy stored equally from hour 17:00 to 19:00; maintain 85% or 80% efficiency</li> </ul>	<ul style="list-style-type: none"> <li>Increase capacity credit of utility-scale solar</li> <li>Distributed storage modelled per Solar Energy Industries Association (SEIA) report</li> </ul>	<ul style="list-style-type: none"> <li>All PV siting</li> </ul>	<ul style="list-style-type: none"> <li>Inverter Max MW rating varies per location</li> <li>MWh rating = 2 hours x Max MW</li> <li>Total utility-scale PV: 2.4 GW</li> <li>Total distributed: 3.9 GW</li> </ul>
<p>Energy arbitrage:</p> <ul style="list-style-type: none"> <li>Store energy during curtailment (low locational marginal price), discharge during higher price</li> <li>Production cost model determines the time of charging and discharging</li> <li>No limit on the number of cycles</li> <li>Minimum charge level is 5%</li> </ul>	<ul style="list-style-type: none"> <li>Increasing wind energy delivery by reducing curtailment</li> <li>Energy arbitrage</li> </ul>	<ul style="list-style-type: none"> <li>Top 30 sites with highest curtailment and with most effective energy storage performance</li> <li>Top 30 sites with most effective energy storage performance</li> </ul>	<ul style="list-style-type: none"> <li>Inverter Max MW rating varies per location</li> <li>MWh rating = 6 hours x MW</li> <li>Total reducing curtailment: 8.1 GW</li> <li>Total energy arbitrage: 3.3 GW</li> </ul>
<p>50% participate in energy-arbitrage, 50% reserved for frequency and small signal (not storage as a transmission-only asset [SATO])</p> <ul style="list-style-type: none"> <li>Store energy during low prices, discharge during higher</li> <li>Production cost model determines the time of charging and discharging</li> <li>No limit on the number of cycles</li> <li>Minimum charge level 50%</li> </ul>	<ul style="list-style-type: none"> <li>Frequency response and small signal support</li> </ul>	<ul style="list-style-type: none"> <li>Sites identified during 50% RIIA Phase 2 operating reliability-dynamics studies</li> </ul>	<ul style="list-style-type: none"> <li>Inverter Max MW rating varies per location</li> <li>MWh rating = 1 hour x MW</li> <li>None for RIIA 40% milestone</li> </ul>

**Table EA-6: Detailed assumptions of energy storage operation and siting for the co-location scenario**

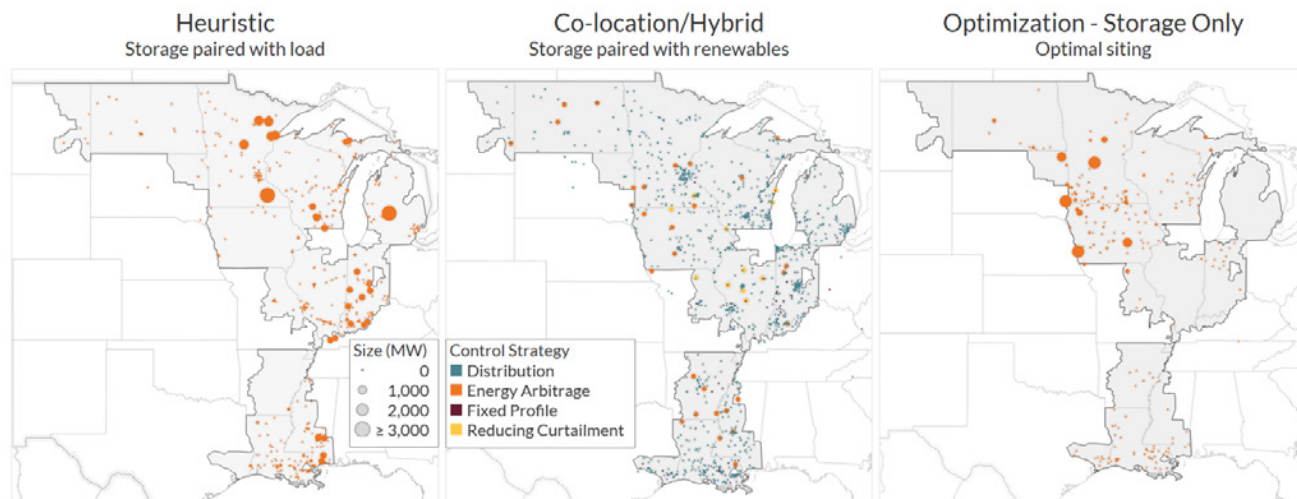


**Figure EA-62: Location of energy storage and control strategy for the energy storage scenarios examined**

**Finding:** Storage, without adequate transmission capacity in the system, may help increase renewable energy delivery but may not sufficiently aid in meeting penetration targets

In Table EA-7, the results of all scenarios for the energy storage sensitivity are summarized. None of the scenarios reached the 38% penetration target; the ‘balanced’ optimization run, where both storage and transmission were available as solution candidates, comes closest to reaching the study penetration target. These results suggest that storage alone, without adequate transmission capacity in the bulk electric system, may not be sufficient to reach renewable penetration targets. In the following sections, each scenario is discussed in more detail.

*Storage alone, without adequate transmission capacity in the bulk electric system, may not be sufficient for meeting renewable penetration targets*

Scenario	Heuristic	Co-location or Hybrid	Optimization Run ‘Balanced’	Optimization Run ‘Storage Only’
40% renewable penetration level	32.3%	35.9%	37.3%	36.2%
Storage location	Storage sited near load	Storage paired with renewables	Optimized expansion of transmission and storage	Expansion of only storage
Comment	No additional transmission	With RIIA transmission solutions up to 30%	With RIIA transmission solutions up to 30%	With RIIA transmission solutions up to 30%

**Table EA-7: Summary of simulation results for the energy storage sensitivity**

**Heuristic:** In Figure EA-63, the annual fuel mix and renewable curtailment were compared before and after adding 30 GW of energy storage, but without including any RIIA transmission solutions (i.e. BaseT model). Without adequate transmission capacity in the system, renewable energy is significantly curtailed due to transmission



constraints and the maximum penetration level is 31.9% (the bottom horizontal stacked bar). After including 30 GW of energy storage near loads in the system, the storage increased renewable energy delivery, which is reflected in a 0.4% increase in the renewable energy penetration level. However, this small increase is not enough to meet the renewable penetration target for the 40% milestone.

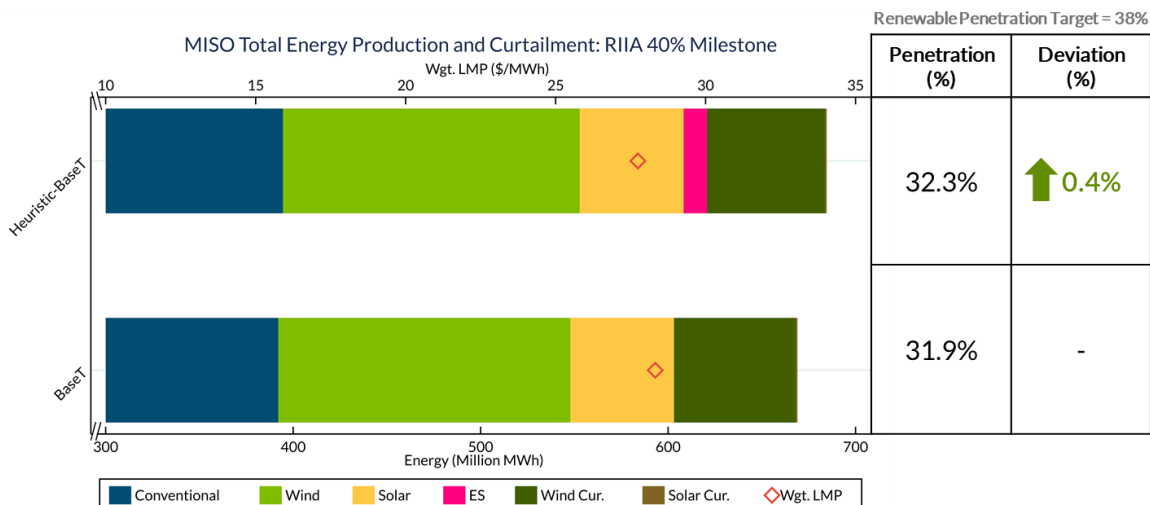


**Figure EA-63: Fuel mix of the heuristic scenario of the energy storage sensitivity, assuming the base transmission (BaseT) model**

In Figure EA-64, the same heuristic scenario was examined with the inclusion of all RIIA transmission solutions up to 40% milestone (Phase II-Final model). Interestingly, even with adequate transmission capacity in the system, including 30 GW of storage near load only increases renewable energy delivery by 0.5% of the annual energy.

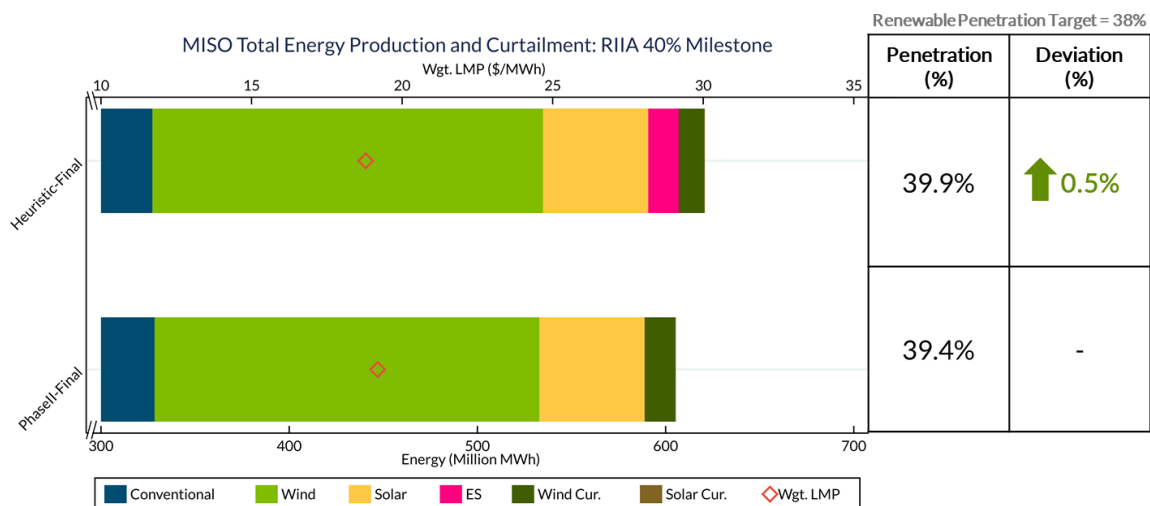


**Figure EA-64: Fuel mix of the heuristic scenario of the energy storage sensitivity, assuming RIIA transmission solutions through the 40% milestone (Final model)**

Nonetheless, transmission solutions do provide synergy for the efficient operation of storage. When adequate transmission capacity is available in the system, the average charging and discharging of battery storage is notably higher (the right panel of Figure EA-65). Please note that battery charging and discharging shown in Figure EA-65 is consistent with the simulation settings: charging during low LMP hours and discharging during high LMP hours.

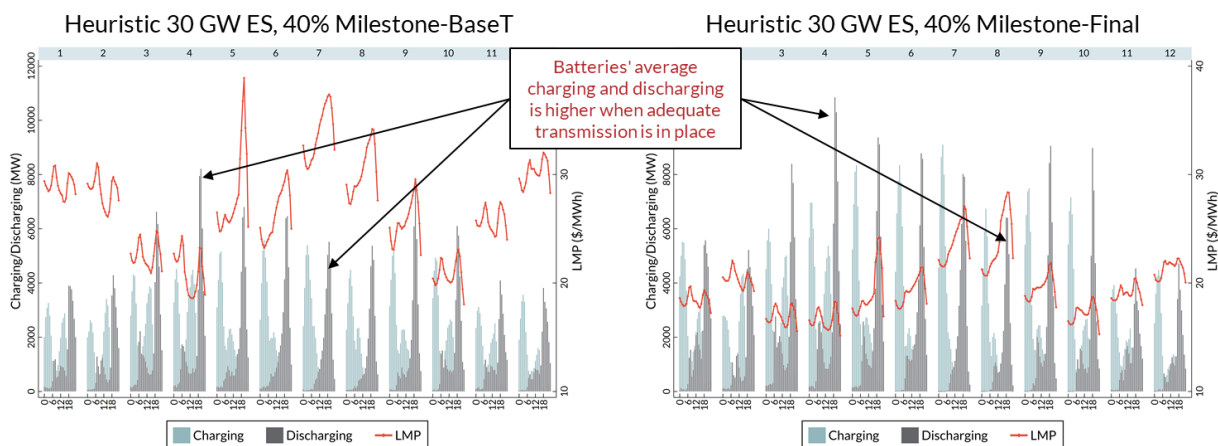


**Figure EA-65: Monthly diurnal average of battery charging and discharging in the heuristic scenario of the energy storage sensitivity, with base transmission (BaseT, left) and RIIA transmission solutions (Final, right)**

**Finding:** Storage paired with renewables is more effective in increasing renewable energy delivery than when it is paired with load

**Co-location:** In Figure EA-66, the annual fuel mix and renewable curtailment are compared before and after including 6 GW of energy storage co-located with solar sites and 12.1 GW of storage co-located with wind sites. Both simulations include RIIA transmission solutions up to the 30% milestone (i.e. Start model). Compared with the heuristic scenario, the co-located batteries are more effective at increasing renewable delivery; the penetration level increased by 2% after including 18.1 GW of co-located battery storage (top of Figure EA-66) compared to the case without battery storage (bottom). In a later section, it will be shown that the MISO-developed optimization also chooses to site energy storage mostly near renewable resources instead of near load (Figure EA-70), which reinforces the finding here.

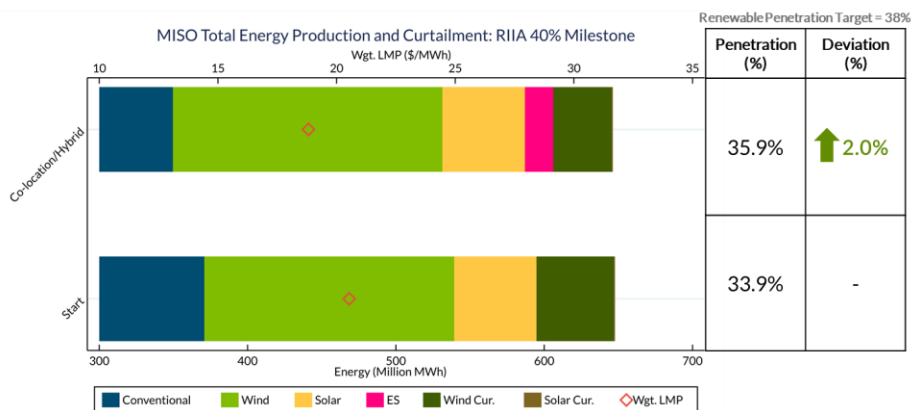


**Figure EA-66: Fuel mix of co-location scenario of the energy storage sensitivity for the 40% milestone, with RIIA transmission solutions through the 30% milestone added (Start)**

**Finding:** Computer-aided optimized expansion demonstrates a combination of storage and transmission is an effective way to meet renewable targets

In both the heuristic and co-location scenarios discussed in previous sections, the choice of energy storage quantity and location is primarily based on engineering judgement and no costs were considered. Hence, in the MISO-



developed optimization scenario, a computer-aided optimization technique was used to explore “optimal” or “balanced” solutions to reach renewable penetration targets. This computer-aided optimization technique included the capital costs of transmission and energy storage as well as system production cost. In Figure EA-67, the total cost varies across different expansion scenarios, from a transmission-only solution (on the left) to a storage-only solution (on the right). Figure EA-67 provides two key observations. First, transmission is more cost effective than storage at increasing the renewable energy penetration, as the total cost of (1), the transmission-only solution, is much lower than the total cost of (5), the storage-only solution. Second, transmission and storage together may achieve the best overall value, as (2) had the lowest total cost.

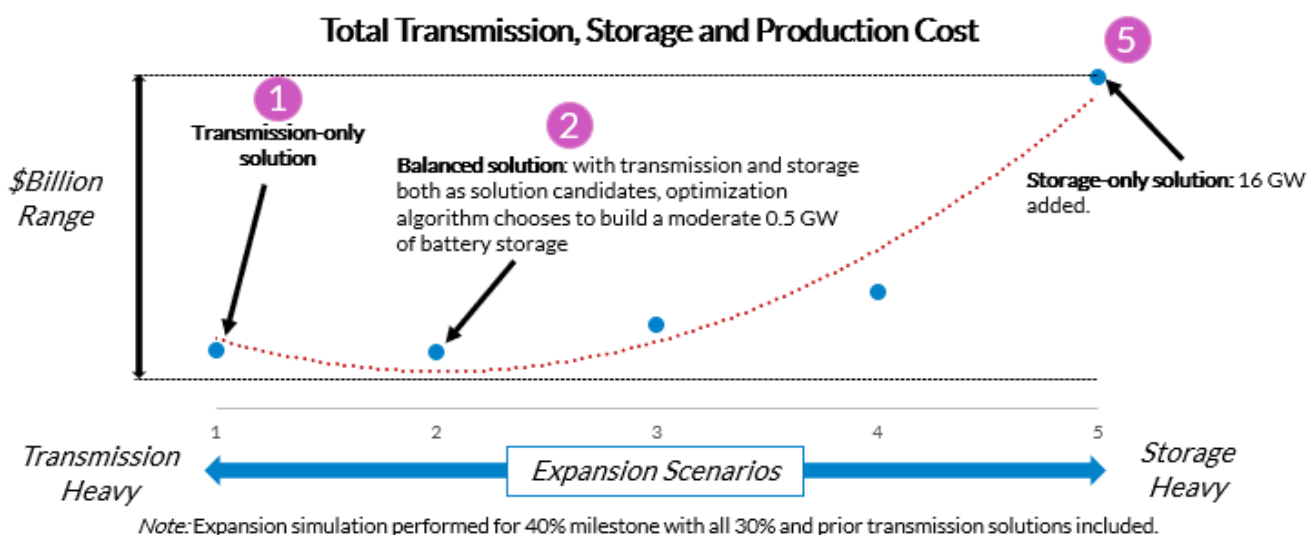


**Figure EA-67: Total cost of transmission, storage, and production for different combinations of transmission and storage in the MISO-developed optimization scenario of the energy storage sensitivity**

When considering renewable energy delivery, Figure EA-68 shows that transmission is necessary to facilitate the transfer of renewable energy to load. When including transmission as a candidate solution (1 and 2), renewable energy penetration comes very close to the target for the 40% milestone while the storage-only scenario (3) with 16 GW of storage cannot reach the same penetration level as solutions with transmission.

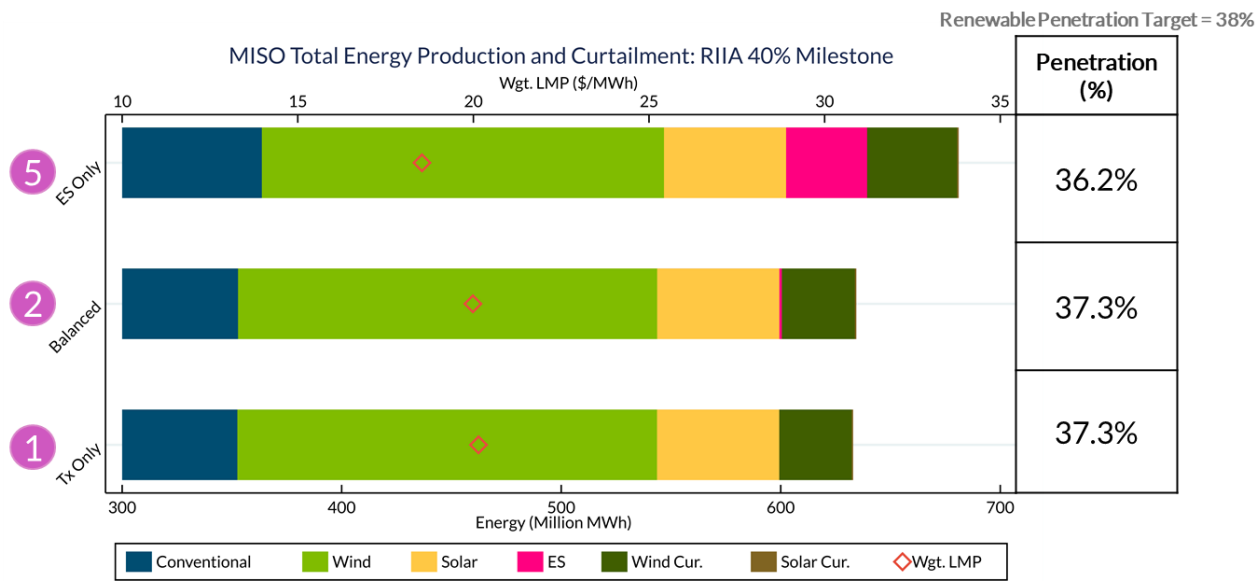


**Figure EA-68: Fuel mix and renewable energy penetration of the MISO-developed optimization scenario of the energy storage sensitivity**

Similar to the finding illustrated in Figure EA-65, the MISO-developed optimization scenario found that storage participation in the balanced scenario (2) is higher than in the storage-only scenario (5), measured by utilization rate or capacity factor of battery storage (Figure EA-69). This suggests that storage and transmission may mutually benefit each other, depending on the relative magnitudes of transmission line rating, generation, and load. If the transmission rating is smaller than the minimum of the load or the maximum power from variable generation paired with the battery, building more transmission may reduce congestion and increase battery utilization. However, when the line rating is greater than the minimum of the load MW or the maximum power from variable generation, adding more batteries could be a cost-effective measure to increase renewable penetration and increase flow on transmission lines.

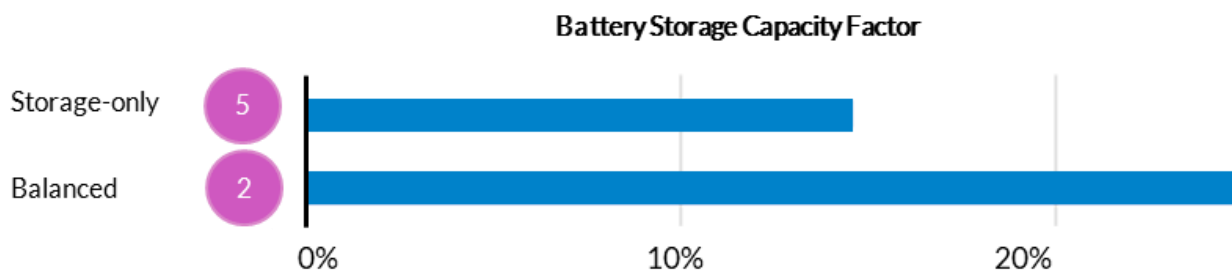


**Figure EA-69: Utilization of battery storage in the MISO-developed optimization scenario of the energy storage sensitivity**

**Finding: Storage is more cost-efficient to mitigate short-duration congestion of moderate severity**

In the MISO-developed optimization scenario, it is possible to examine the types of batteries chosen and their locations in order to make additional conclusions about the role that energy storage might play in a high-renewable future. The top two charts of Figure EA-70 compare the number of installations for each MISO region for the two



different optimization solutions. In both cases (storage-only and balanced), shorter duration batteries are shown to be preferred for most locations, comprising approximately 85% of the selected batteries. In the bottom two charts of Figure EA-70, the locations of the storage installations are compared for the three MISO regions. For both the storage-only and balanced optimizations, most storage is sited near renewable resources instead of near load (99% and 93%, respectively). This suggests that storage is a cost-efficient way to mitigate short-duration congestion driven by renewable output.

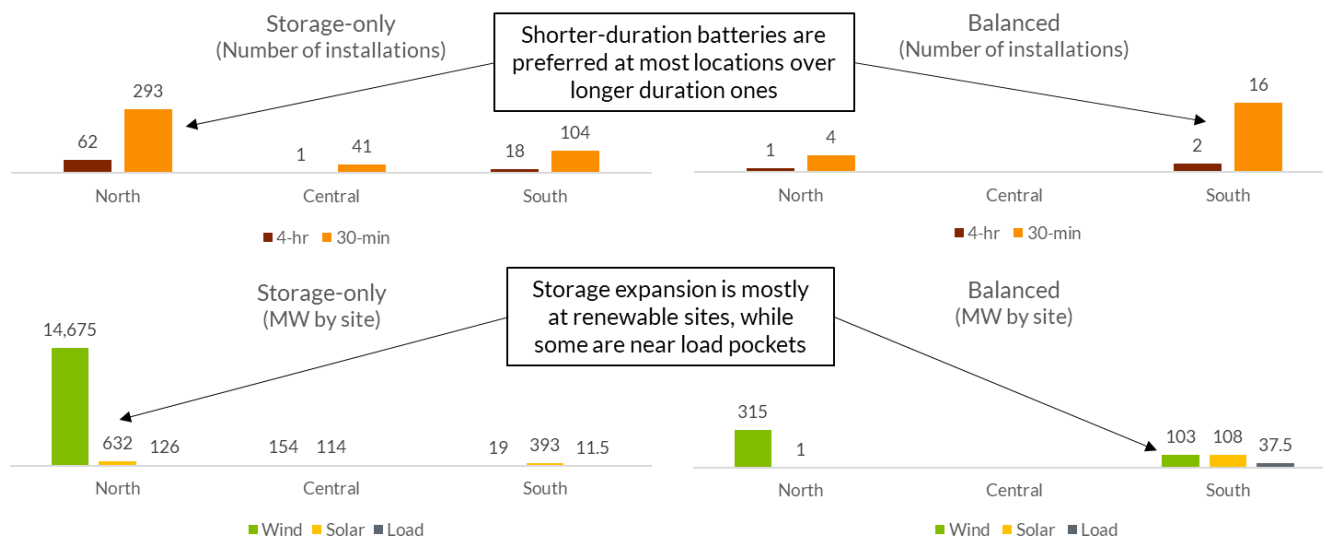


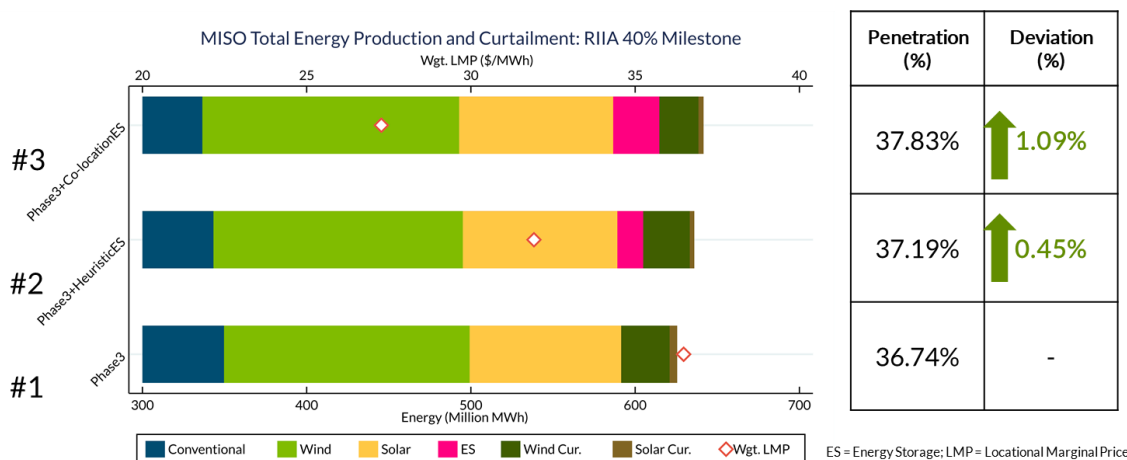
**Figure EA-70: Battery storage duration compared for the MISO-developed optimization scenario of the energy storage sensitivity**

Lastly, to reinforce our key findings that storage alone may not be sufficient for meeting penetration targets if without adequate transmission in the bulk electric system, RIIA performed three additional Phase3 sensitivities (Table EA-8) by combining multiple Phase 2 sensitivities while using the BaseT transmission model. Figure EA-71 shows the annual fuel mix and renewable curtailment were compared between the three Phase 3 sensitivities. First, for the #2 and #3 of Phase3 sensitivities, none of them reached penetration targets. These results re-validated our previous argument that without adequate transmission capacity in the system, energy storage alone is not enough to meet the renewable penetration. Second, #3 of Phase3 sensitivities provided a higher incremental improvement in terms of penetration target when compared with #2, which also supported our finding that storage paired with renewables is more effective in increasing renewable energy delivery.



Sensitivity	Sourced from Phase 2s Assumption	#1	#2	#3
Generator characteristics	<ul style="list-style-type: none"> <li>Generator characteristics from MISO proprietary data</li> </ul>	✓	✓	✓
Siting	<ul style="list-style-type: none"> <li>Wind/Solar ~50/50 at 50% milestone</li> <li>Localized expansion/siting by LRZ load ratio</li> </ul>	✓	✓	✓
Energy Storage - Heuristic	<ul style="list-style-type: none"> <li>Storage capacity sourced from another MISO storage study</li> </ul>		✓	
Energy Storage - Co-location	<ul style="list-style-type: none"> <li>Assume batteries co-located with wind and solar resources</li> </ul> <p>Solar sites: batteries with fixed charging and discharging profiles</p> <p>Wind sites: batteries are price responsive</p>			✓

**Table EA-8: Summary of simulation settings for the Phase3 energy storage sensitivity**



2

**Figure EA-71: Fuel mix of the Phase 3 sensitivities, assuming BaseT transmission for the 40% milestone**



## Energy Adequacy – Market and Operation

### Overview

In-depth analyses into the market and operational needs for identifying the challenges and opportunities of novel market products and operational processes was studied. This section describes the Energy Adequacy – Market and Operation Focus Area, also named the Portfolio Evolution Study (PES). This work was conducted in parallel with the core RIIA analysis. Many of the assumptions are the same, but some are different as seen in Methodology.

The scope of this work includes:

- The evaluation of system needs
  - Market system requirements (including ancillary services) and their expected evolution
  - Performance of market and operational constructs
- Exploration of Solutions
  - Platforms for analyses of potential market and operational adaptations to effectively accommodate new resources

### Key Findings

The PES finds that:

- Flexibility needs at around the 40% renewable level are significant.
- Wind and solar increase hourly and multi-hour flexibility needs.
- Solar growth increases intra-hour needs due to its diurnal patterns and unique intra-hour profiles.

To illustrate the growing flexibility needs across and within hours due to increasing wind and solar production, Figure EAM-3 shows 15-minute net ramp, the average 30-minute headroom need, the average 1-hour net load ramp, and the maximum 4-hour persistent net load ramp-up for two different future portfolios and how it compares to current market. Under the 40% renewable scenario with 50% of that renewable comes from solar, ramping needs are considerably higher, highlighting potential operational issues.

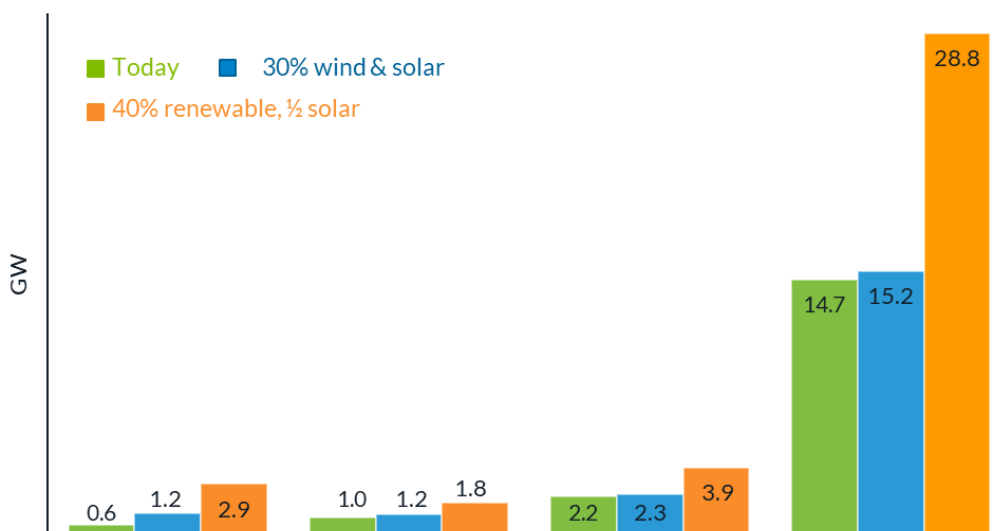
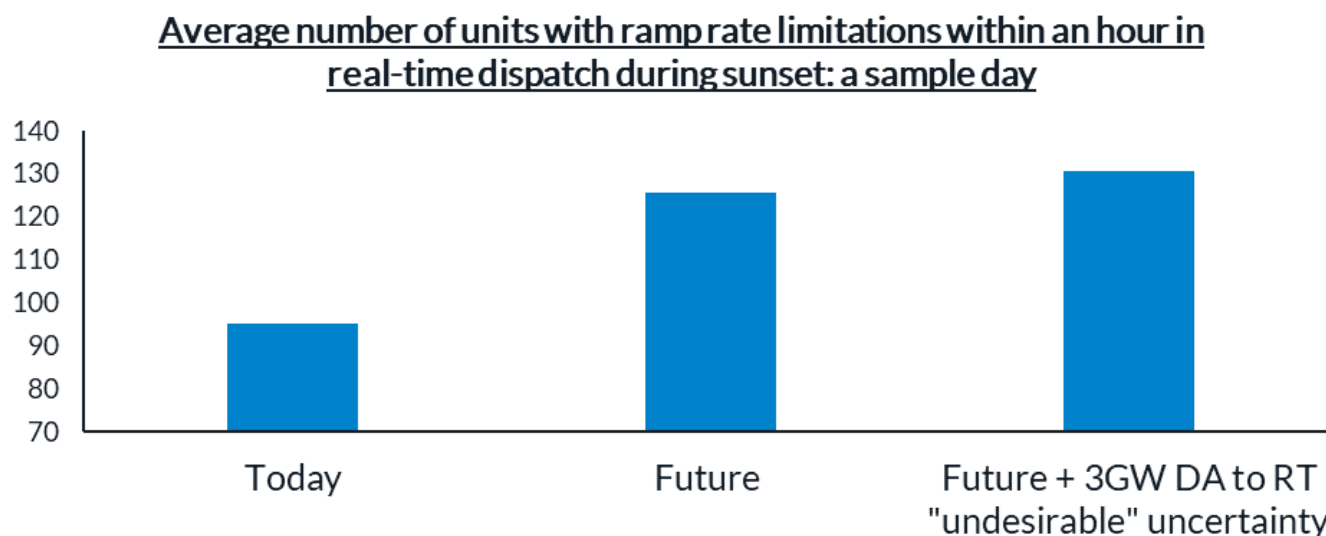


Figure EAM-1: Net ramp capability for different time horizons for different scenarios



Figure EAM-2 further shows that ramping capability may be becoming tight or insufficient when net-load changes rapidly in real-time. The number of generation units that experience binding ramp rate constraints increases sharply in the simulated future scenarios.



**Figure EAM-2: Average number of units with binding real-time dispatch inter-hour ramp constraints during sunset for a sample day.**

Additional observations from Figure EAM-1 and Figure EAM-2 include:

- The sunset time periods may be challenging to manage
- Fleet ramping capability is needed to manage discrepancies between solar reduction, wind pickup and load variation
- The operational challenges can be both inter-hour and sub-hourly
- Additional volatility within the hour at this timeframe could increase the need
- Real time actions influence the outcomes

In terms of deliverability, PES also finds such need will grow without transmission adaptation to the new resource mix. Within the analysis scope of PES, deliverability is indicated by the marginal congestion component (MCC) of locational marginal price. Figure EAM-3 illustrates the deliverability of 30-minute headroom within the 40% renewable penetration case, in which “good deliverability” from rampable MWs with lower marginal congestion component (MCC). On the other hand, ramp MWs that must come from resources with increasing congestion or higher MCCs are categorized as “bad deliverability.” Figure EAM-3 shows that (1) deliverability issue will become even more crucial in the future along with increasing needs of flexibility; and (2) transmission builds, flexible transmission management, and market enhancements could improve deliverability outcomes.



### Deliverability\* of 30-min headroom for 40% renewable: a worst case

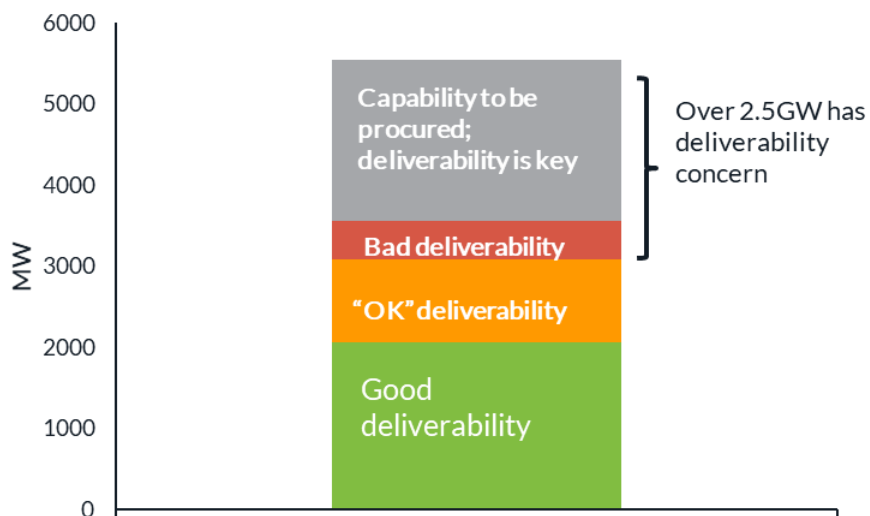


Figure EAM-3: Net ramp capability for different time horizons for different scenarios

Last, PES finds that without market or operations changes, greater variability and uncertainty could result in real-time resource scarcities. Figure EAM-4 shows, via real-time energy prices for a sample day, that higher prices and reduced capability are more likely to occur among future resource portfolios if without changes to current market practices. Findings suggests that in future market operator may run into Real-time capacity or reserve scarcities if variability and uncertainty are not well prepared for accommodating evolving future portfolio.

### Real-time Energy Prices (ExAnte): Sample Day

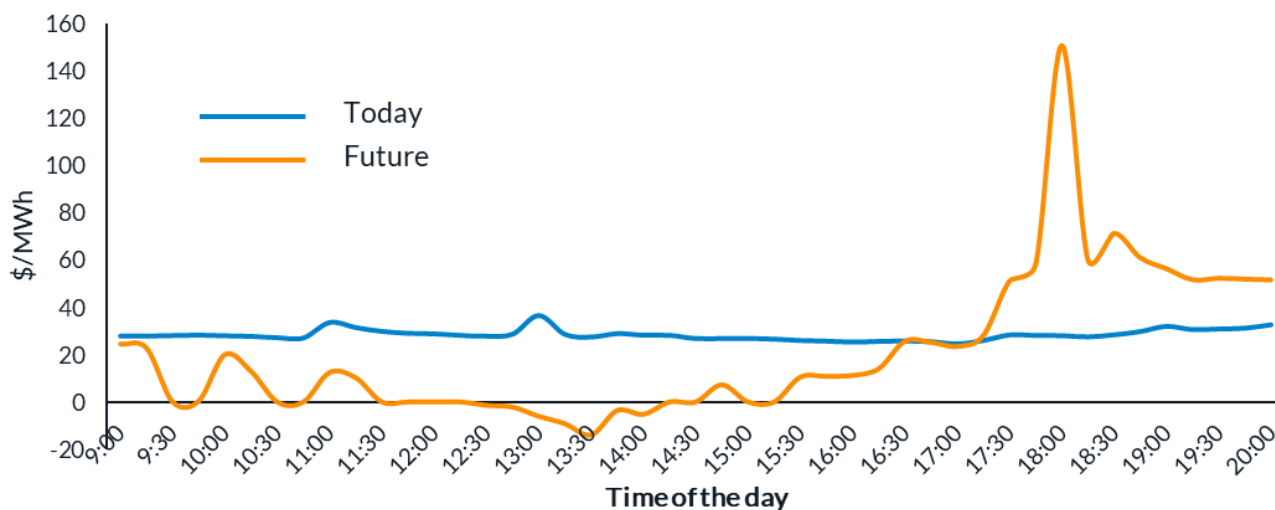


Figure EAM-4: Comparison of ex-ante real-time energy prices, today vs future (sample day)



## Energy Adequacy – Uncertainty and Variability Trends

### Overview

The goal of energy adequacy is to ensure that all system demand is reliably, and cost effectively met. Ensuring cost-effective and reliable energy delivery to meet the expected system demand requires a review of three key metrics: Flexibility, uncertainty and variability. The previous sections on Energy Adequacy – Planning and Markets and Operations, highlight the need for flexibility as a key metric. Understanding the uncertainty and variability associated with the supply and demand can help with planning and designing the energy market to improve its effectiveness or efficiency. Uncertainty is the deviation of the actual value of the supply or demand during the real-time in comparison to the forecasted value in the day-ahead timeframe while variability is the deviation of supply or demand over a certain time period. RIIA analyzed the forecasted uncertainties and variability associated with increased amounts of renewable generation penetration within the MISO region. The issues as well as the solutions associated with uncertainty and variability highlighted in the results below are currently under review in the MISO Forward Report<sup>2</sup> and the MISO's response to the reliability imperative<sup>3</sup>

### Key Findings

**Finding:** Uncertainty and forecast error increases in the wind forecast varies across different months of the year.

Forecast error or uncertainty associated with wind and solar generation is the deviation in the respective generation output between the Day-Ahead and Real-Time markets. Uncertainty with the wind and solar generation if not handled appropriately, may have an impact on the efficiency of unit commitment and dispatch within the MISO market. It is therefore imperative for MISO to have a better understanding on the un-certainty from the renewable generation resources in order to provide an appropriate mechanism to handle it appropriately and improve market efficiency. Figure EAD-1 shows the forecast error associated with the wind generation across different milestones. In whisker charts like this, the lower whisker represents the first quartile (the lowest 25% of the values), the upper whisker represents the fourth quartile (highest 25% of the values), and any dots represent outliers. The thick middle portion is the second and third quartiles (middle 50% of the values) and the median is the horizontal line. From this figure, it is observed that the magnitude of the forecast error for wind generation would increase as renewable penetration increases in the MISO footprint.

---

<sup>2</sup> [https://cdn.misoenergy.org/MISO%20FORWARD\\_2020433101.pdf](https://cdn.misoenergy.org/MISO%20FORWARD_2020433101.pdf)

<sup>3</sup> <https://cdn.misoenergy.org/MISO%20Response%20to%20the%20Reliability%20Imperative504018.pdf>

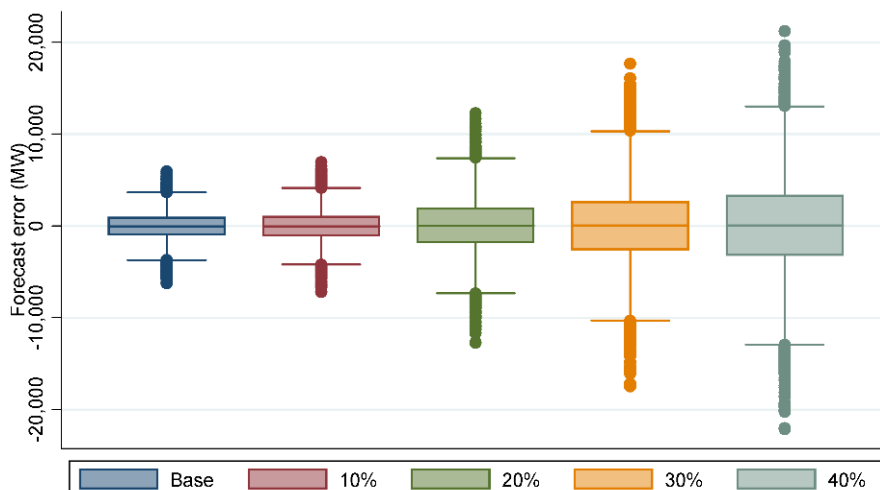


**Figure EAD-1: Wind forecast error for various renewable milestones**

Figure EAD-2 shows the forecast uncertainty broken down on a monthly basis for the base renewable penetration and the 40% renewable penetration. The forecast error is expected to be higher during the months with higher renewable output.

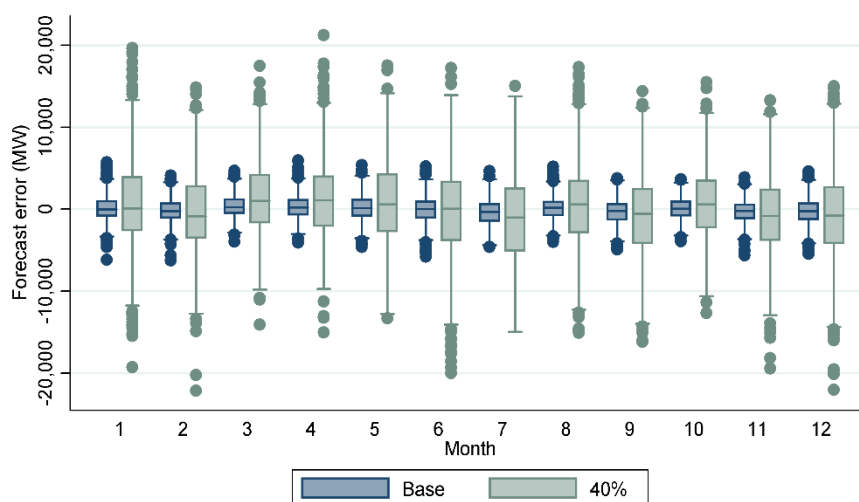


**Figure EAD-2: Monthly breakdown of the wind forecast error for the base and 40% renewable milestones**

**Finding: Variability of the wind and solar generation decreases with geographic diversity**

Variability is defined as the change in generation or demand over a pre-defined time interval. Figure EAD-3 shows the ramp rates associated with the wind and solar generation over an hourly interval. It is observed that variability in the aggregated generation reduces when the generation resources are geographically diverse. Any local variations in the renewable energy output can be easily compensated by the renewable generation within the same local resource zone (LRZ) or other parts of the footprint if adequate transmission capacity is built.

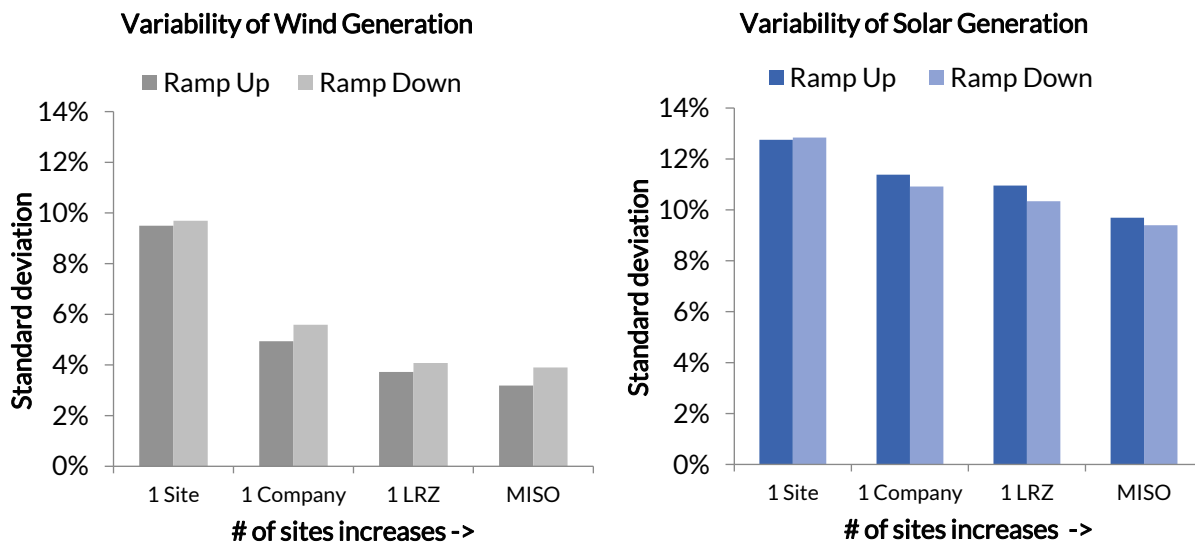


**Figure EAD-3: Variability of wind and solar generation based on geographical aggregation**

Finding: Increases in net load ramp is observed due to variability associated with the wind and solar generation

Figure EAD-4 and Figure EAD-5 shows that the variability or ramp from wind and solar generation increases in magnitude with increase in renewable penetration. The variability of wind and solar generation combined with the 1.4% variability associated with load leads to the net load ramp requirements increasing for the rest of the generation fleet (Figure EAD-6). The net load ramp is estimated by netting out the renewable generation amount from the hourly load. The variability of the wind and solar generation along with the increase in the net load ramp requirement calls for better coordination between the renewable generation resources and thermal generation in order to reliably serve load.

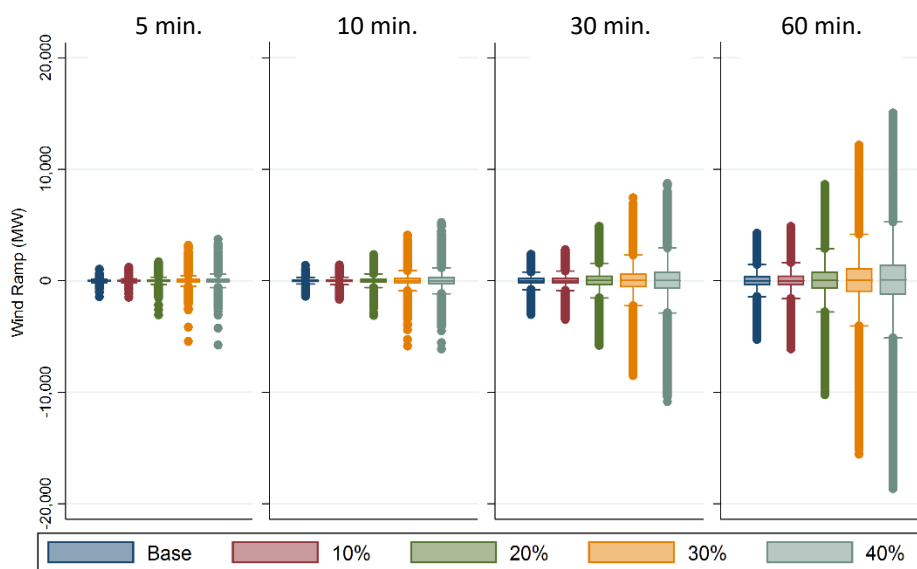


**Figure EAD-4: Wind ramp for various renewable penetration milestones**

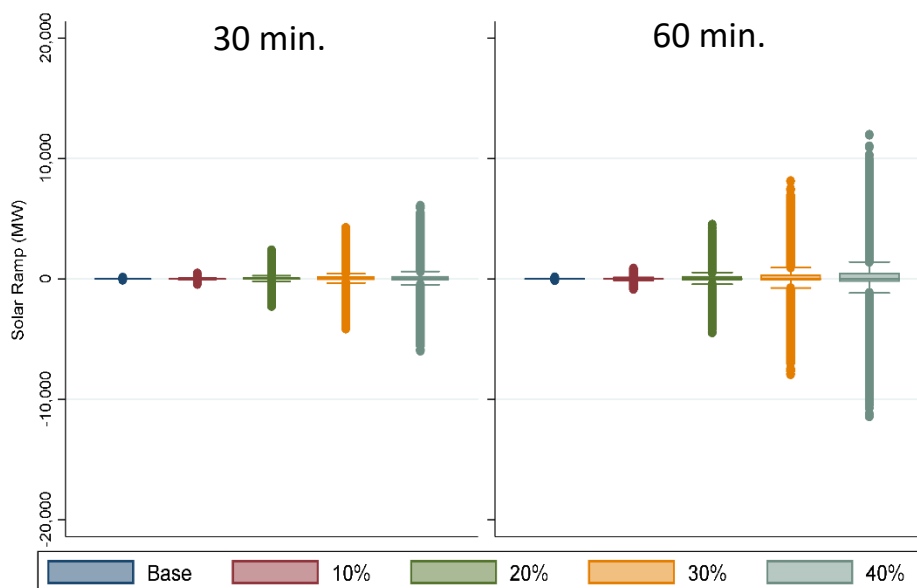


Figure EAD-5: Solar ramp for various renewable penetration milestones

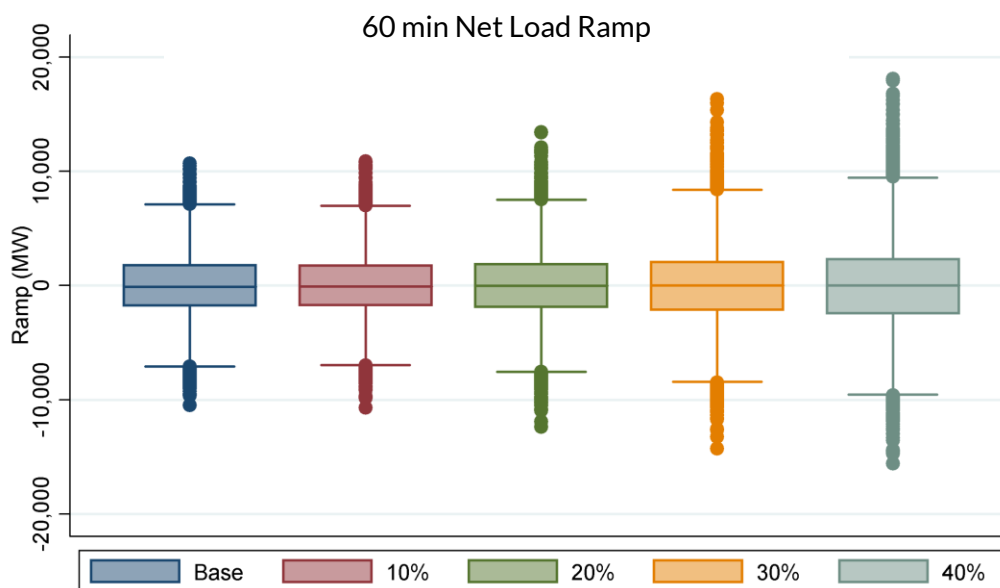


Figure EAD-6: Net load ramp for various renewable penetration milestones



## Operating Reliability – Steady State

### Overview

The purpose of steady-state reliability studies is to prevent the transmission system from exceeding its thermal and voltage ratings during normal and abnormal system operation, when deviations from normal operating conditions can occur without warning. Steady-state reliability studies are performed for a finite number of operating points. Traditionally, these points were chosen to align with periods of high system stress using engineering judgement, such as peak load. As renewable penetration increases, the times of transmission system stress also change. RIIA demonstrates that peak system stress is not necessarily coincident with the conditions traditionally studied -- peak system load or shoulder load -- in systems with high penetration of renewable generation. This is significant because traditional transmission planning presumes maximum system stress would be coincident (or nearly coincident) with peak system load.

Within the RIIA OR-SS analysis, two primary concerns were examined:

- Will there be enough voltage-regulating equipment to support stable transmission system operation in high-stress conditions, since voltage-regulating controls, unlike regulating frequency, are a local resource, rather than a network-wide resource?
- Is there enough transmission capacity on long-distance transmission lines for the bulk electric system to operate reliably in case of unplanned outages?

In a world with high renewable penetration, RIIA suggests that there will be fewer thermal generators close to loads and more renewable generators remotely located from load centers, requiring longer transmission paths. Longer transmission paths increase the potential for thermal overloads as the older paths may not have been designed for the same level and direction of geographic power transfer. As a result, the complexity of the system increases with increasing renewable penetration (Figure OR-SS-1).

In summary, RIIA OR-SS analysis shows:

- As renewable penetration grows, system conditions and timing at which transmission stress occurs change
- The location of transmission stress changes significantly beyond 20% renewable penetration
- Steady-state complexity increases beyond 20% renewable penetration and is largely driven by mitigating thermal violations on transmission lines

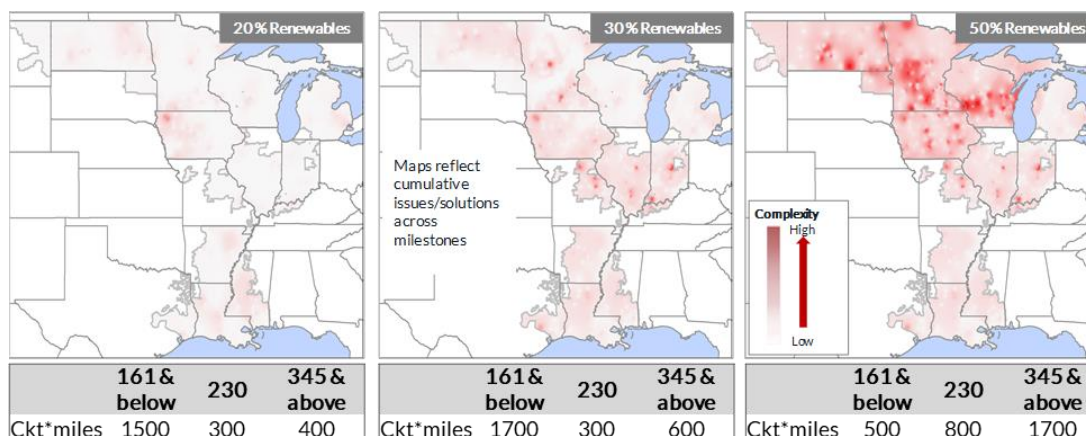


Figure OR-SS-1: Steady-state results summary (thermal and voltage-support mitigations)



## Key Findings

**Finding:** System conditions during and timing of transmission stress change as renewable penetration grows.

In the RIIA system models, the MISO load peaks in July at around 125 GW, while the lowest load levels of 55-60 GW are observed in the spring and fall seasons during night hours. At these very low load hours, a system with a higher share of wind energy in the renewable resource mix can experience very high instantaneous penetration (refer to “% Renewable at reference point” and bar chart on Figure OR-SS-2. Increase in solar installed capacity in the Siting sensitivity (discussed in Siting and Scenario Development), creates a new stressed operating point during the shoulder load periods, which may need further review in Operating Reliability).

Detailed steady-state and dynamic stability analysis was conducted on a total of 15 models (3 models for each of the 5 snapshots of 10% to 50% annual renewable energy) with instantaneous renewable penetration ranging from 5% to 89%. RIIA demonstrates total renewable output in the 50% milestone varies significantly throughout the year, with moments of high instantaneous renewable penetration reaching 89% in the MISO region, compared to 24% for the 10% milestone (Figure OR-SS-2). The shoulder periods studied in RIIA can differ greatly from the shoulder periods traditionally studied.

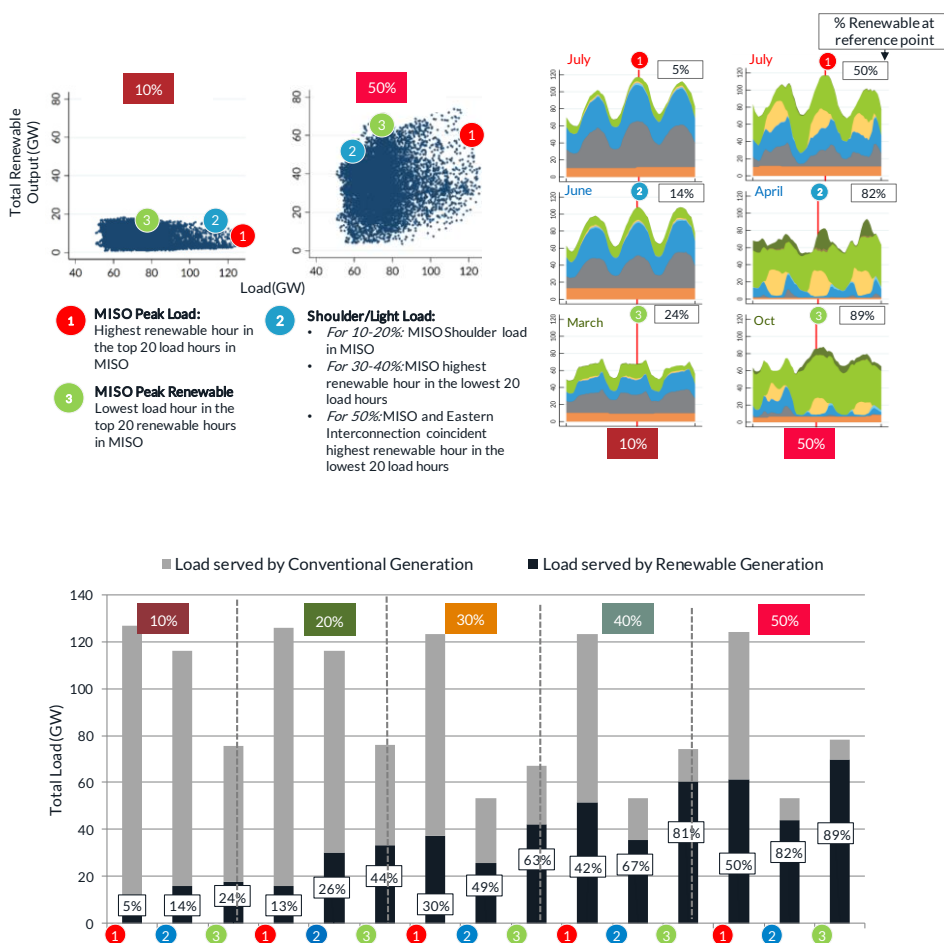


**Figure OR-SS-2: Changing conditions during stress and changing timing of stress on the transmission system**



During these periods of high instantaneous renewable penetration, conventional units are displaced by low-cost renewable energy. This displacement introduces new reliability risk periods, which are no longer aligned with the traditional risk-period (peak load) and represents new periods of stress on the transmission system (more detail on this is in sections below). An adaptive planning process is essential to evaluate new periods of risk as renewable penetration increases. Based on RIIA findings, MISO is actively engaging stakeholders to update dispatch assumptions used in the MTEP reliability process<sup>4</sup>.

#### Finding: The location of transmission stress changes significantly beyond 20% renewable penetration

RIIA steady-state analysis indicates that in absence of any upgrades of existing transmission network or addition of new transmission equipment, the bulk electric system experiences significant post-contingent low voltages beyond the 20% renewable penetration level. As the renewable penetration increases, more power flows from the northwestern part of MISO to load centers in the central and southern parts of MISO. As a result of this changing flow pattern, several acute issues arise in different locations in MISO and progressively become worse as the renewable penetration increases (Figure OR-SS-3). Low-voltage issues can be mitigated by installing shunt reactive power devices (e.g. capacitors) or by adding transmission lines. Voltage issues becoming more severe and resulting in transient instability may require installing dynamic compensation devices, such as STATCOMs or VSC-HVDC devices (refer to the Operating Reliability – Dynamic Stability section).

---

*As a result of changing flow patterns, several acute issues arise in different locations in MISO and progressively become worse as the renewable penetration increases.*

---

Because these voltage issues are exacerbated as the penetration level increases, cost-effectively mitigating voltage issues will require a forward-looking approach, tackling both steady-state and dynamic stability issues.

A similar pattern is observed in thermal overloads; as renewable penetration increases, the number and severity of thermal overloads increases and expands into different geographic areas (Figure OR-SS-4). Initially, overloads are concentrated near the renewable expansion areas. With increasing renewable penetration, however, more overloads appear between renewable expansion areas and load centers. With the base-siting, this is driven by two major factors – (a) limited transmission capacity in the wind-rich northwestern part of MISO’s footprint for delivering low-cost wind to other parts of MISO, and (b) conventional units, typically sited near large load centers, being displaced or retired due to economics as the renewable penetration increases.

---

*An adaptive planning process is essential to evaluate new periods of risk as renewable penetration increases.*

---

---

<sup>4</sup> Refer to MISO PSC presentation “Wind / Solar Generation Dispatch Assumptions In The Reliability Planning, Models”, Oct 2019, available online [here](#).

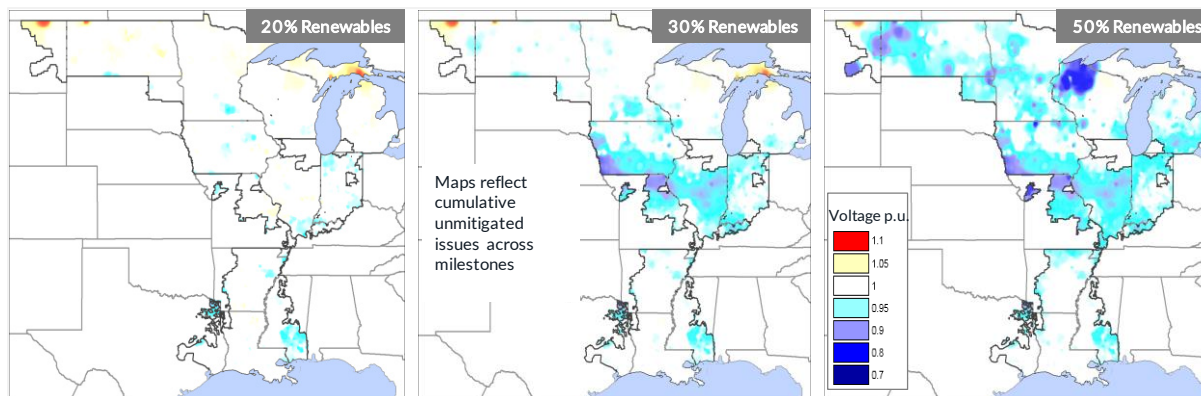


Figure OR-SS-3: Locations of low voltages in MISO

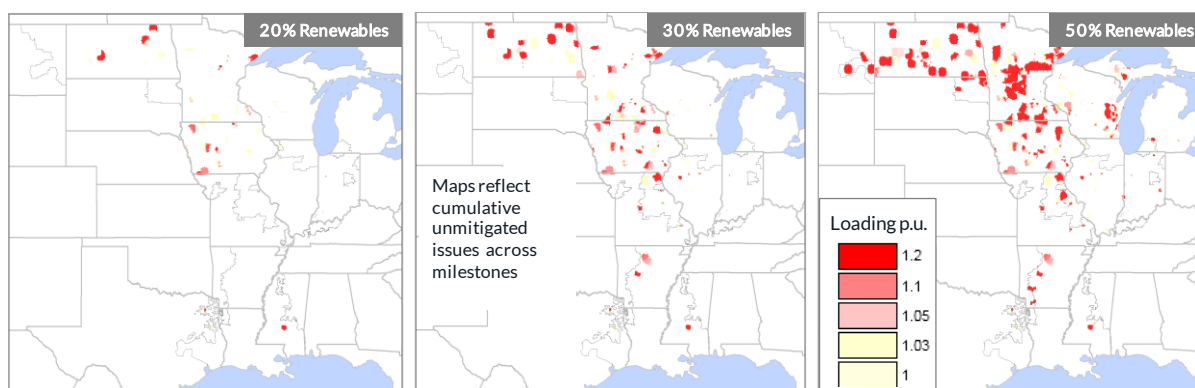


Figure OR-SS-4: Locations of thermal overloads in MISO

Finding: Steady-state complexity increases with renewable penetration levels after 20% and is largely driven by mitigating thermal violations on transmission lines

Transmission line upgrades to mitigate thermal limit violations comprise the largest driver of complexity for resolving steady-state issues. Upgrading transformers for thermal limit violations or installing shunt reactive devices for voltage issues make up a much smaller percentage of the complexity (Figure OR-SS-5). Although RIIA demonstrates that increasing renewable penetration will require considerable shunt reactive power devices to ensure acceptable voltage performance, the investment cost pales in comparison to the need for upgrading transmission lines.

---

*Increasing renewable penetration will require considerable shunt reactive power devices, but the investment cost pales in comparison to the need for upgrading transmission lines.*

---

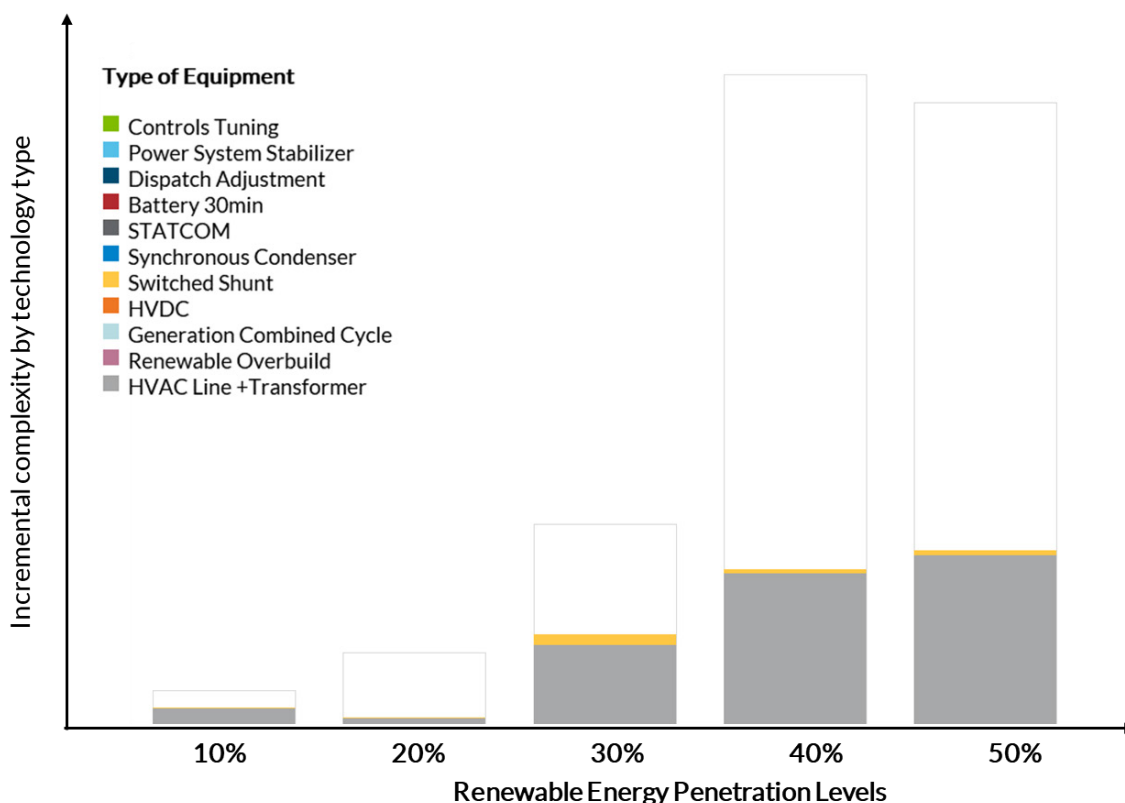


Figure OR-SS-5: Incremental complexity to resolve steady-state issues, by equipment type

Finding: As renewable penetration increases, more thermal mitigations on higher voltage lines are needed

Another interesting finding related to transmission grid stress can be distinguished by the fact that as the penetration increases more thermal overloads are seen on higher voltage lines. Typically, conventional generators are located near load centers, and have one point-of-interconnection (POI) to the electrical-grid and generate at or near their full capacity most of the time, whereas renewables resources are geographically dispersed, need more POIs and more nameplate capacity<sup>5</sup> is required to serve the same load (due to natural variations of irradiance and wind speeds).

---

*With subsequent increases in renewable penetration, the transmission bottlenecks shift to higher voltage lines, akin to freeways getting congested.*

---

At lower RIIA milestones, the production-cost-model sourced generation dispatch and load levels in the power-flow models indicated the energy from these renewable resources tends to cause overloads on lower voltage lines -- akin to city streets getting congested. With subsequent increases in renewable penetration, the transmission bottlenecks shift to higher voltage lines, akin to freeways getting congested. This pattern provides an important insight into transmission infrastructure planning; while high-voltage transmission lines will be needed as backbones to enable more renewable delivery, lower voltage lines will also need upgrades to enable the last-mile delivery of renewable energy.

---

<sup>5</sup> Nameplate capacity is defined as MW injection at full output

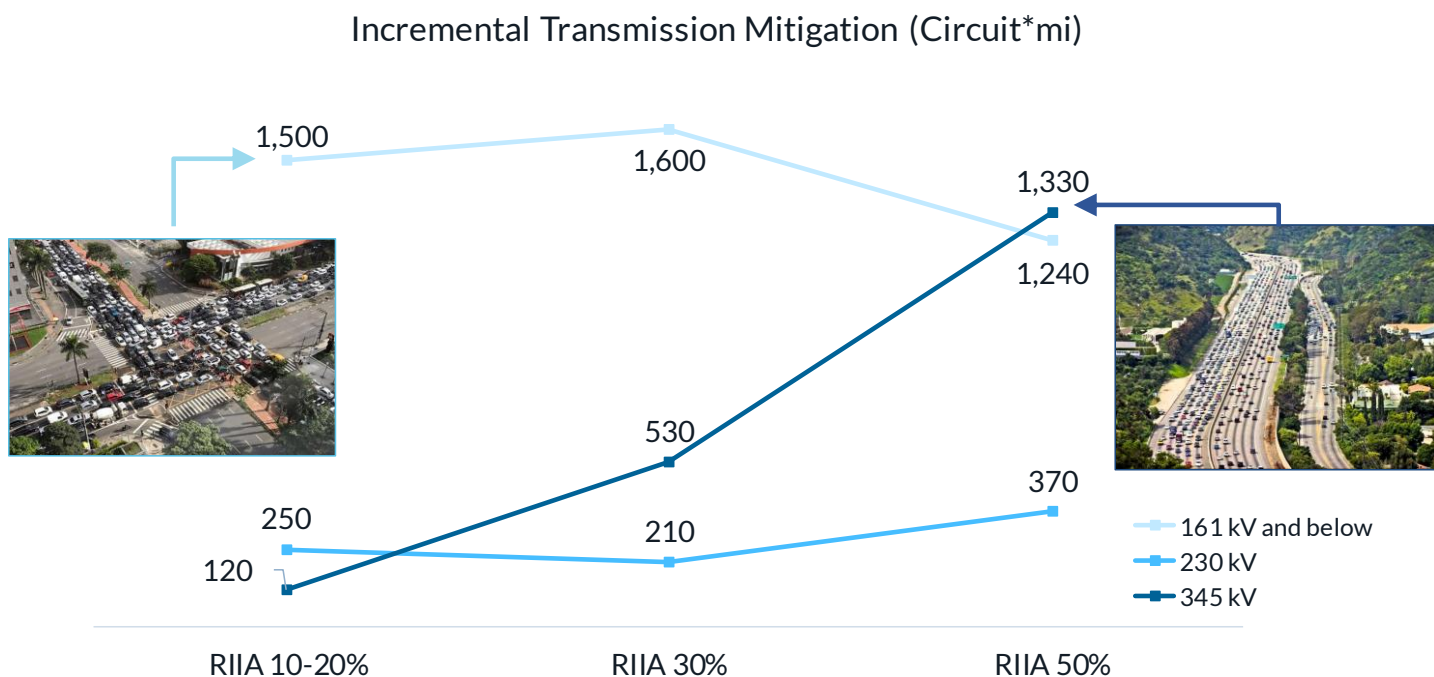


Figure OR-SS-6: As renewable penetration increases, the amount of higher voltage line upgrades increases

## Operating Reliability – Dynamic Stability

### Overview

Dynamic Stability is comprised of maintaining operating equilibrium post electric-grid disturbance in three distinct elements – (a) voltage stability, (b) adequate frequency response, and (c) rotor angle stability (Kundur<sup>6</sup>, 2004). The equilibrium should be characterized by a well-damped, non-oscillatory behavior of electrical quantities (MW, Mvar, frequency). Dynamic stability looks at the timeframe within seconds of power system disturbances and involves laws of physics and fast-automatic-action of equipment responding to the event without any operator action. Similar to steady-state analysis, it is performed on a limited number of specific scenarios.

<sup>6</sup> P. Kundur, J. Paserba and S. Vitet, "Overview on definition and classification of power system stability," CIGRE/IEEE PES International Symposium Quality and Security of Electric Power Delivery Systems, 2003. CIGRE/PES 2003., Montreal, Quebec, Canada, 2003, pp. 1-4, doi: 10.1109/QSEPDS.2003.159786.

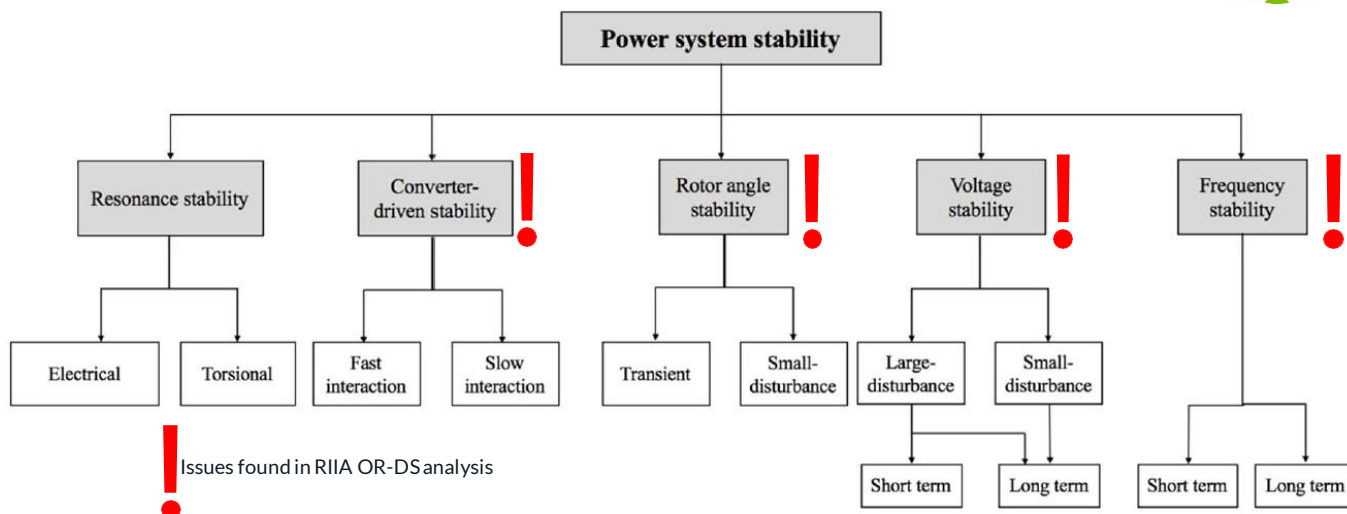


**Figure OR-DS-1: Power system stability categories defined by IEEE and issues identified in RIIA**

Within the RIIA operating reliability-dynamic stability (OR-DS) analysis, the following key concerns were examined within the context of three key elements of dynamic stability:

- What will the impact of high penetrations of renewable (inverter-based) resources be on frequency, transient and voltage stability, damping, and local grid strength (weak areas)?
- What actions will be required to maintain adequate performance? When will they be necessary?

RIIA identifies potential issues with all three elements of dynamic stability and an additional category of “converter-driven stability<sup>7</sup>” associated with inverter-based equipment defined in the new IEEE report (Figure OR-DS-1, IEEE PES- TR77<sup>8</sup>, May 2020). With respect to voltage stability and inverter-driven stability, the RIIA assessment demonstrates that as inverter-based resources increase in penetration, there is a corresponding decrease in online conventional generation, which intensifies reliability issues. The same phenomenon is also responsible for frequency stability. As the increased penetration of inverter-based generation continues, the number of conventional units available to provide inertia and damping decreases. The result is the potential compromise of the system’s ability to arrest a frequency excursion in the timeframe necessary to prevent involuntary load shedding, and, due to the displacement of conventional units with power system stabilizers, an Eastern Interconnection (EI) wide undamped oscillation (also known as “inter-area small-signal oscillations”) appearing. The analysis was also conducted to gauge the rotor angle stability of the remaining online convention units by calculating critical clearing time (CCT<sup>9</sup>). The analysis indicates overall, CCT increases as renewable penetration increases denoting a positive impact of renewable penetration; however, RIIA finds that CCT may decrease at certain locations experiencing very high instantaneous penetration.

<sup>7</sup> Converter-driven stability is associated with resources (wind, solar or battery) or dynamic devices (STATCOM, HVDC) utilizing inverters to connect to AC grid.

<sup>8</sup> Nikos Hatziargyriou, P. Pourbeik, *et al*, “Stability definitions and characterization of dynamic behavior in systems with high penetration of power electronic interfaced technologies”, May 2020

<sup>9</sup> CCT is defined as the maximum number of cycles a conventional unit can remain in synchronism during a faulted condition. 1 cycle = 1/60 second



The key findings of operating reliability-dynamics are summarized below, which are discussed in detail in the subsequent sections.

- Potential dynamic stability issues due to weak grid increase sharply beyond RIIA 20% milestone.
- Frequency response is stable up to 60% instantaneous renewable penetration, but may require additional planned headroom beyond.
- Small signal stability may become a severe issue beyond 30% RIIA milestone and can be addressed by specially tuned batteries or must-run units equipped with power system stabilizers.
- Overall, critical clearing time (CCT) becomes better as large units are displaced, but some locations may observe a decrease and may require installation of new protection techniques or transmission devices.
- Grid-technology-needs evolve as renewable penetration increases leading to an increased need for integrated planning and a blend of transmission solution types.

The dynamics stability concerns by the rank of severity are summarized in Table OR-DS-1, as follows: 1) transient voltage stability in weak areas, 2) small-signal and frequency response, and 3) rotor angle stability. The thumbs up and thumbs down on the rotor angle stability row indicates that some CCT values improve and others worsen, with the relative proportion indicated by the size of the symbol.

After analyzing a range of reliability issues pertaining to weak-areas, RIIA proposes several mitigation techniques (Figure OR-DS-2). Wherever applicable, low-cost solutions, such as tuning of controls of inverters and re-dispatch of generators can be applied. However, to address severe voltage and inverter-driven stability issues, adding synchronous condensers to the existing AC transmission system and utilizing advanced technologies, such as Flexible Alternating Current Transmission System (FACTS) devices and Voltage Source Converter (VSC) based HVDC transmission lines can be pursued. Frequency -related issues can be addressed by maintaining additional planned headroom on resources, including renewables and by storage. Although renewable resources have the capability (hardware) to provide frequency response and ramping, they cannot provide sustained response unless they maintain a certain amount of headroom (energy reserve) by operating below their maximum possible power output. Thus, wind and solar resources need economic incentives or regulations adopted to “spill” energy to maintain headroom.

Inter-area small-signal issues can be resolved by ensuring units with power system stabilizers (PSS) installed are committed or by installing specially tuned batteries at strategic locations. Additional research and pilots into advanced technology, such as grid-forming inverters, should be pursued to help counteract these risks or minimize cost. Inverter-based resources (IBR) can be equipped with Fast Frequency Response (FFR) to mitigate issues caused by reduced governor response and reduced inertia, due to retired or off-line thermal generating units. IBR and FACTS could also be equipped with stabilizing control loops.

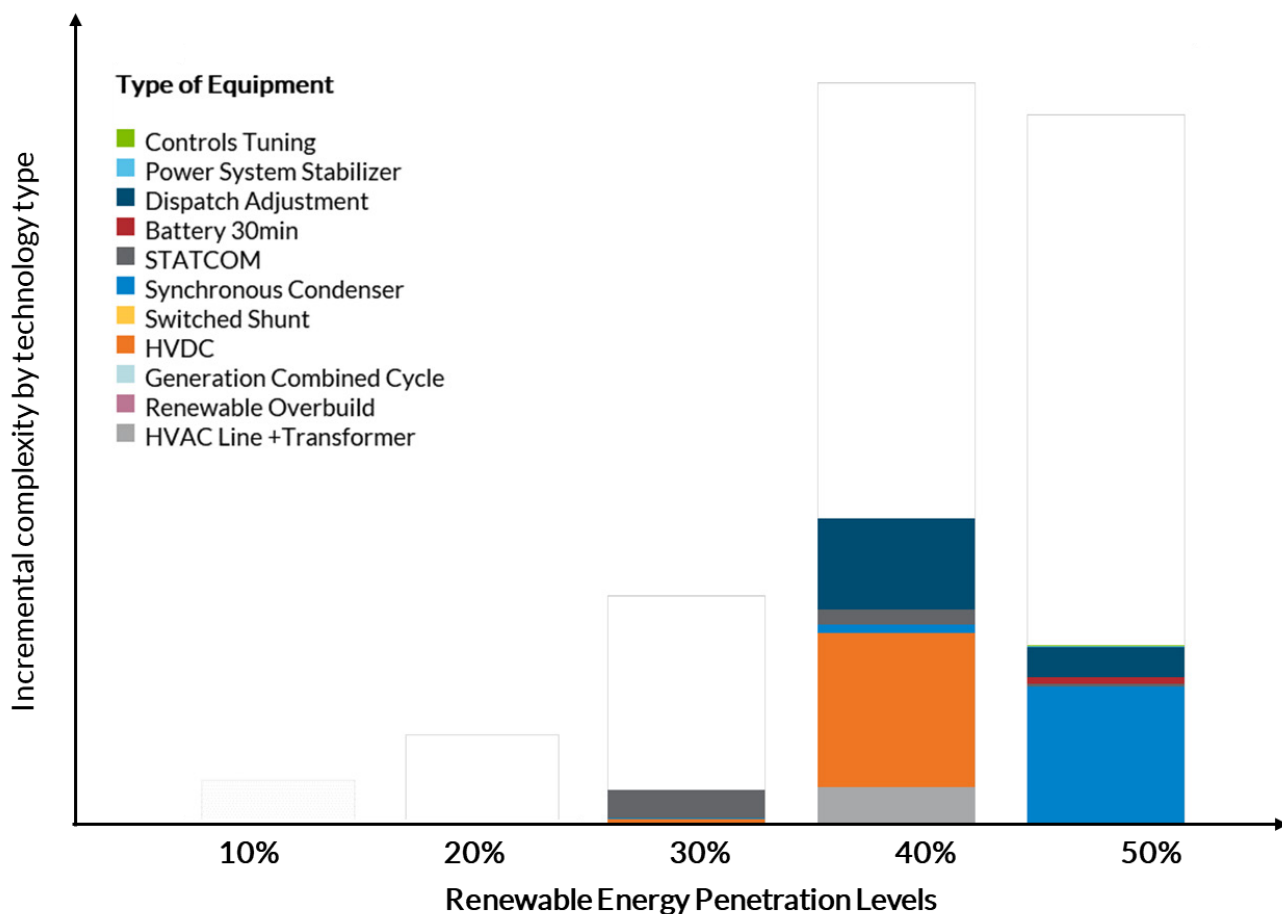


**Figure OR-DS-2 :Different technology types used to solve operating reliability issues at each RIIA milestone**

The analysis also indicates that to bring down the cost of grid-integration (particularly at high penetration levels) there is benefit to improving characteristics of inverter-based resources such as the following.

- Research and development should be pursued to develop better control-techniques (such as deploying “grid-forming” technique) to enable reliable operation in weak-grids. This can have the effect of reducing the need for synchronous condensers and transmission lines – both AC and DC.
- Interconnection-wide small signal oscillations in the range of 0.1-0.8 Hz can appear at high penetration of renewables. Currently, renewable resources are not known to have the capability to arrest inter-area oscillations, and it is uncommon to install power system stabilizers (PSS) on synchronous condensers (SC). Through detailed analysis, strategic locations can be identified where installing appropriately tuned and designed supplemental power oscillation damping (POD) controllers on renewable resources, batteries, SVC, STATCOM, or HVDC can help to improve small signal stability. Hence, RIIA makes a recommendation to the renewable resource owners (including electric storage) and dynamic device manufacturers to facilitate the addition of POD controllers to mitigate such issues in the future.
- Pilot-programs demonstrating the reliable operation of these new techniques should be pursued to educate and familiarize the electric grid operators and assets owners, and to facilitate mass adoption.



Area of stability	Ranked concern	Performance metric	Impacts	Possible mitigations	Concerned MISO group	Issue first seen	Impact of renewable penetration	Capital cost share to mitigate
Inverter-based stability and voltage stability	1. Transient voltage stability in weak areas	Short circuit ratio, undamped voltage and current oscillations, interactions between the controls of equipment	Local area, observed at many substations system-wide	<ul style="list-style-type: none"> <li>Control tuning</li> <li>Synchronous condensers</li> <li>STATCOM</li> <li>HVDC</li> </ul>	EP*, GI†	30%		
Frequency stability	2. Frequency response	Frequency nadir, rate of change of frequency (RoCoF), NERC BAL-003 obligations	Interconnection wide	<ul style="list-style-type: none"> <li>Additional planned online headroom</li> <li>Batteries</li> </ul>	Operations	50%		
	3. Small signal stability	Damping ratio of low frequency oscillations	Interconnection wide	<ul style="list-style-type: none"> <li>Must-run units with power system stabilizers</li> <li>Specially tuned batteries</li> </ul>	EP*, Operations	30%		
Rotor-angle stability	4. Transient rotor angle stability	TO's local planning criteria, NERC criteria	Local area	<ul style="list-style-type: none"> <li>Faster protection schemes</li> <li>Transmission facilities</li> </ul>	EP*, GI†	50%		-

\*EP: Expansion Planning  
†GI: Generator Interconnection

**Table OR-DS-1: Summary of dynamic concerns by ranking, performance metrics, possible mitigations and impacted**

## Key Findings

**Finding: Weak areas: Short circuit ratio (SCR) at several locations decrease with an increase in penetration due to a reduction in conventional generation and the increase in inverter-based generation.** Grid-following inverters face difficulties in operating reliably in areas known as “weak-area” or “weak-grid” and can be identified by calculating the short circuit ratio (SCR<sup>10</sup>). Low SCR defines weak areas. Typically, weak-area instability arises in long radial electric networks or local networks with high concentrations of inverter-based renewable resources with little or no conventional generation or synchronous condensers. Conventional generators, by design, improve SCR, thus making the grid stronger.

Existing inverter-based resources use a combination of phase locked loop (PLL) and extremely fast current-regulated controls to keep the current being injected into the grid by the inverters in synchronism with the grid frequency. Thus, in weak areas, following severe faults on the grid there is no strong grid frequency reference for the PLL to lock into, and present technology can have significant challenges with recovering and remaining connected to the grid post-fault. Advances in power electronic converter technologies, such as so-called “grid-forming” inverters, will be needed in the future as penetration increases. Some of these approaches are based on inverters that are able to create their own internal frequency reference and thus do not need a PLL for keeping synchronism with the grid and can thus avoid both the issue with PLL dynamics and not being able to lock into the grid post-fault, and moreover can provide inherent services such as virtual-inertia. Much of this still requires more research and development, but such technologies show promise for the future.

PLL in the grid-following inverter-based resource is one of the sources of reliability concern, and instabilities may also arise from a combination of challenges in weak grids such as

<sup>10</sup> SCR is calculated as available fault MVA at a network node divided by MW injection by inverter-based resource. Other methods are also used to determine SCR. Refer NERC: Integrating Inverter Based Resources into Low Short Circuit Strength Systems Reliability Guideline, December 2017



- tracking of voltage and frequency using PLL,
- inverter-based resources behaving as current-controlled sources,
- sensitivity of power electronics to external disturbances (unlike conventional generation units able to survive under instantaneous high current or high voltage conditions),
- interactions between the high bandwidth controllers of inverters, and
- interactions between inverter controllers and other equipment (series compensation or long lines).

The focus may need to be to understand the conventional grid was planned and built for traditional synchronous generators serving machine loads. However, the trends in both loads and generation sources are moving towards increased penetration of power electronics-based resources introducing a different set of constraints needing further research and mitigations.

The heatmaps below show the geographical locations of the weak areas denoted by orange color (SCR<sup>11</sup>) in different RIIA milestones (Figure OR-DS-3). The intensity of color denotes severity of the weak-area issue; thus, darker areas are most likely to have a stability issue. A combination of renewable resources located in areas with limited grid strength (such as North Dakota, parts of Iowa, and southwest Minnesota) with displacement of conventional generation increases the number of locations with low SCR (Figure OR-DS-4) and exacerbates challenges faced by inverters. The potential reliability issues arising in the weak areas can manifest into different forms, ranging from undamped oscillatory behavior of electrical quantities to voltage and inverter-based stability issues. SCR is merely an indicator, much like a high temperature may indicate a person is ill, but it does not tell the exact ailment. To ascertain the nature of complications, 15 detailed EI-wide dynamic stability models (3 each for the 5 milestones of 10% to 50%) were developed, and findings are discussed below.

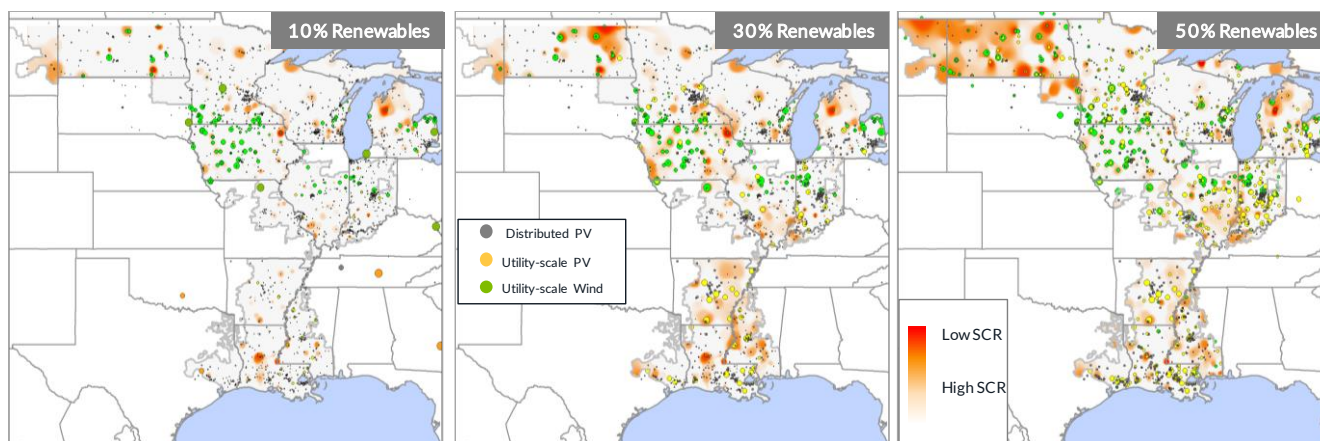


Figure OR-DS-3: Projected weak areas in MISO with growing penetration of renewables

<sup>11</sup> SCR was calculated using PSSE module

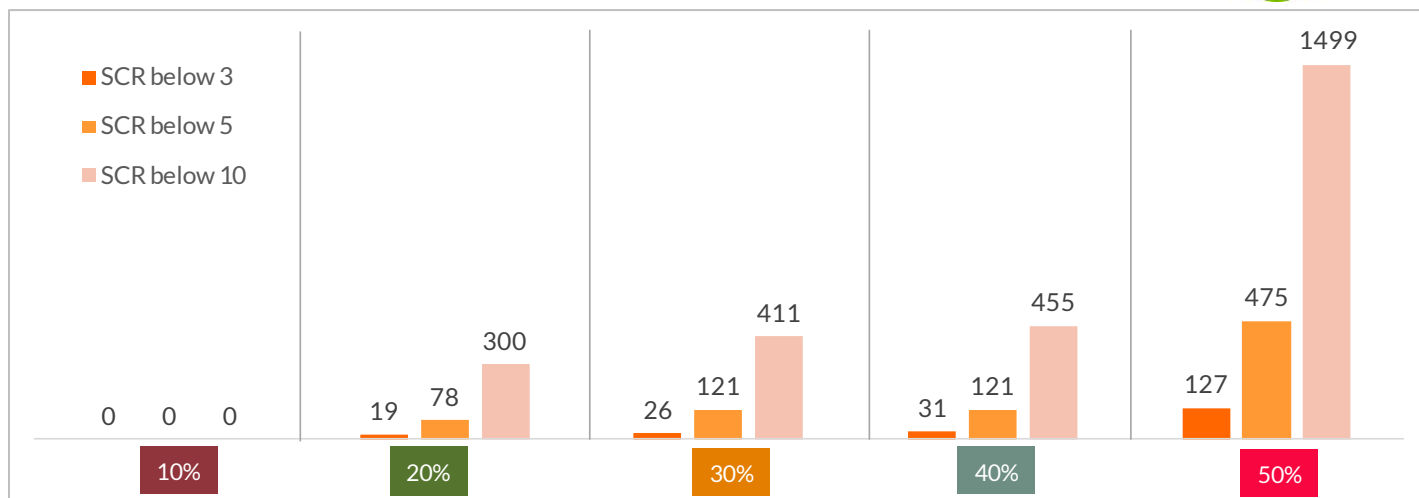


Figure OR-DS-4: Short Circuit Ratio (SCR) distribution in MISO (number of substations)

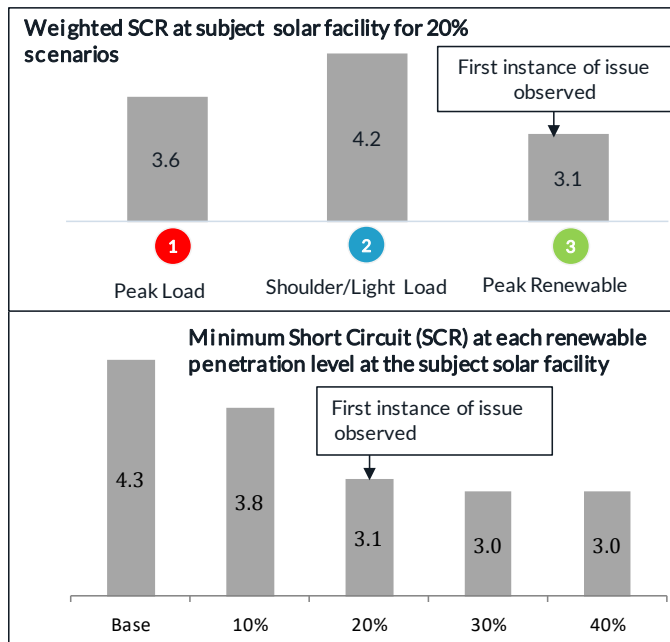
Finding: Weak areas: dynamic issues such as low -frequency undamped oscillations of electrical quantities are likely to appear during high renewable and low load conditions, which can be fixed by tuning wind and solar plant controls.

The stability issue likely to appear first in the list of “reliability issues due to weak-area” is low frequency undamped oscillatory behavior of electrical quantities (MW and Mvar) at renewable resource’s POI. Such issues can be fixed at relatively low cost by performing detailed modeling and analysis (positive sequence or electromagnetic transient (EMT) type simulations) of the renewable resource. Then tuning the control gains correctly resolves the instabilities. RIIA observes this issue for the first time in the 20% peak-renewable case at a non-MISO location. A solar farm of 600 MW capacity was modelled in the base case at that location, and the minimum SCR was found to be 4.3. At 20% RIIA milestone, a higher renewable capacity sited at that location, coupled with displacement of a nearby conventional generator lead minimum SCR to fall to 3.1 (Figure OR-DS-5). Interestingly, the minimum SCR coincides with the scenario of system-wide low load and high renewable penetration, because at higher system load more conventional units are committed to serve load and meet other requirements such as ramping. Lower SCR causes undamped oscillations at the terminal voltage and was fixed by tuning the gains of the inverter controls.

---

*Dynamic issues, such as low-frequency undamped oscillations, are likely to appear during high renewable and low-load conditions.*

---



Undamped voltage oscillations in low SCR area fixed by tuning the gains of solar plant A

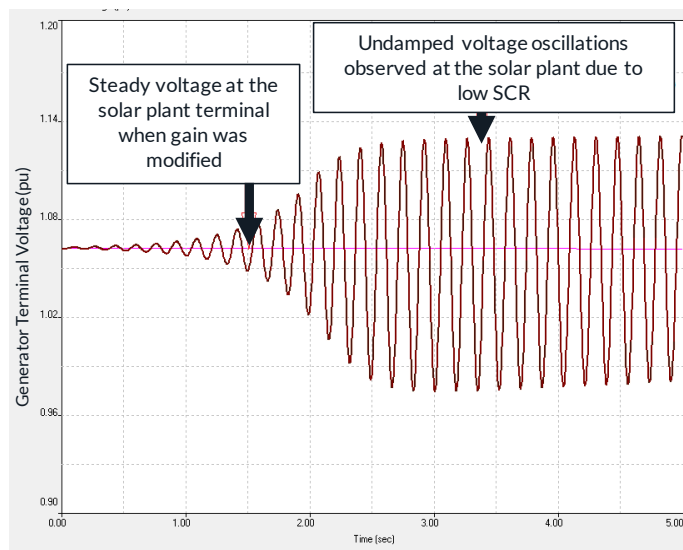


Figure OR-DS-5: Low-frequency undamped oscillations due to weak areas fixed by tuning of wind and solar plant controls

Finding: Weak areas: Wind and solar plants may require retuning of controls as system conditions change.

RIIA finds that as system conditions change over the years with increasing amounts of renewables and displacement or retirement of conventional generators, there could be a need to retune the gains of wind and solar plant controls. Analysis indicates that at 50% milestone the set of control parameters used to model future renewable resources had to be updated at several locations (Table OR-DS-2) to mitigate voltage oscillations in the range of 5-6 Hz (Figure OR-DS-6). The gains had to be reduced, and randomization<sup>12</sup> was introduced to prevent any unwanted unstable interactions between the renewable resources found by initially using the same parameters for all the new generation in the model. The finding even though surprising, can be well explained by the fact that at the 50% milestone several locations in MISO demonstrate low values of SCR, which is an indication of overall degradation of system strength (Figure OR-DS-3 and Figure OR-DS-4).

The finding also sheds light on an important emerging issue and deviation from the norm. Generally, after going through an interconnection study, inverter-based renewable resources rarely require retuning of the controls in the following years. However, there is significant possibility of an RTO or Transmission Owner with renewable resources conducting periodic studies to ensure that the control parameters ensure reliable operations as the adjacent system changes. Wind, solar, and hybrid plant owners will likely see a new normal of needing to retune their controls often, thus requiring a close coordination with transmission owners. It also provides another important insight; a renewable asset owner would need the control-hardware of the generation site to be easily accessible when necessary to modify it. In the

---

*An RTO or Transmission Owner with renewable resources may need to conduct periodic studies to ensure the control parameters provide reliable operations, as the adjacent system changes.*

---

<sup>12</sup> The randomization simulated the natural differing control settings the developers of renewable generation sites will employ as they commission their generation sites



likelihood some of the control-gains reside within the equipment installed on the wind-turbine, an easy and secure access to the equipment ensures minimal delay and downtime to resolve the issues required by the Transmission Owner before resuming operation.

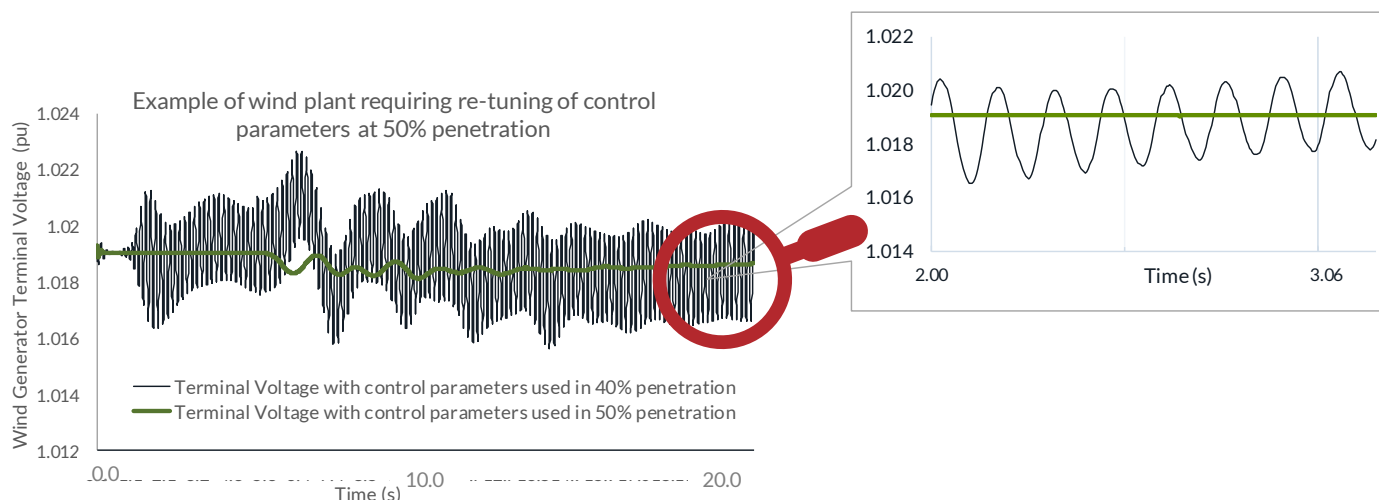


**Figure OR-DS-6: Renewable resource retuning of controls as system conditions change**

Control Parameters that were re-tuned	Value at 40%	Value at 50%*
Kp, Reactive power PI control proportional gain (pu)	4 or 10	1.60 - 2.40
Ki, Reactive power PI control integral gain (pu)	2 or 5	0.75 - 1.25
Kpg, Proportional gain for power control (pu)	0.25	0.2 - 0.28
Kig, Integral gain for power control (pu)	0.25	0.2 - 0.28
Kvi (pu), Voltage regulator integral gain	40	30-50

\*Random values in the specified range chosen to minimize control interactions. Only RIIA sited wind and solar units were re-tuned.

**Table OR-DS-2: Renewable controls tuning parameters**

**Finding: Weak grid: Power delivery from low short circuit areas may need transmission technologies equipped with dynamic support capabilities: A holistic approach is needed to develop solutions to solve the myriad of reliability issues**

Energy adequacy analysis indicates that transmission solutions were needed to achieve 40% renewable energy penetration target (Figure EA-4). A least-cost solution proposed new AC transmission lines to be placed in the weak areas of ND and Iowa to reduce curtailment and increase wind power delivery. Per the study process these new AC transmission lines were then modeled in power-flow models, and steady-state contingency analysis was performed to identify additional thermal and voltage solutions, which were subsequently fed into initial 40% dynamics models. During the dynamics analysis, even after applying a combination of AC only solutions (new AC transmission lines



only, AC lines and synchronous condensers only) the bulk electric system was unstable. For example, applying only new AC lines in absence of any synchronous condensers demonstrated severe voltage stability issues<sup>13</sup> at several nodes. New synchronous condensers were then modeled at these locations; they ensured the model initialized; however, the system was still unstable for several critical contingencies. Additionally, due to the large size of synchronous condensers located electrically very close to each other, low-frequency interactions were observed, and they created additional reliability issues<sup>14</sup>.

For the purposes of RIIA analysis, the only workable solution found was addition of Voltage Source Converter (VSC) HVDC transmission lines (Figure OR-DS-7). Utilizing the older LCC HVDC technology in weak areas was found inadequate and indicated further system enhancements needed to keep the system stable (Figure OR-DS-8).

The need for VSC HVDC technology to successfully solve a myriad of issues (reducing curtailment, ensuring power delivery, solving weak-area instability) demonstrates dynamic stability will become increasingly important for any large or small transmission expansion project in high renewable penetration scenarios, and the transmission design needs to be specifically vetted for dynamic

---

*To port power from wind-rich zones located in weak-areas, building a VSC- HVDC line into those weak-areas may be more economical than incrementally installing a combination of AC transmission lines with many synchronous condensers.*

---

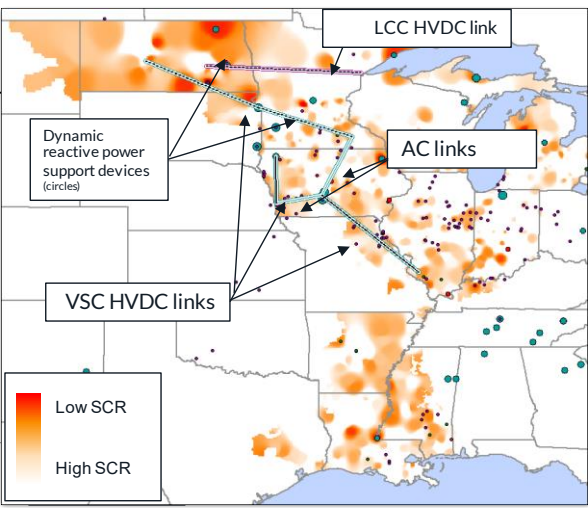
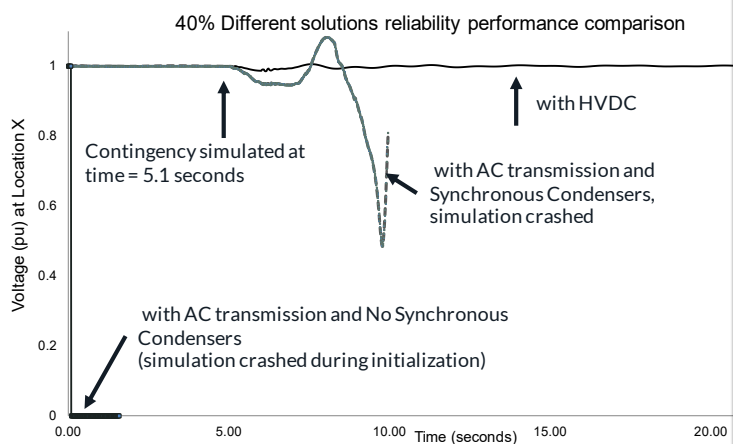
performance. To port power from wind-rich zones located in weak-area, building a VSC-HVDC line into those weak-areas may be more economical than incrementally installing a combination of AC transmission lines with many synchronous condensers and mitigating the small signal stability issues created by installing the rotating masses of those synchronous condensers (Figure OR-DS-9). It also re-emphasizes the desire to develop new technology, such as grid-forming inverters and pilot projects, to demonstrate their effectiveness to bring down the cost of grid-integration of renewable resources.

Modern HVDC-VSC technology does not require filter banks. Modern HVDC systems can be tapped to form multi-terminal systems.

---

13 Severe voltage stability was denoted by solution infeasibility at certain nodes within acceptable iterations limits.

14 Similar results were reported by ERCOT in “Dynamic Stability Assessment of High Penetration of Renewable Generation in the ERCOT”, 2018 available [online here](#).



Contingency: Loss of 4500 MW generation.

Heat Map represents Short Circuit Ratio (SCR)

**Figure OR-DS-7: Power delivery from low short circuit areas may need HVDC transmission technologies**

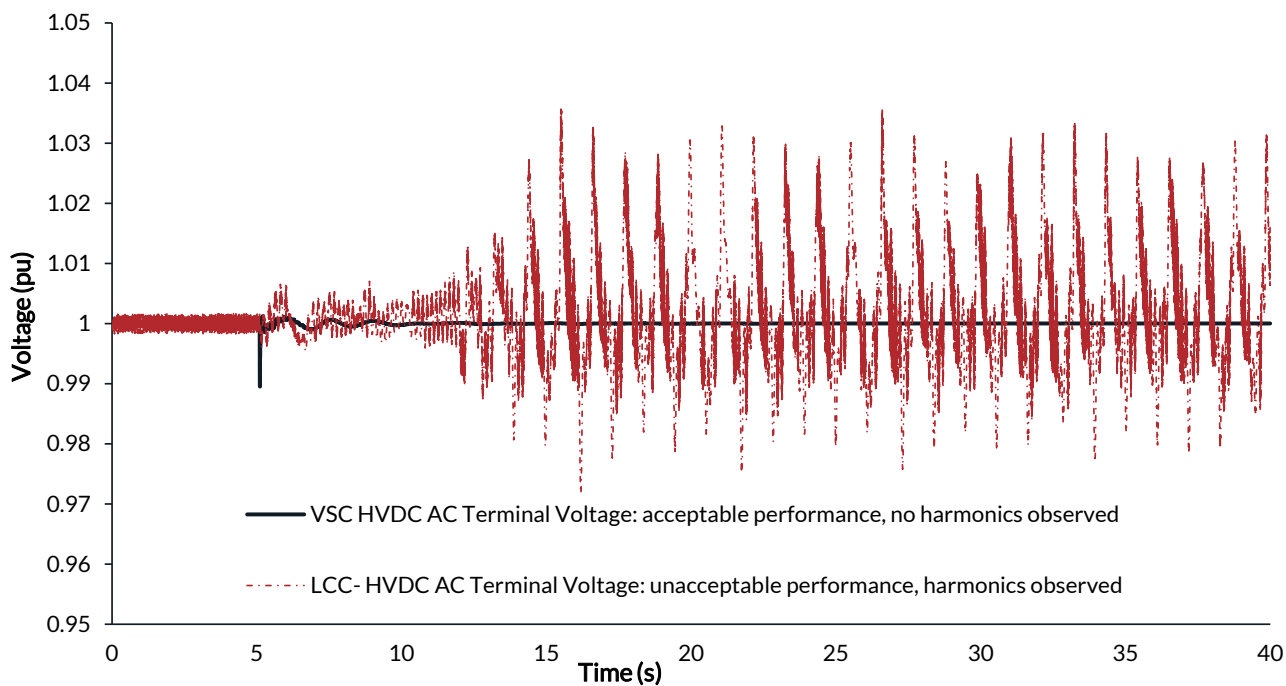
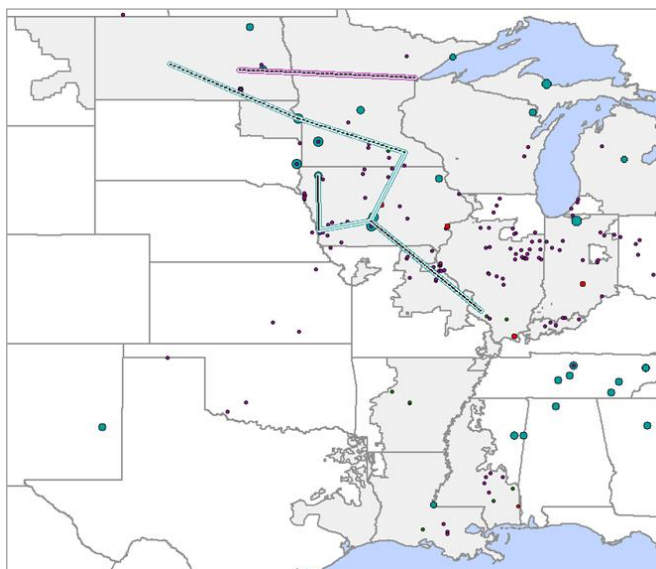
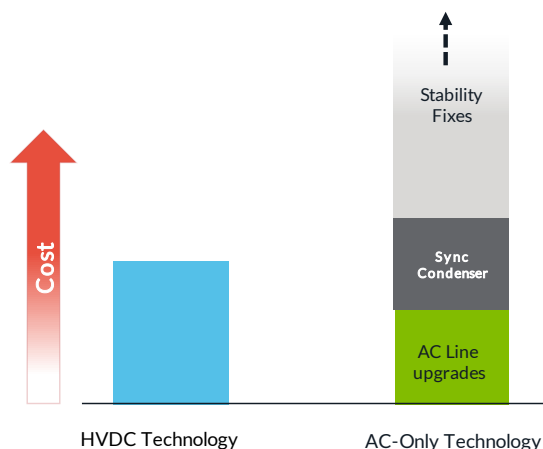


**Figure OR-DS-8: LCC vs VSC terminal voltage comparison**



Qualitative cost comparison for different transmission technologies for equal reliability performance



To port power from wind-rich zones located in weak-area, building a VSC- HVDC line into those weak-areas may be more economical than incrementally installing a combination of AC transmission lines with many synchronous condensers and mitigating the small signal stability issues created by installing the rotating masses of those synchronous condensers

**Figure OR-DS-9: A holistic approach is needed to develop solutions to solve the myriad of reliability issues**

**Finding: Weak-grid: Voltage stability remains the main driver of dynamic complexity at 50% and may require system-wide installation of synchronous condensers.**

Energy adequacy simulations indicate that at the 50% milestone MISO could experience several hours of very high instantaneous renewable penetration where ~90% of load for that hour may be served by renewable generation, and very few conventional units will be online. Simulations indicate such conditions are precarious for the grid-following<sup>15</sup> technology, as it needs a strong grid (voltage source) to perform reliably. Installation of several synchronous condensers provides a stabilizing impact on the voltage of the grid, thus mitigating the chattering observed in the 50% milestone voltage waveform (saw-tooth type waveform observed in Figure OR-DS-10). However, to verify the need for several synchronous condensers across the footprint, a new model beta<sup>16</sup> model (regc\_b) was also tested and gave the same results. The cost of renewable integration can be reduced if renewable manufacturers make inverter technology more grid friendly.

---

*Installation of several synchronous condensers can provide a stabilizing impact on the voltage of the grid.*

---

<sup>15</sup> RIIA utilized the industry-vetted WECC 2nd generation renewable model (regc\_a), which is a current-source model representing commercially available inverters. However, as noted in the WECC documentation and papers, this model has its limitations, particularly the potential for numerical issues when used under very weak-grid conditions. Thus, some new models have been developed to address some of these issues, the so-called REGC\_B model.

<sup>16</sup> regc\_b was under development by WECC when RIIA simulations were done.

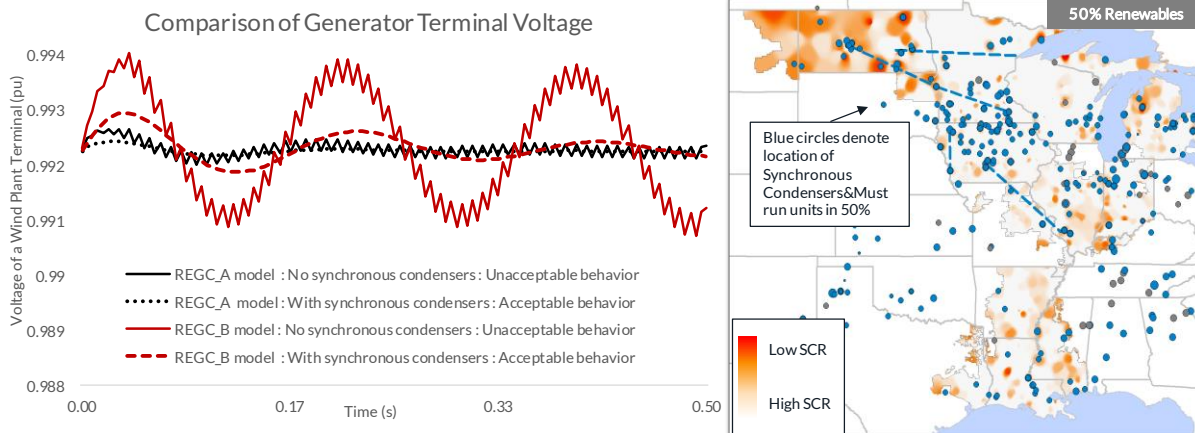


**Figure OR-DS-10: At 50% milestone system-wide installation of synchronous condensers may be required**

### Finding: Weak-grid stability: Summary of issues and solution

In summary, integration complexity to maintain reliability in weak areas rises sharply beyond the 20% milestone (Figure OR-DS-11), which creates a range of reliability issues. Short circuit ratio (SCR) decreases with an increase in inverter-based generation and reduction in fault current from conventional generation not being online. These dynamic instability issues can be solved by inverter-control-gain tuning, or by installing synchronous condensers, static var compensators (SVC), STATCOM, HVDC, or keeping more conventional generation online. Deployment of innovative new technologies such as properly tuned hybrid renewable resources, Type-5<sup>17</sup> wind, or grid-forming inverters can bring down the cost of additional transmission reinforcement required due to low SCR.

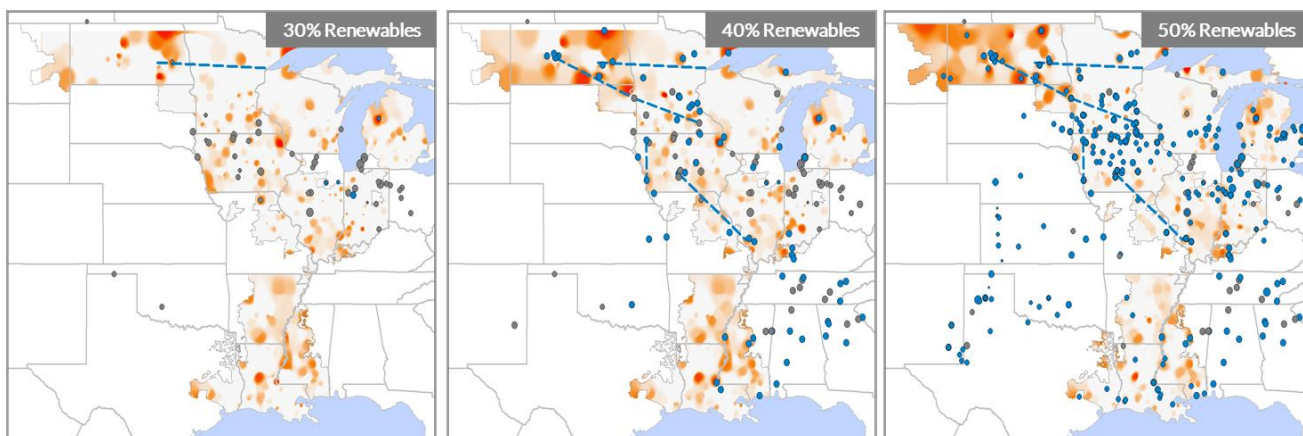


**Figure OR-DS-11: Weak area instability is the main driver of dynamic complexity**

<sup>17</sup> Type-5 wind technology concept has been around since as early as 2006, although it has not gained any significant commercial success. Other avenues are likely to be more successful (i.e. BESS, grid-forming inverter-based PV and Wind, and batteries etc.).



Finding: Frequency response is stable up to 40% renewable penetration\*, but at 50%, planned headroom is required to remain above Under Frequency Load Shed (UFLS) threshold.

Inertial and primary frequency response remains one of the major concerns, as frequency response in the Eastern Interconnection has been relatively steady but just slightly above adequate levels for several years (IEEE, NERC 2017,2018), and performance of MISO’s conventional resources during the primary frequency response period has been at adequate but not greatly above minimum compliant levels (refer to section -Operating Reliability – Dynamic Stability Focus Area). In addition, although renewable resources have the capability to provide frequency response and ramping, they cannot provide sustained response unless they maintain a certain amount of headroom by operating below their maximum possible power output. Thus, wind and solar resources need economic incentives or regulations adopted to “spill” energy to maintain headroom. Hence, the RIIA study assumes wind and solar will not preserve any headroom unless simulations identify the need.

Frequency response analysis was studied using dynamic models benchmarked with real-time measurements from MISO’s phasor measurement units (PMU) (Figure TA-30), improved governor modeling<sup>18</sup> and considering non-responsive behavior of MISO’s and EI’s existing conventional units (Figure TA-31). Further details, such as types of contingencies, method to calculate primary frequency response, EI and MISO’s BAL-003-1 obligations can be found in Technical Assumptions Summary – Operating Reliability – Dynamic Stability Focus Area.

RIIA finds that frequency response is stable up to 60% instantaneous renewable “system-wide” penetration but may require additional planned headroom beyond. As a rule of thumb, the highest instantaneous % of renewables in a given year can be near 2 times the annual renewable energy penetration level. The assessment indicates frequency response may be stable up to the 40% annual energy-wise renewable penetration milestone; however, certain hours at the 50% milestone can be at risk of load disconnection through automatic controlled action of Under Frequency Load Shedding (UFLS) protection schemes, which initiates if

---

*...frequency response may be stable up to the 40% milestone; however, certain system conditions at the 50% milestone can be at risk of load disconnection.*

---

frequency dips below 59.5 Hz in the Eastern Interconnect. The rise in risk can be primarily attributed to the displacement of conventional resources ( Figure OR-DS-13), which decreases the electric system’s inertia and available online headroom. For example, at lower milestones (like 10%), the highest instantaneous penetration is around 24%; this increases to 89% at the 50% milestone<sup>19</sup>. The composition of the fuel mix of 50% snapshot-3 ( Figure OR-DS-13) indicates the majority of the remaining 11% conventional units are comprised of nuclear units and a very small fraction of combined-cycle units. Nuclear units in the Eastern Interconnection are not assumed to provide primary frequency response, due to their normal operation being at maximum capacity, for efficiency. Gas-based units are also known for withdrawing their frequency response after a period of 30-35 seconds due to supplemental controls<sup>20</sup>. These conditions may lead to scenarios where the grid does not have sufficient primary frequency response to sustain tripping of a large generator or plant.

---

18 N.Mohan “Governor Modeling Improvement’, MISO MUG meeting 2017, available online [here](#).

<sup>19</sup> As a rule of thumb, the highest instantaneous % of renewables in a given year can be around 2 x annual renewable energy penetration level

<sup>20</sup> Several articles discuss the impact of “Outer-Loop Control” in Gas units. Refer to the following documents:

- (1) NERC, “Primary Frequency Response – Natural Gas/Combined Cycle Webinar”, November 13, 2018
- (2) NERC, “Reliability Guideline Application Guide for Modeling Turbine Governor and Active Power-Frequency Controls in Interconnection-Wide Stability Studies”, June 2019

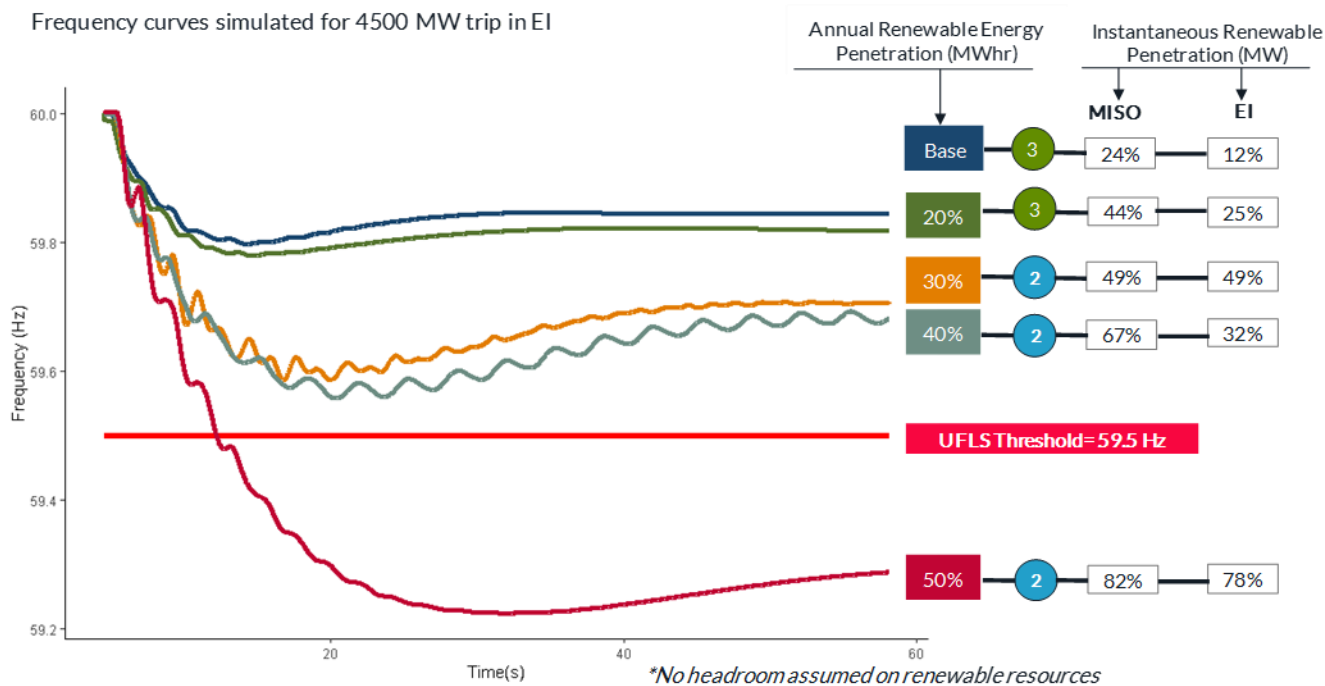


**Figure OR-DS-12: Frequency response curves for all milestones in RIIA**

Analysis indicates periods of low load with very high instantaneous penetration of renewables are most concerning, as described in the subsequent sections. To counteract frequency related risks, additional online headroom on resources (including wind and solar) can be procured in real-time grid processes to automatically respond without any operator intervention. Additionally, installation of fast response batteries can be also be done.

**Finding:** Periods of high renewable penetration during low load become important for frequency stability.

Frequency response analysis was conducted on various scenarios representing different system-wide load levels and instantaneous renewable penetration levels. These scenarios of high instantaneous renewable penetration can be divided into three main categories – (1) system wide near-peak load occurring in summer, (2) off-peak or low load conditions occurring in Spring, and (3) highest renewable output during low load hours occurring in the Fall months. The assessment shows the most concerning periods for frequency stability are scenarios 2 and 3, which can be explained by examining the composition of the types of generation (renewable versus conventional) at these scenarios and load levels ( Figure OR-DS-13).

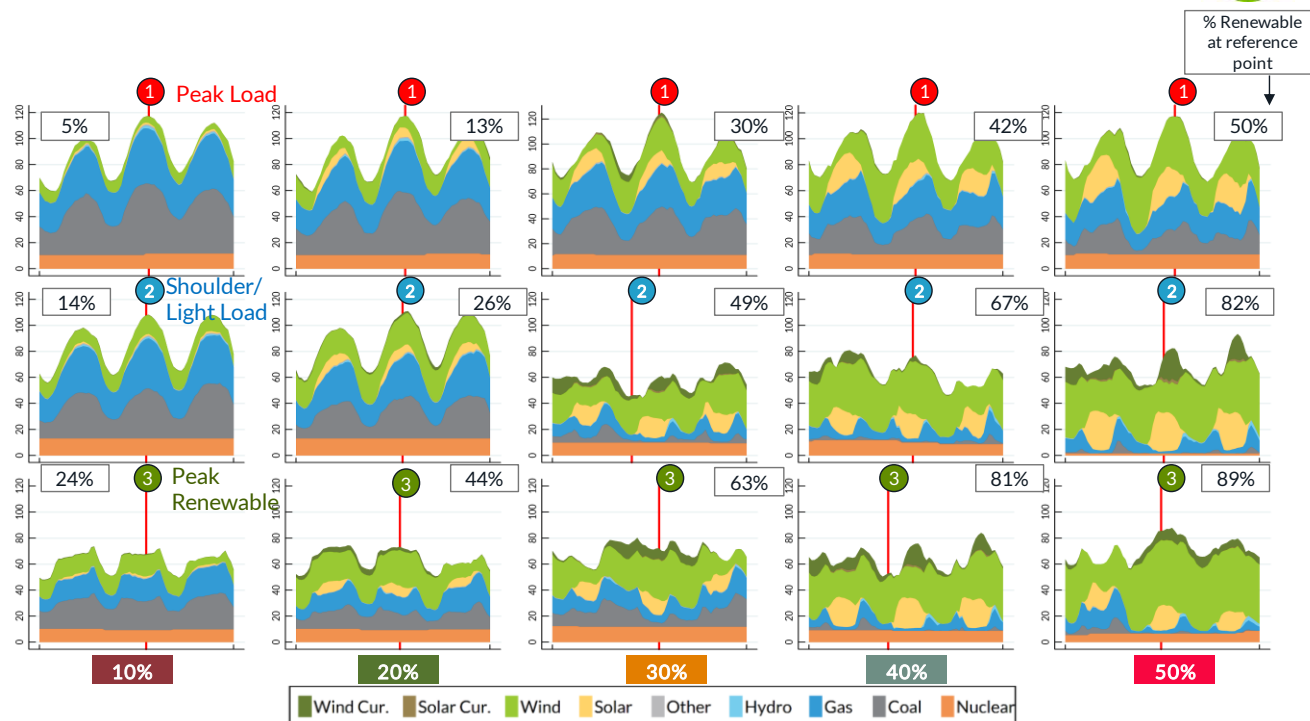


Figure OR-DS-13: Changing dispatch pattern and timing of stress on the transmission system

Even at higher RIIA milestones, the summer scenarios are characterized by relatively low penetration of renewables (2%-36% in EI), and more conventional units being committed, and a substantially higher load (>~95% of peak load). These conditions help maintain sufficient inertia and online headroom on the grid. It is worth noting

rotating loads also provide a stabilizing impact on frequency performance of the grid because those motor-loads (comprising a large share of the total electric grid) slow down after the sudden dip in the frequency post a generator trip, thus consuming reduced power and helping to support the grid. However, in scenarios 2 and 3, a combination of various factors such as (a) a very high amount of instantaneous renewable penetration, (b) low amount of conventional units and (c) lower amount of load result in conditions where frequency response diminishes rapidly, and load can be at the risk of automatic disconnection through the action of UFLS.

---

*A combination of various factors such as: (a) very high instantaneous renewable penetration, (b) few conventional units, and (c) lower load result in frequency response diminishing rapidly.*

---

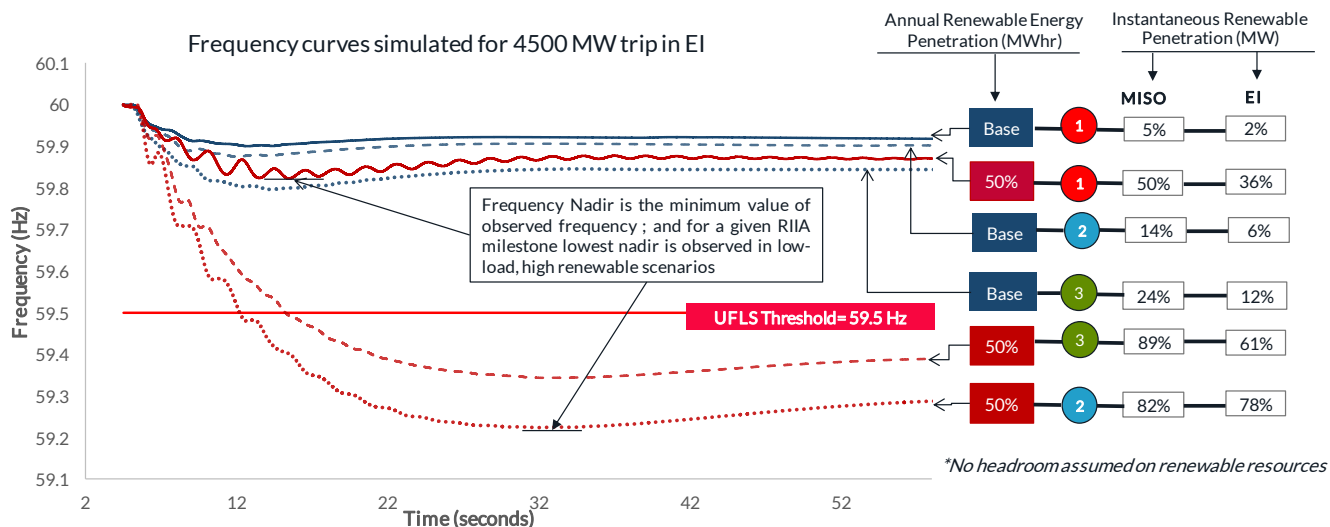


Figure OR-DS-14: Hours of high renewable penetration during low load become important for frequency stability

The trend of frequency nadir for all scenarios and simulated contingencies was plotted in Figure OR-DS-14. A significant finding revealed by assessment is the rapid reduction in system stability margin, particularly in the 50% milestone. For 50% scenario 2, it can be seen that following the loss of 2700 MW of generation (considerably lower than the largest simulated contingency of 4500 MW) frequency nadir is at the UFLS threshold of 59.5 Hz.

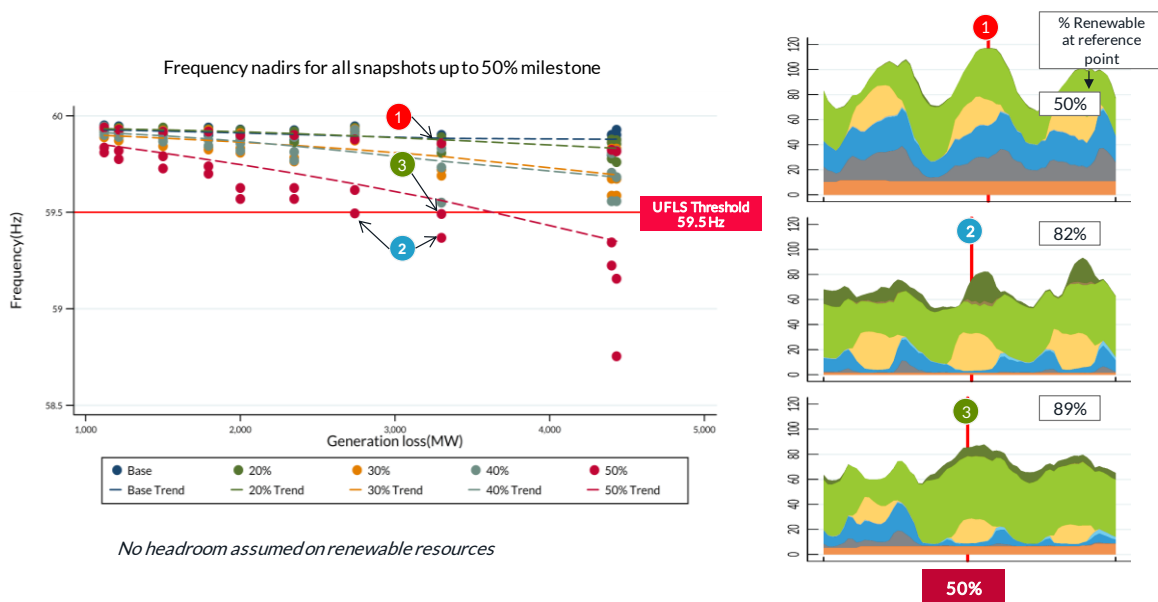


Figure OR-DS-15: Frequency nadir trend for all scenarios in RIIA

Finding: At higher renewable penetration, additional online headroom for primary frequency response may be needed to achieve NERC BAL-003 performance criteria.

NERC BAL-003-1 is the reliability standard requiring the grid operators to maintain primary frequency response, and it quantifies the performance of a synchronous interconnection (EI, WECC, Texas RE) by accounting for the amount of generation tripped and measuring average frequency deviation in the time period of 20-52 seconds



following tripping of a large generator<sup>21</sup> (Figure TA-27, Figure TA-28). The standard also determines a minimum performance threshold for Eastern Interconnection and individual Balancing Authorities such as MISO, PJM etc. The assessment indicates the average performance of MISO is satisfactory up to the 30% milestone; however, starting at 40% there can be a few hours in a year where MISO's BAL-003-1 performance may be marginally above the threshold (Figure OR-DS-16) for a large generator trip, and, rather unsurprisingly, performance dips below the threshold several times at the 50% milestone. The root cause of the degradation of performance is similar to factors described above – displacement of conventional units, and reduction in inertia and online headroom.

Similar to the frequency nadir trend, the assessment indicates periods of low load with very high instantaneous penetration are most concerning. BAL-003-1 performance can be improved if additional planned online headroom is preserved on any resource, including renewables or storage.

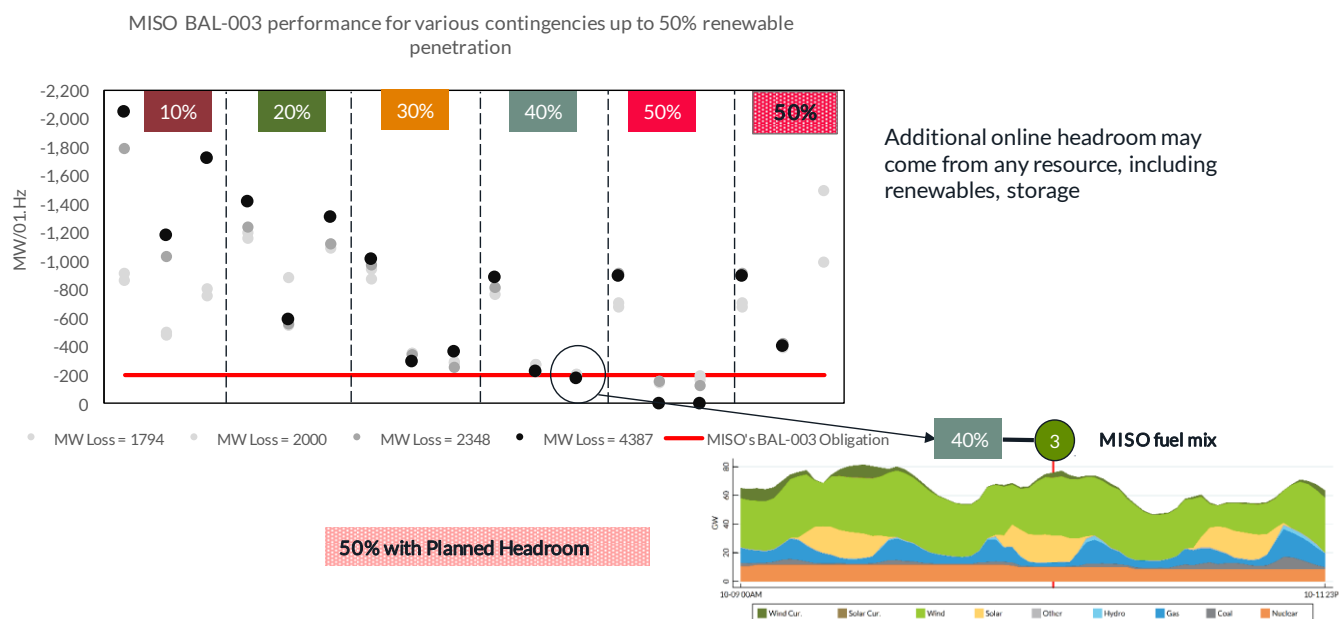


Figure OR-DS-16: MISO's projected trend per NERC BAL-003-1 requirement

Finding: Average primary frequency response for MISO and the Eastern Interconnection remains satisfactory at 50%; however certain hours are at risk for UFLS.

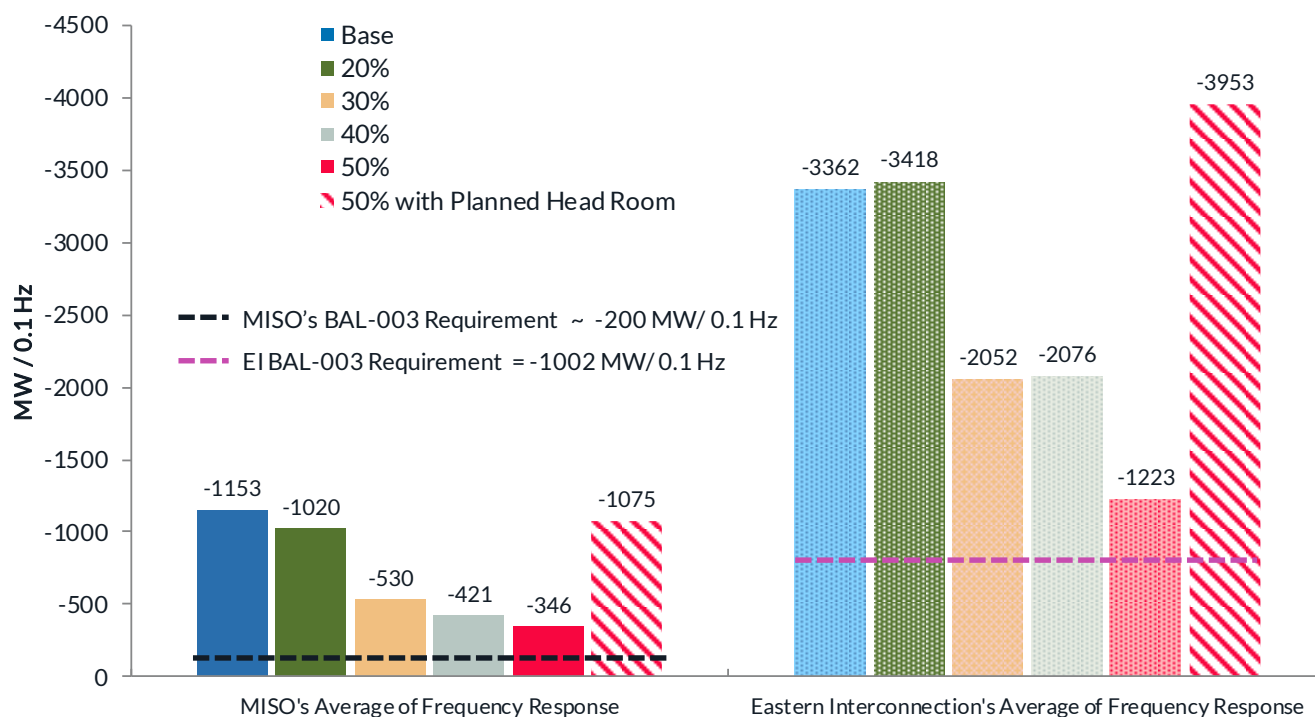
Currently, NERC evaluates the BAL-003-1 performance of the interconnection and Balancing Authorities by sampling data of several generator trip events from a year and averaging the calculated frequency response (FR) values for each event. The pass-fail criteria do not depend on any single event. The assessment indicates that the average performance of MISO and EI are satisfactory at all milestones studied in RIIA (Figure OR-DS-16); however, at the 50% milestone, there can be scenarios (as described on page 122) where load is at risk of automatic disconnection. While the current performance evaluation process may be suitable for the near future, the assessment points to a lacuna in the process stating averaging FR values may mask certain

*It may not be prudent to continue with the present BAL-003 evaluation process; instead, the industry may need to transform it proactively as further degradation in frequency response is observed.*

<sup>21</sup> Refer to Technical Assumption section for details. The units of primary frequency performance metric are MW/0.1Hz (MW per 1/10 of a Hz)



hours where EI is at high risk of losing load. This is analogous to considering a student graduated even though the person failed the mid-term exam, but shined in the finals, versus a student who consistently performed well through all the tests and passes with flying colors. Being a reliable grid-operator is like being a student who needs to perform well in all the tests. This raises an important issue to the grid operators and auditors; it may not be prudent to continue with the present BAL-003 evaluation process; instead, the industry may need to transform it proactively if further degradation in frequency response is observed.



Negative sign in Primary Frequency Response value indicates under-frequency event. Average performance in absence of planned headroom remains high largely due to good performance in Peak Snapshot and smaller generator (MW) trip events.

**Figure OR-DS-17: Eastern Interconnection and MISO's average BAL-003-1 performance**

**Finding:** Analysis with conservative model parameters indicates a primary frequency response inflection point lies between 30% and 40% milestones.

While a considerable amount of effort was put into developing dynamic models to produce realistic frequency response behavior (Figure TA-30, Figure TA-31) the assessment acknowledges some optimism may still be present in the frequency response results, due to a modeling issue discovered mid-way during the course of the analysis (Figure TA-32). Last

*Thus, the frequency response should be monitored, and future projections should be evaluated through improved modeling practices.*



year NERC released a report<sup>22</sup> discussing some of these issues in detail. As part of RIIA, a study was conducted to evaluate the impact on the validity of the RIIA frequency response results, and it indicated the need for planned headroom may arise at earlier stages i.e. 30% annual penetration level to meet BAL-003-1 obligations. Thus, the frequency response should be monitored, and future projections should be evaluated through improved modeling practices. Figure OR-DS-18 presents the difference between the original model parameters and the results following the change in settings.

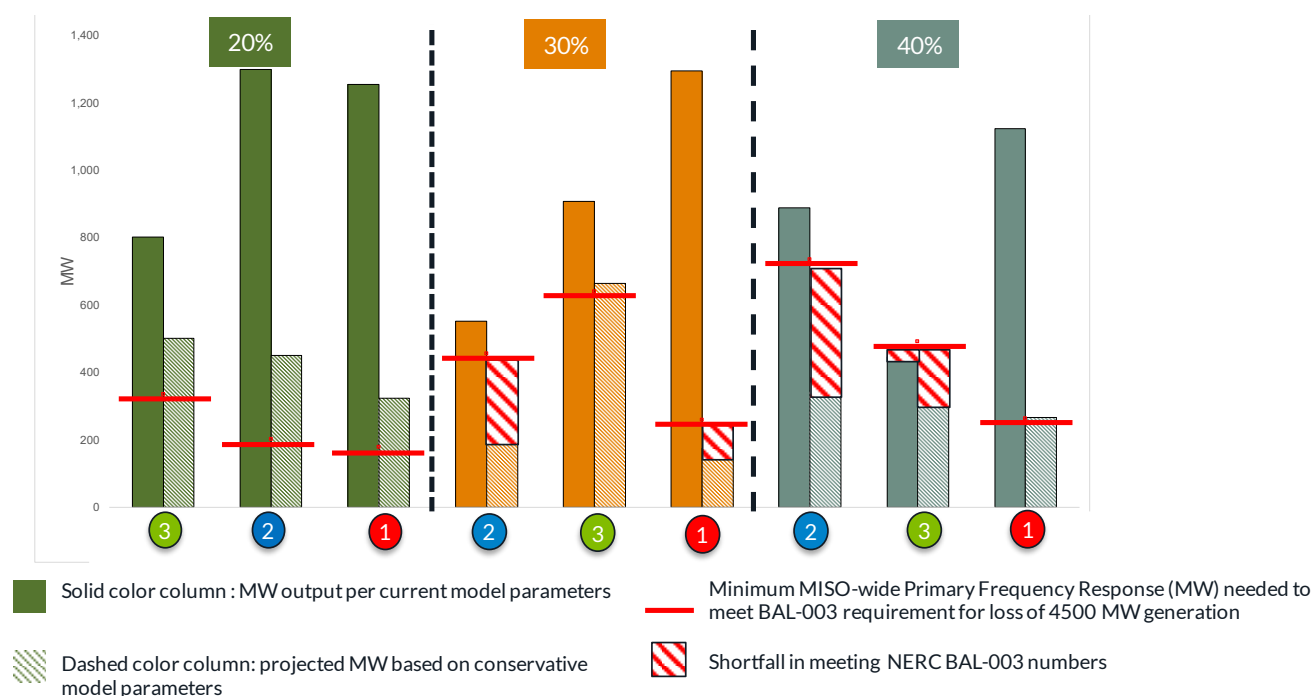


**Figure OR-DS-18: Estimation of optimism in RIIA’s BAL-003 analysis with conservative model parameters**

**Finding:** Linear prediction models show system conditions will be in the caution zone 5% of the time for 30% penetration and increase to 73% in 50% penetration.

RIIA assesses the impact of renewable penetration on the frequency response of the grid by studying three snapshots at each milestone (total 15 scenarios). To gauge the impact on the frequency response throughout the year with changing fuel mix, a linear regression model was developed to predict the frequency nadir throughout the entire year. Inputs to this model were system load (MW), total conventional generation (MW), and total renewable generation (MW) obtained from production cost simulations for every hour of the year (8760). For the purposes of this analysis, the zone between the nominal frequency of 60 Hz to an empirical value of 59.7 Hz (denoted by the green line) is chosen as a low-risk zone, the zone between 59.7 Hz to the UFLS frequency threshold of 59.5 Hz is defined as the caution zone (zone between green and red color), and the zone below 59.5 Hz is automatic tiered load-shedding zone (denoted by red color, a zone of operation to avoid).

22 NERC Reliability Guideline: “Application Guide for Modeling Turbine-Governor and Active Power Frequency Controls in Stability Studies”, June 2019

[https://www.nerc.com/comm/PC\\_Reliability\\_Guidelines\\_DL/Reliability\\_Guideline-Application\\_Guide\\_for\\_Turbine-Governor\\_Modeling.pdf](https://www.nerc.com/comm/PC_Reliability_Guidelines_DL/Reliability_Guideline-Application_Guide_for_Turbine-Governor_Modeling.pdf)



Analysis indicates that as the penetration increases, the number of hours of system conditions which are in the caution zone increase from 5% of the time in 30% milestone to 73% in the 50% milestone, and several hours are at the risk of automatic disconnection due to UFLS in 50% (Figure OR-DS-19).

A similar exercise was done for MISO's BAL-003-1 performance; however, results are less concerning partly due to the reasons discussed on page 126 (averaging the performance may be leading to underestimating the issue).

*Analysis indicates as the penetration increases, the number of hours of system conditions in the caution zone increase from 5% of the time in the 30% milestone to 73% in the 50% milestone, and several hours are at the risk of automatic disconnection due to UFLS in the 50% milestone.*

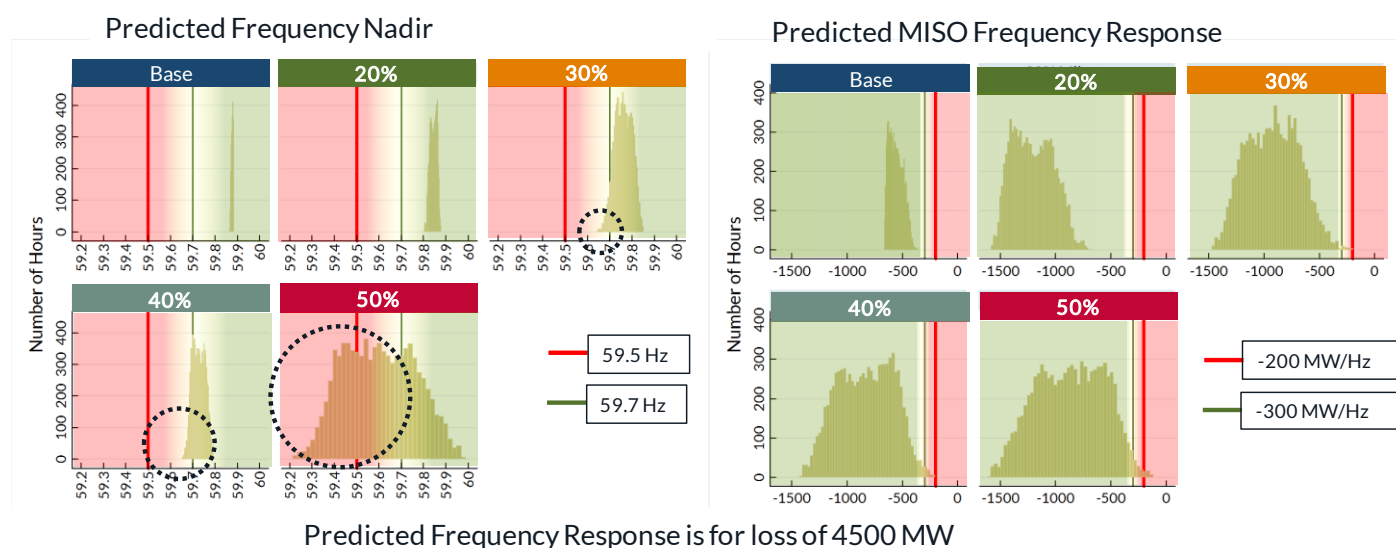


**Figure OR-DS-19: Output of linear prediction model output to estimate frequency performance for 8760 hours of system conditions will be**

**Finding:** Frequency response is stable up to 60% instantaneous renewable penetration but may require additional planned headroom beyond.

RIIA discusses the impact on the frequency response in terms of annual renewable energy penetration (10%, 20%, 50%, etc.). Rather, instantaneous renewable penetration is a superior metric to annual energy, as the frequency of the grid is maintained on a real-time basis for every second, every minute, and grid operators and planners are more concerned about real-time wind and solar output. Thus a few natural questions arise as follow.

- (1) Since assessment denotes 50% annual renewable penetration is concerning, could there be periods in 40% or 30% milestone where frequency response may have been inadequate?
- (2) Is there a way a better metric could be developed to track frequency nadir trend?

A study was conducted to draw a relationship between instantaneous renewable penetration and frequency response by utilizing the linear regression model described on page 128. The plot of frequency nadir against all possible ranges of instantaneous renewable penetration within each RIIA milestone is shown in Figure OR-DS-20.



For example, the instantaneous renewable penetration at the 30% milestone ranges from as low as ~10% to as high as 60% in MISO. The corresponding range of frequency nadir based on system conditions range from 59.8 Hz to 59.6 Hz, which is also the first time the predicted frequency nadir trend enters into the caution zone.

Thus, analysis provides long-term situational awareness to grid-operators and planners that starting at the 30% milestone they would need to:

- Prepare for the operations of the future
- Modify infrastructure
- Update processes to maintain stable frequency response

Another important finding this analysis points to is the rate at which frequency nadir trend declines due to increasing renewable energy penetration; for a 30% energy penetration system, 60% instantaneous scenarios look quite different from the 60% instantaneous scenarios in a 50% energy-wise system.

The former scenario (60% in 30% milestone) indicates minimum predicted frequency nadir dropping to 59.6Hz, thus entering in the “caution-zone”. In the latter scenario (60% instantaneous in 50% milestone), the minimum predicted frequency nadir slides to “automatic-load-shedding-zone” and at a much higher speed, denoted by a higher slope of the line.

---

*Frequency can be stable up to 60% instantaneous system-wide penetration and may need additional planned headroom beyond that 60% value.*

---

These results can be explained by examining the dispatch pattern at the two milestones. In the 30% renewable energy penetration system, at 60% instantaneous renewable penetration, the RIIA study indicates some coal, gas, and nuclear units are still committed ( Figure OR-DS-13). However, in 50% energy system, during 60% instantaneous penetration, the majority of the thermal units have been displaced or retired, and only a few nuclear units and combined-cycle units are expected to be committed. Thus the overall system inertia-wise becomes “very light,” which leads to faster degradation of frequency nadir performance.

Lastly, given all the analyses performed, parameters considered, and some remaining optimism in modeling, RIIA concludes instantaneous renewable penetration should be used to monitor frequency response, and further arrives at the conclusion that frequency can be stable up to 60% instantaneous system-wide penetration, but may need additional planned headroom beyond that 60% value. However, electric storage can change the conclusion about the “60%” number given that it was not considered in the simulations for the above results. The application of electric storage can significantly improve and preserve the frequency response trend (both primary and nadir) and is discussed in the following sections.

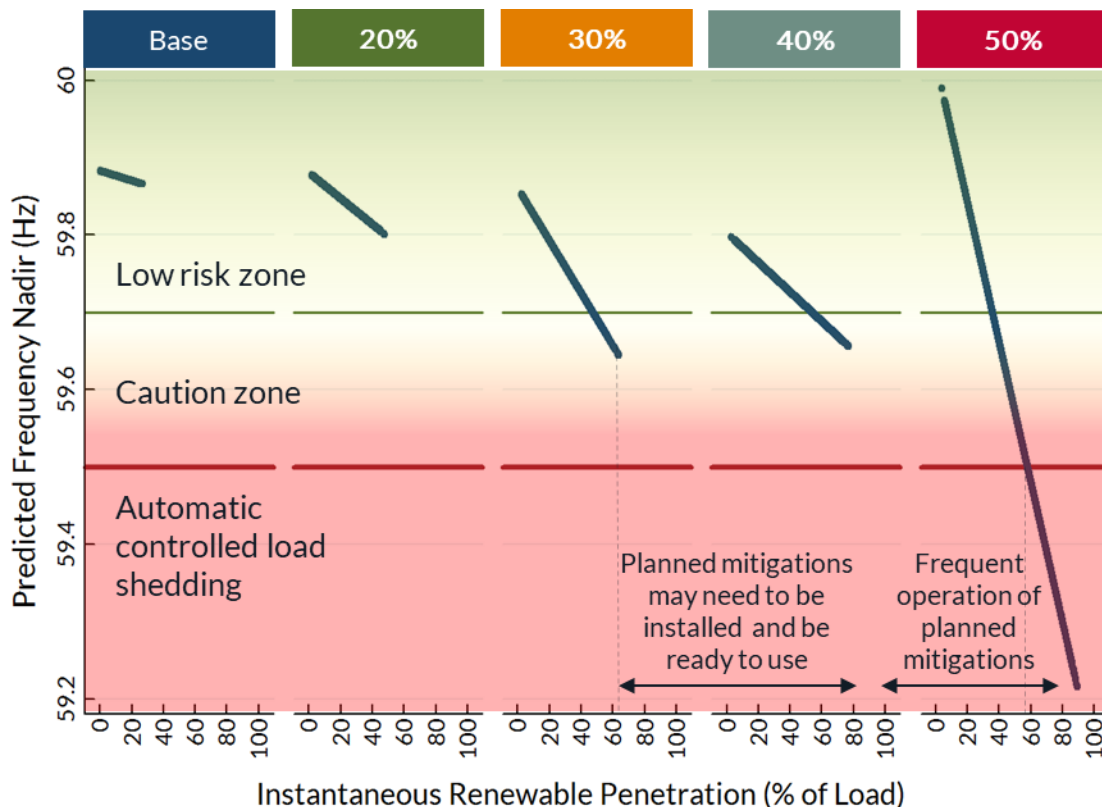


Figure OR-DS-20: Predicted frequency nadir across all RIIA milestone for 8760 hours of different system dispatch

Finding: Online available curtailment may be utilized to mitigate frequency response issues at certain hours but...

RIIA explores several techniques to resolve frequency response issues. Energy adequacy simulations indicate curtailment could be used for congestion management, particularly at higher milestones (Figure EA-1). Wind and solar resources can provide primary frequency response, even if they are curtailed due to congestion. Snapshot 2, Figure OR-DS-13, from the 50% milestone indicated approximately 80 GW of wind and solar may be curtailed (Figure OR-DS-21) in the Eastern Interconnect.

*Battery storage may be needed to ensure sustained frequency response at very high instantaneous penetrations.*

The production cost simulations indicated some of the wind farms can be curtailed down to zero MW output<sup>23</sup>. A wind farm owner informed the RIIA team that if a dispatch signal from an RTO or ISO is sent to the wind farm to operate near 0 MW, then roughly 15% of the turbines remain online and produce ~0 MW, and the remaining 85% of the turbines may be shut off. However, for primary frequency response, generation resources are needed on a “hot-stand-by”, meaning they should be online and ready to inject power automatically. Considering all these factors, a conservative assumption was made that out of the 80 GW curtailment, only 30 GW of headroom could be utilized for frequency response.

<sup>23</sup> These results were validated against historical data which indicated that some wind farms in MISO were also curtailed down to near zero output to manage short periods of congestion, particularly during periods of very high system-wide wind output.



Results indicate frequency response is stable (Figure OR-DS-21) if renewables carry 30 GW of headroom for the 50% milestone; less may be needed for milestones less than 50%. To pragmatically implement curtailment as a solution to provide support during frequency response, RTOs and ISOs need to develop tools to obtain visibility on the amount of curtailed renewables (particularly wind) available online in the system.

However, the scenario-3 from the 50% milestone simulation indicates that banking on online curtailment only is insufficient to remedy frequency response issues at other hours. More on this follows.

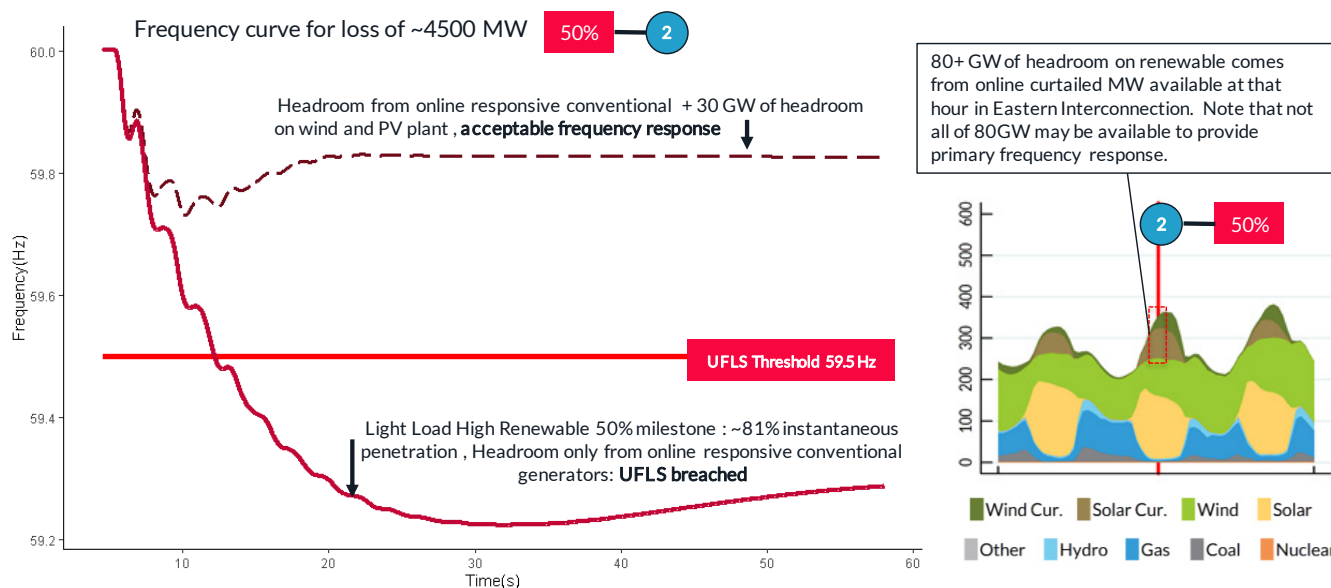


Figure OR-DS-21: Headroom from curtailed renewables can be used to provide frequency response

Finding: Battery storage may be needed to ensure sustained frequency response at very high instantaneous penetrations

The simulation of both scenarios 2 and 3 at the 50% milestone indicates potential frequency stability issues following the simultaneous tripping of 4500 MW generation. Similar to the approach described in the previous page, the curtailed renewable resources were assumed to be frequency responsive, with a difference that all of the 14 GW of headroom on renewable units is assumed to be available for frequency support (which is a very optimistic assumption). The simulations unearth some very interesting complications. Initially, the frequency response of the red dash-dot curve seems to be recovering after tripping the 4500 MW of generation; however, during the period of 30-35 seconds following the trip, frequency declines and slides back to settle near the UFLS level. This kind of performance is unacceptable, as it does not demonstrate a “sustained” frequency response in the defined 20-52 second window. Upon investigation, it was found the decay can be attributed to two major factors -- (a) the majority of conventional units are gas-fueled, and these units withdraw their response either due to hitting equipment limits, or due to outer-loop controls described on page 129, and (b) the real-power output of some renewable units in weak areas starts to decline as the voltage gradually decreases to a value lower than ~0.8 pu following the generation loss causing low voltages -- renewable units hit limits of their maximum current injection into the grid as they struggle to stabilize voltage and frequency simultaneously.

To remedy these complications, 6 GW of batteries in EI (600 MW in MISO) were modeled, and subsequent frequency response was found to be stable (maroon dashed line on Figure OR-DS-22). The application of batteries drastically improves the frequency nadir, as batteries inject power at a very high rate into the grid with almost no delay, given they have control systems to support this.

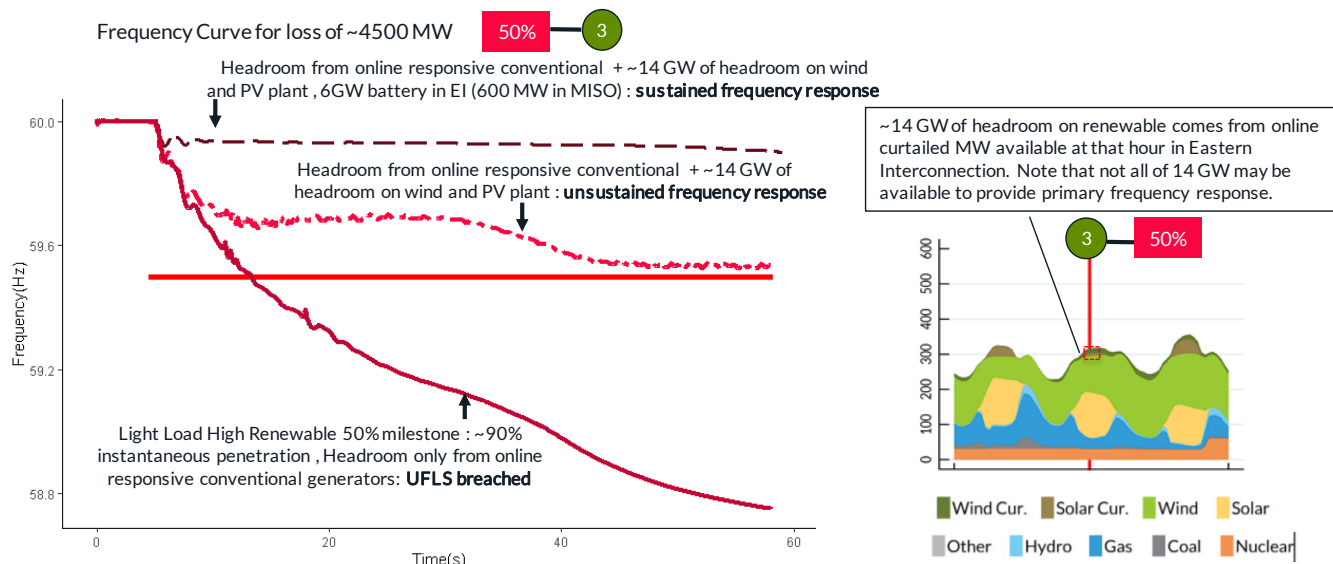


Figure OR-DS-22: Batteries storage can provide frequency response during system conditions of low curtailment

Finding: Large scale stability issues may occur due to displacement of units with power system stabilizers operating

Of all the challenging phenomena and issues discovered in RIIA, perhaps the most interesting and somewhat surprising finding was the observance of small-signal inter-area oscillations at 30% milestone, particularly for one contingency in one snapshot only (Figure OR-DS-23). Small-signal inter-area issues are low frequency (~0.1 Hz to 0.8 Hz) oscillatory behavior of several interconnected generating machines (dynamic devices). Any given frequency of oscillation is called a “mode”. There can be several “modes” in an electric system. A well damped mode (damping ratio  $\geq 5\%$ ) does not create any reliability issues. Historically, small-signal stability has been a major concern in the western part of the United States (WECC) and has been extensively studied. On the other side, EI is also known to have certain modes that can initiate large-scale issues impacting the whole interconnection due to small-signal instability; however, these modes are generally well-damped and are not problematic. When inter-area small-signal stability issues show up in real-time, they are difficult to mitigate, as wide-area coordination between different grid-operators is needed. The non-availability of any real-time tool to pinpoint to the root cause adds to the complexity. The NERC report<sup>24</sup> pointed out the challenges faced to mitigate inter-area stability in EI in 2019.

The report states: “RCs [Reliability coordinators] were aware of the oscillation event relatively quickly by using both SCADA data and advanced applications and PMU measurements. RCs sought coordination activities, including use of the RC hotline; however, the RC hotline was inoperable due to technical issues. RCs were forced to call neighboring RCs individually that led to misinformation and mischaracterization of the event initially. Wide-area operator action did not contribute to mitigating the oscillation event, and most tools were ineffective at identifying a source location for the oscillation”.

<sup>24</sup> The most recent small-signal inter-area stability issue occurred in EI in Jan 2019 where a generator in Florida initiated a 0.25 Hz (mode) oscillation across the EI. Refer NERC, “Eastern Interconnection Oscillation Disturbance January 11, 2019 Forced Oscillation Event”, released December 2019, available online [here](#).



To remedy small-signal inter-area issues, numerous conventional units are equipped with a supplemental control system called power system stabilizer (PSS), that counteract the inter-area oscillations. The impact of inter-area small-signal stability issue is on a large-scale i.e. interconnection-wide. For example, the 30% milestone shows MISO may observe 700 MW peak-to-peak oscillations on its tie-lines due to this phenomenon(Figure OR-DS-23). The assessment indicates the problem progressively worsens at the 40% milestone as three more “modes” enter the poorly-damped region and became severe at 50% to the point that dynamic stability models would exhibit undamped oscillations for a no-disturbance test (Figure OR-DS-24). The root cause of inter-area oscillations observed is the displacement of thermal units with PSS installed due to the dispatch of renewables. To verify this hypothesis, the RIIA study was performed on unmitigated models using SSAT<sup>25</sup> on all the 15 snapshots. The study indicated that, starting at the 30% milestone, certain modes may have damping less than 5%, which can lead to interconnection-wide issues. The study also indicated that renewables did not contribute to this issue; however, certain Synchronous Condensers, added as mitigation, participated in the oscillations, thus making matters worse.

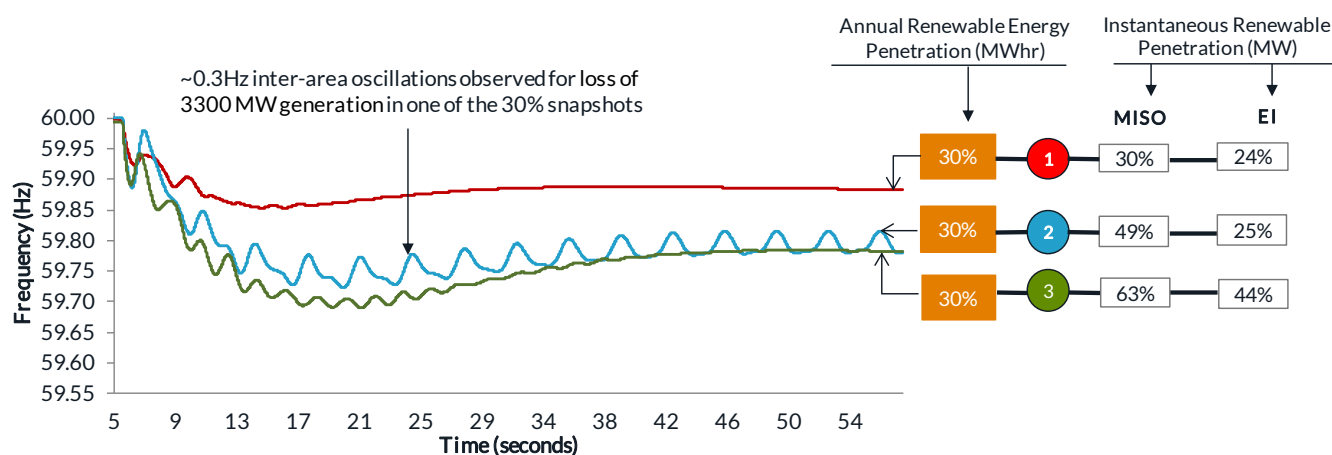


Figure OR-DS-23: Inter-area small signal stability issues observed in low-load high renewable in 30% milestone

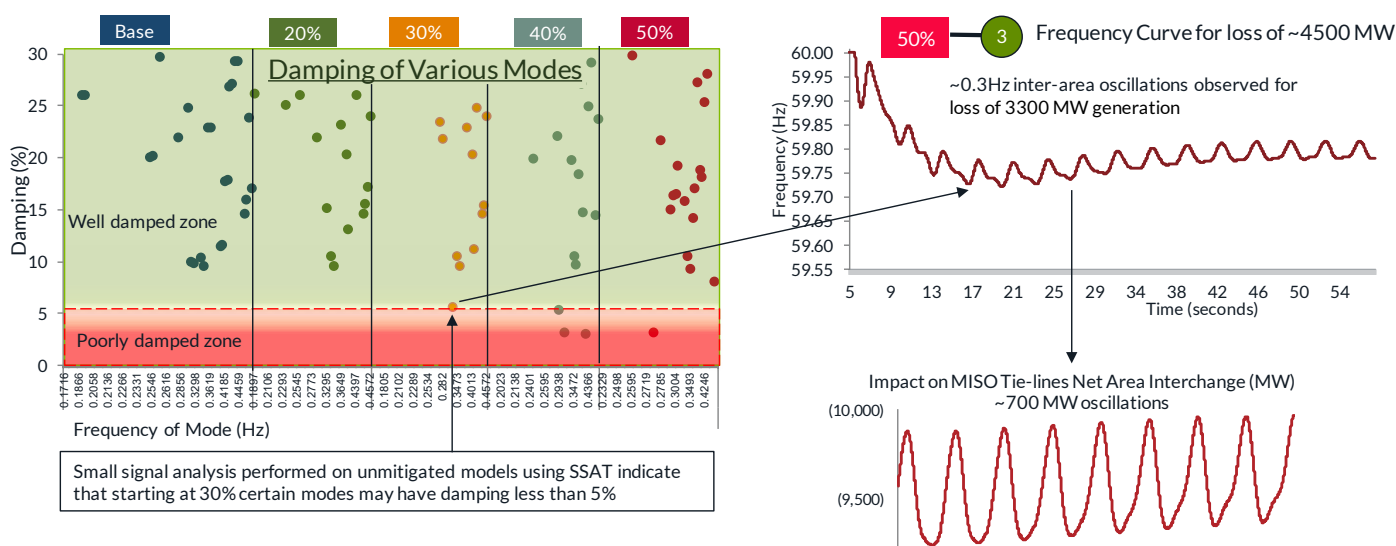


Figure OR-DS-24: Trend of damping of inter-area small-signal stability modes for all RIIA milestones

<sup>25</sup>SSAT is a tool produced by PowerTech Labs which helps determine the root cause of small-signal inter-area instability, modes, and units contributing to the issue.



## Finding: Various techniques can be utilized to mitigate frequency and small-signal stability issues simultaneously

There are various methods to mitigate small-signal stability issues. The first method can be to study the network conditions and ensure the units with PSS installed are committed in real-time operations. For example, the analysis indicated to mitigate instability due to small-signal issues at the 50% milestone (maroon color line with 1600 PSS ON in Figure OR-DS-23), turning on at their minimum output 100 additional thermal units with PSS installed, combined with 14 GW of headroom on renewable was sufficient to completely address both frequency response and small-signal stability issues (light green color line in Figure OR-DS-23). However, such a study and practice would involve a close coordination among all grid-operators in EI.

The assumption that grid-operators may be able to turn on the units with PSS has some practical limitations -- some of the units could be unavailable due to maintenance, or even could have retired. An alternative is to install specially tuned batteries across the entire EI. The study indicates that 7.2 GW of battery with small-deadband ( $\pm 10$  mHz compared to  $\pm 36$  mHz traditionally used in EI) and high droop (126 compared to 20 traditionally used in EI) can provide a sustained frequency response (blue color line in Figure OR-DS-25) and damp-out small-signal oscillations. Such storage devices can operate automatically, thus minimizing the challenges stated above.

When small-signal inter-area stability issue appear in real-time, they are difficult to mitigate, as wide-area coordination between different grid-operators is needed. The non-availability of any real-time tool to pinpoint the root cause adds to the complexity. Per the NERC report pointing out the challenges faced to mitigate inter-area stability in EI in 2019 - "RCs [Reliability coordinators] were aware of the oscillation event relatively quickly by using both SCADA data and advanced applications and PMU measurements. RCs sought coordination activities, including use of the RC hotline; however, the RC hotline was inoperable due to technical issues. RCs were forced to call neighboring RCs individually leading to misinformation and mischaracterization of the event initially. Wide-area operator action did not contribute to mitigating the oscillation event, and most tools were ineffective at identifying a source location for the oscillation".

In summary, RIIA concludes the following regarding small-signal inter-area oscillations:

- Small signal stability issues may arise at higher renewable penetration levels
  - Renewable generation displaces conventional generators and creates different dispatch patterns.
  - Conventional units installed with Power System Stabilizers (PSS) may not be committed or could retire, which decreases the damping effect.
  - Must run operations of units with PSS may be needed or new PSS may be installed to increase damping.
- Currently, renewable resources are not known to have the capability to arrest inter-area oscillations in the range of 0.1-0.8 Hz, and it is uncommon to install PSS on Synchronous Condensers. Through detailed analysis, strategic locations can be identified where installing appropriately tuned and designed supplemental power oscillation damping (POD) controller on renewable resources, batteries, SVC, STATCOMs, or HVDC can help to improve small signal stability. Hence, RIIA makes a recommendation to



the renewable resource owners (including electric storage) and dynamic device manufacturers to facilitate addition of POD controller to mitigate such issues in the future.

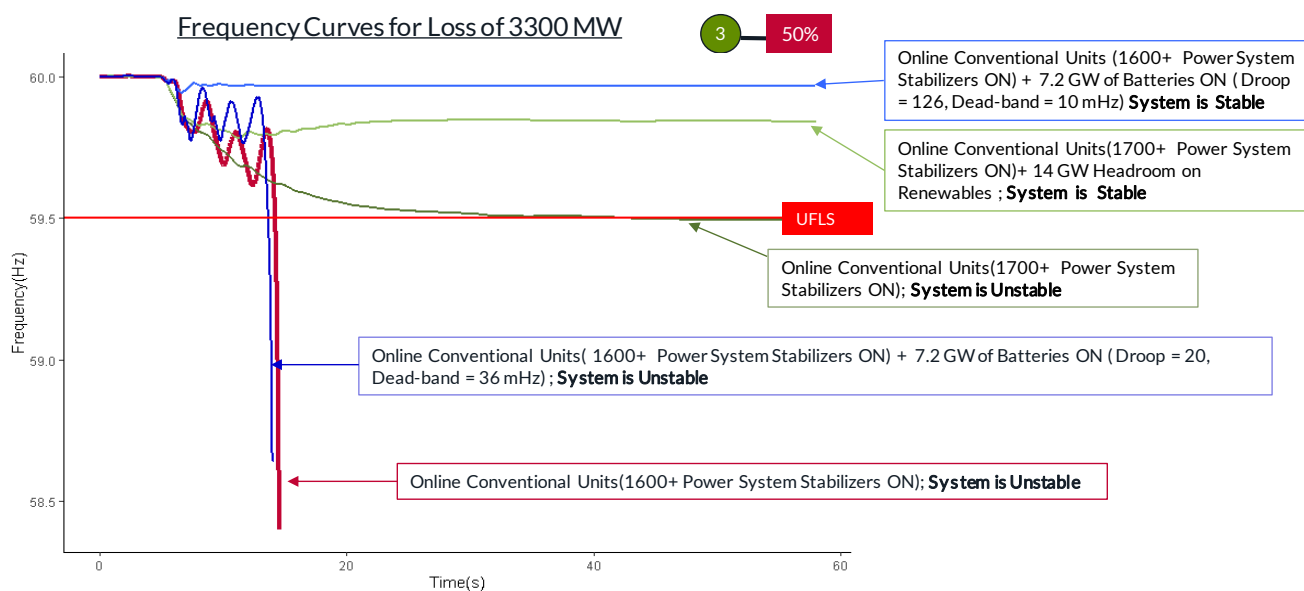


Figure OR-DS-25: Different techniques used to mitigate inter-area small signal stability issue

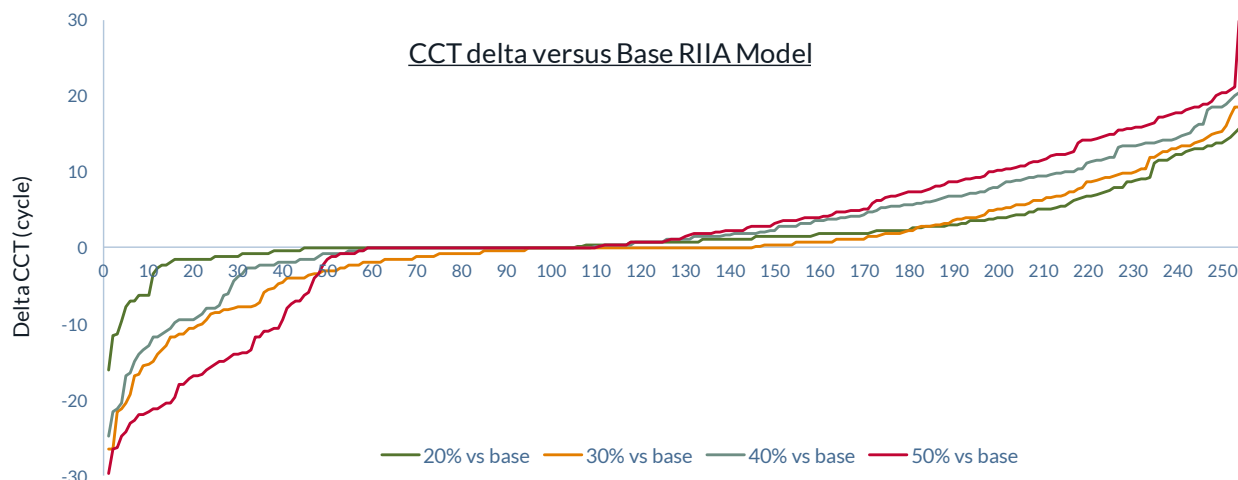
Finding: Overall, CCT increases as renewable penetration increases but may decrease at certain locations at very high instantaneous penetration

To evaluate the impact of renewable penetration on the rotor angle stability of conventional rotating machines (thermal and hydro) a study was performed to calculate the safety margins by calculating critical clearing time (CCT) at each milestone. The study utilizes the same snapshots, and tools used for frequency response analysis. The study utilizes the same snapshots and tools used for frequency response analysis. A sub-group of contingencies (270) utilized in MTEP<sup>26</sup> planning process was used to evaluate CCT. Thus, utilizing 3 snapshots at each milestone, minimum CCT for each of 270 contingencies valid in the RIIA models was calculated, and difference from the minimum base CCT was calculated. The trend (Figure OR-DS-26) indicates that overall, CCT increases as renewable penetration increases; however, certain geographical locations witness a decrease in CCT at the 50% milestone<sup>27</sup>(Figure OR-DS-27). The following section discusses one of the reasons contributing to the increase in the CCT.

Significant decrease in CCT can cause problems in protecting circuits following disturbances, as the relaying and breaker-opening times may be greater than the CCT needed to keep the system from becoming unstable and causing widespread loss of load.

<sup>26</sup> Refer to MISO, "Determining Material Changes in Stability Between Planning Scenarios", available online [here](#).

<sup>27</sup> A study performed by EirGrid and System Operator of North Ireland found a similar impact on CCT due to increase penetration of wind. Refer to "Ensuring a Secure, Reliable and Efficient Power System in a Changing Environment", available online [here](#).



- Graphs represent the delta in CCT between Base and 20%, 30%, 40% scenarios
- Total of 270 disturbances were simulated

**Figure OR-DS-26: Trend of CCT for all RIIA milestone**

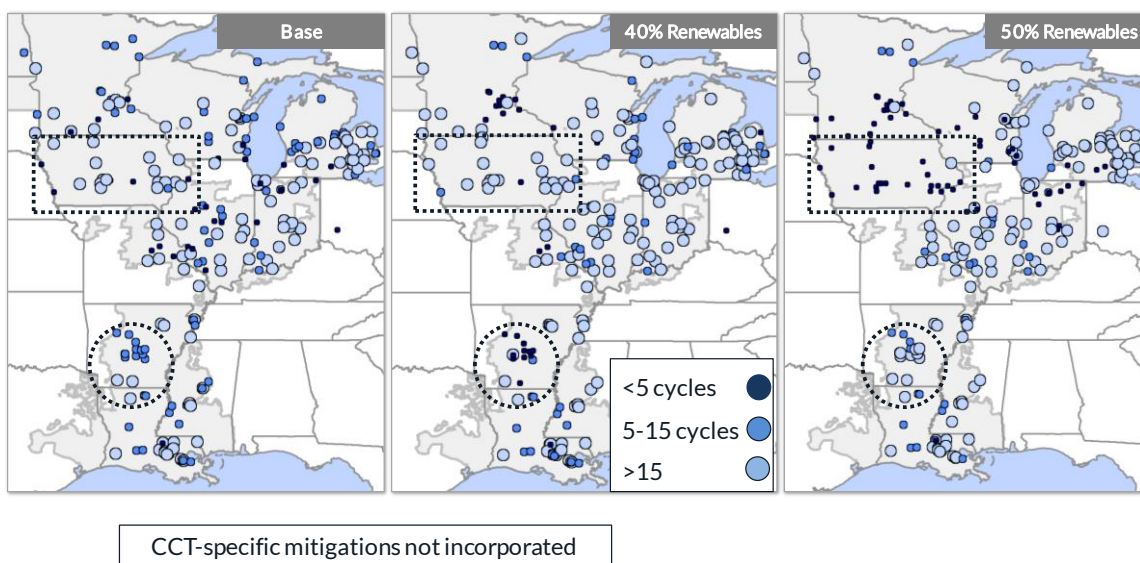


**Figure OR-DS-27: Geographical trend of CCT for RIIA milestone**

**Finding:** CCT increases are due to displacement of large units

The generation output of Energy Adequacy results indicates as renewable penetration increases, conventional units will be generally dispatched down, and few thermal units will be committed. Based on this result a hypothesis is proposed that the increase in CCT can be attributed to the general trend that conventional units will be dispatched down or will be turned off. To test this hypothesis, a study was performed on 2 conventional units, one in the northern part of MISO, the other in southern footprint, and impact on CCT of nearby units utilizing contingencies in the local area near those units was calculated under two scenarios as listed in Table OR-DS 1. The results confirm the hypothesis that CCT of nearby units increases when the test unit is turned off, versus when the test unit was



dispatched at maximum output (Figure OR-DS-28). Further, results confirm that due to local network topology, CCT of some nearby units may decrease as can be observed from the CCT trend in MISO south.

Test Unit Location	Scenario	Power output
North	1	Maximum Generation
	2	Turned Off
South	1	Maximum Generation
	2	Turned Off

Table OR-DS 1 Scenarios to study the impact on CCT of near-by units due to dispatch of a thermal generation

Delta CCT with large thermal units off vs at P-max/ cycles 40% 2

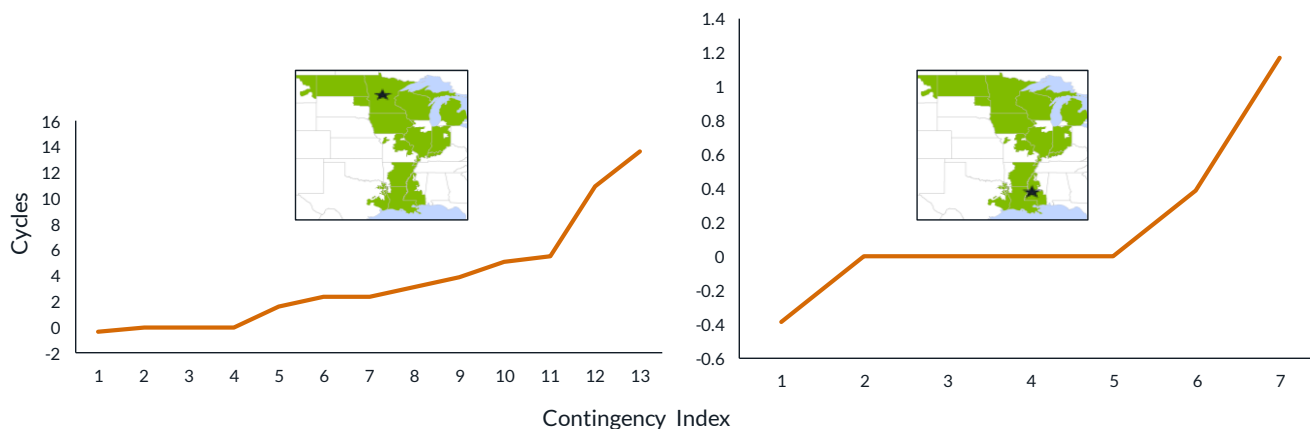


Figure OR-DS-29: Dispatch of thermal units impacts the CCT of nearby units



# Technical Assumptions Summary

The technical assumptions summary serves as a detailed summary of the data, methods and process used for the Renewable Integration Impact Assessment (RIIA) analysis.

The primary purpose of the Renewable Integration Impact Assessment (RIIA) is to methodically find system integration inflection points driven by increasing levels of renewable generation. Industry studies<sup>28</sup> have shown that the complexity for renewable integration escalates non-linearly with increasing penetrations of renewables. Over certain ranges of renewable penetration, complexity is constant when spare capacity and flexibility exist, but at specific penetration levels when they are depleted, complexity rises dramatically. These are system inflection points, where the underlying infrastructure or system operations need to be modified to reliably achieve the next tranche of renewable deployment. This assessment aims to find those inflection points and examine potential solutions to mitigate them.

This assessment is designed to be “year agnostic” in that it does not intend to develop pathways for achieving high levels of renewable penetration, but instead intends to examine system conditions under renewable penetration levels assumed to have been reached in any year. The assessment does not attempt to develop an optimal resource mix, and the generation changes in the model are assumed to occur regardless of external drivers and timelines.

---

*This assessment is designed to be “year agnostic” in that it does not intend to develop pathways for achieving high levels of renewable penetration, but instead intends to examine system conditions under renewable penetration levels assumed to have been reached in any year.*

---

These technical assumptions section discusses the details of data and processes used in the three focus areas that comprise RIIA. The RIIA concept paper provides a detailed explanation of the assessment background, goals and structure. Together these two documents serve as the scope of work for the assessment.

## Process

The RIIA process is made up of three focus areas: (1) Resource Adequacy, (2) Energy Adequacy and (3) Operating Reliability. Resource Adequacy is defined as the ability of available power resources to reliably serve electricity demands when needed across a range of reasonably foreseeable conditions. This focus area assesses changes in renewable resource capacity credit by calculating the Loss of Load Expectation (LOLE) and the Effective Load Carrying Capability (ELCC). Energy Adequacy looks at the ability of a system to be operated continuously. This involves analysis of ramping, over/under production, capacity factors, coordination, operating reserves and congestion. Operating Reliability studies the ability of the system to withstand sudden disturbances to system stability or unanticipated loss of system components. This focus area will look at voltage support, thermal overloads, dynamic stability issues such as voltage, inverter-driven, rotor angle and frequency stability.

These three focus areas flow together in a complex and robust process (Figure TA-1).

---

<sup>28</sup> The RIIA concept paper includes a detailed list of relevant industry studies.

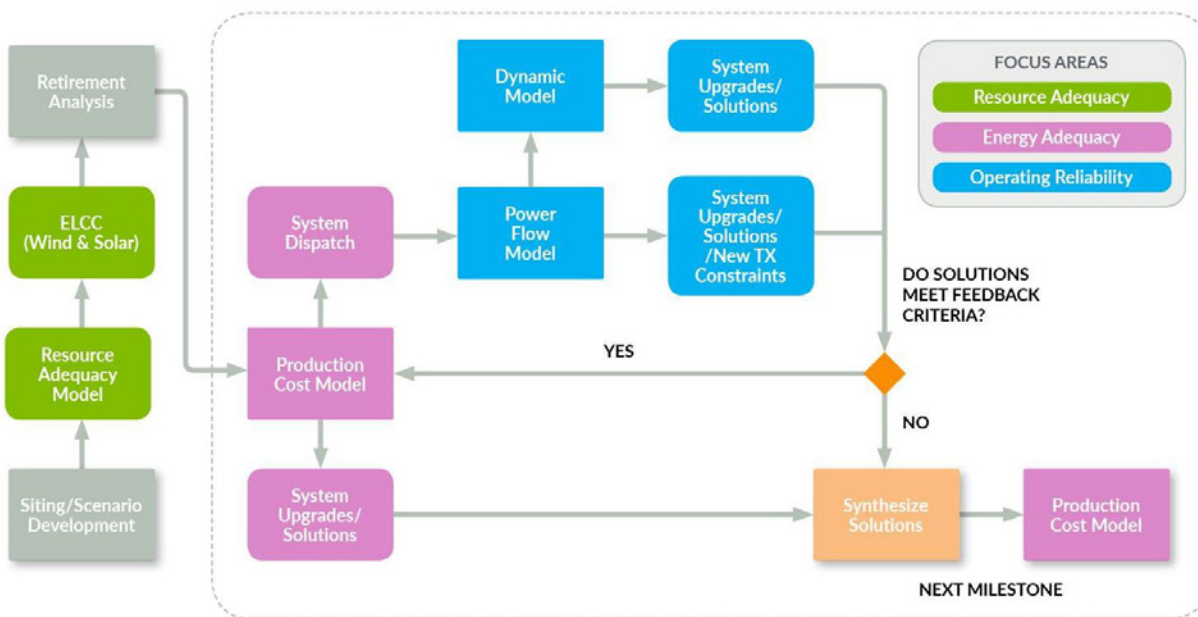
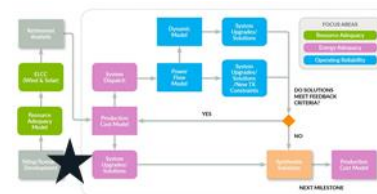


Figure TA-1: RIIA process map

First, scenarios are designed for use throughout the entire assessment. The scenarios represent different levels of renewable energy penetration that increment in 10% intervals, or milestones. Wind and solar resources are added and sited in each model region (MISO, PJM, NYISO, etc.) such that each region meets the desired milestones as seen in the next section. (Page 141). The first focus area, Resource Adequacy, then analyzes the system with the added resources to determine their ELCCs at each milestone. (Page 159). These values are used to determine the appropriate amount of retirements (page 164) to ensure the system is not over or under built. Once the expansion and retirements are determined, Energy Adequacy models are built and analyzed. Energy Adequacy (page 166) uses a production cost model for its analysis, which produces a full year of hourly dispatch based on the constraints present. Several hours of this dispatch are selected for study in the Operating Reliability focus area (pages starting 178 and 184) and the dispatch is passed from the production cost model to the power flow model and the dynamic model. These models assess the reliability of the system during the selected stressful hours. If any of the focus areas encounter problems preventing the reliable operation of the system that need to be addressed, solutions are developed and passed along to subsequent focus areas' models. The following sections discuss the process in greater detail.

## Siting and Scenario Development

The base model for RIIA is derived from the MTEP17 model, as described in detail in the Process section. Generator additions and retirements assumed in the MTEP process are not utilized in this study. Instead, additions are calculated and sited using a process developed for this assessment, while retirements are determined based on initial screening results of the PLEXOS model. In this section, the expansion and siting processes are described, with the retirement process to follow in page 164.





## Expansion

1. Determine the GWh of demand in each region from the load profiles developed for this assessment (Table TA-1)

Region	Energy (GWh)
MISO	677,466
SPP	264,805
TVA	222,637
SERC	469,283
PJM	829,073
NYISO	159,970

**Table TA-1: Total demand by region**

2. Assign the split of wind and solar energy to each region based on the ERGIS RTx30<sup>29</sup> scenario (Table TA-2)

Region	Wind	Solar
MISO	75%	25%
SPP	80%	20%
TVA	10%	90%
SERC	10%	90%
PJM	75%	25%
NYISO	75%	25%

**Table TA-2: Split of wind and solar by region**

For solar capacity, installed MW will be split into 70% utility-scale solar and 30% distributed solar, based on current industry trends.

3. Calculate the average capacity factors for new wind sites, existing wind sites, new solar sites and existing solar sites for each region from the 2012 NREL profiles used in the PLEXOS model, described in page 175. For new renewable sites, calculate capacity factors for each penetration level (Table TA-3 to TA-6).

---

<sup>29</sup>NREL Eastern Renewable Generation Integration Study: <https://www.nrel.gov/docs/fy16osti/64472.pdf>



Region	Existing Wind	Existing Solar
MISO	37%	19%
SPP	41%	20%
TVA	37%	19%
SERC	35%	19%
PJM	33%	18%
NYISO	35%	17%

Table TA-3: Capacity factors for existing wind and solar by region

	10%	20%	30%	40%	50%	60%	70%	80%	90%	100%
MISO	44%		45%	44%		43%		42%	41%	
SPP	N/A	N/A	48%	46%						
TVA	38%	36%		37%			36%		35%	
SERC	37%	38%		37%			36%		35%	
PJM	43%	40%	39%	38%		37%				
NYISO	43%	41%	42%	41%	42%					

Table TA-4: Capacity factors for new wind by region

	10%	20%	30%	40%	50%	60%	70%	80%	90%	100%
MISO	19%			18%	19%					18%
SPP	N/A	N/A	22%	23%						
TVA	19%									
SERC	19%									
PJM	18%									17%
NYISO	16%									

Table TA-5: Capacity factors for new utility-scale solar by region



	10%	20%	30%	40%	50%	60%	70%	80%	90%	100%
MISO	17%									
SPP	N/A	N/A	18%							
TVA	17%									
SERC	19%									
PJM	16%									
NYISO	15%									

**Table TA-6: Capacity factors for new distributed solar by region**

4. Calculate the energy needed from new renewables by subtracting the energy produced by existing renewables from the demand.
5. Determine the amount of renewable capacity needed to produce the needed energy calculated in step 4.

This process yields the following capacity expansion (Figures TA-7 to TA-9).

	10%	20%	30%	40%	50%	60%	70%	80%	90%	100%
MISO	1,993	15,511	28,303	41,521	55,168	69,031	84,427	98,097	114,297	129,647
SPP	0	0	4,200	9,900	15,000	20,250	25,675	30,700	36,225	41,750
TVA	675	1,450	2,175	2,800	3,600	4,400	5,200	5,800	6,300	7,300
SERC	1,350	2,800	4,300	5,750	7,250	8,750	10,250	12,000	13,500	15,250
PJM	11,300	29,600	48,750	68,900	87,600	107,700	128,200	147,025	164,900	185,600
NYISO	1,875	5,375	8,525	11,975	15,325	18,400	21,825	25,200	28,500	31,600

**Table TA-7: Wind expansion (MW) by region and milestone**



	10%	20%	30%	40%	50%	60%	70%	80%	90%	100%
MISO	1,050	8,500	15,575	23,125	30,550	37,700	44,900	52,500	59,325	67,975
SPP	0	0	1,600	3,400	5,200	7,100	9,000	10,600	12,600	14,700
TVA	8,200	16,675	25,250	34,625	42,150	50,675	59,300	67,750	76,275	85,275
SERC	16,300	36,550	52,600	70,800	90,625	110,825	126,125	145,100	161,475	180,825
PJM	6,200	15,600	24,800	34,600	45,050	55,250	63,375	72,850	84,600	93,100
NYISO	1,200	3,225	5,250	7,600	9,200	11,300	13,375	15,675	17,775	19,675

Table TA-8: Utility solar expansion (MW) by region and milestone

Region	10%	20%	30%	40%	50%	60%	70%	80%	90%	100%
MISO	1,276	4,711	8,549	12,257	15,415	18,837	22,590	25,994	28,956	32,190
SPP	0	0	1,076	2,065	3,070	4,099	5,066	6,128	7,124	8,139
TVA	3,838	7,854	11,846	15,833	19,872	23,874	27,885	31,891	35,910	40,174
SERC	7,757	16,428	24,935	33,704	42,267	50,864	59,478	68,073	76,757	85,119
PJM	3,126	7,575	12,014	16,547	20,786	25,349	29,523	33,750	37,548	41,174
NYISO	595	1,499	2,363	3,283	4,138	5,064	5,921	6,805	7,667	8,483

Table TA-9: Distributed solar expansion (MW) by region and milestone

## Siting

MISO's current siting process is robust and comprehensive for the circumstances under which it is used, such as MTEP studies. With this study, however, MISO is developing a variation on this process to deal with the large amount of renewables modeled.

1. Identify and map all buses 230 kV and above.
2. Exclude buses as viable siting candidates based on the following criteria.
  - a. *Rural vs urban areas:* For wind, exclude any sites within 0.5 mile of an urban area (>500 people/square mile) or within 10 miles of a high-density urban area (>2000 people/square mile). For solar, exclude any sites within 0.5 mile of an urban area.
  - b. *Airports:* For wind, exclude buses within a 5-mile radius of a regional airport (an airport with a control tower). For wind and solar, exclude areas within a 1-mile radius of any size airport.
  - c. *Military facilities:* Exclude all locations within a 2-mile radius of the boundary of a military facility.
  - d. *Federal lands:* Exclude all locations within a 2-mile radius of the boundary of federal land.



- e. *State lands*: Exclude all locations within a 1-mile radius of the boundary of state land. This assumption may be adjusted at higher levels of renewable generation.
  - f. *Swamp and marsh lands*: Exclude all locations within a 2-mile radius of swamp/marsh lands greater 10 square miles.
  - g. *Retirements*: Buses with existing thermal generation larger than 300 MW may be used when the unit retires.
  - h. *Proximity to existing thermal unit*: If a candidate bus is in close proximity to a low kV bus with a thermal generator larger than 300 MW, exclude the candidate bus until the thermal unit retires.
3. Geographically group the buses and select a subset of buses per group.
- a. The average distance between existing wind farms greater than 100 MW and their 10 closest neighbors of equal or greater size within 200 miles is ~26 miles. A 15-mile grid is therefore appropriate to group buses.
  - b. Select two buses as representative of each grid cell. High kV buses with significant outlets are given first priority. Representative buses must be at least 3 miles apart.
  - c. For New York, SERC and TVA, grid cells include additional representative buses due to a small number of candidate buses relative to needed MW capacity.
4. Calculate the capacity factor of each site using the wind and solar profiles developed by NREL (see page 175). Create capacity factor bins.
5. Prioritize the list of viable buses in each pool based on the following criteria:
- a. Status in the various interconnection queues<sup>30</sup> (Table TA-10)

Status	Priority
Operating	1
Planned	2
Canceled	3
Retired	3
Cold Standby	3
Greenfield	4

**Table TA-10: Siting priorities by unit status**

- b. Capacity factor bins
- c. Rank within grid cell (determined in step 3)

<sup>30</sup> For MISO, use the tiers developed in previous MISO studies and currently used in the siting process. For external regions, sort the list of buses developed in steps 1-5 by queue status to develop proxies for tiers outside of MISO.



- d. Proximity to queue locations
  - e. Outlet capability (measured by number of high kV lines connected to the bus)
6. Fill up and add capacity per bus to achieve desired renewable penetration level at each milestone. Buses are selected based on the priority sorted list.
- a. If a candidate bus is chosen for siting in a particular milestone, that bus must be used for all subsequent milestones. Each bus's sited MW monotonically increases across milestones.
  - b. For SERC and TVA, allow co-location of wind and solar in any milestone. Allow co-location of wind and solar for all other regions only under the following conditions:
    - i. 500 and 765 kV buses can be co-located at 10% penetration
    - ii. 345 kV buses can be co-located at 20% penetration
    - iii. 230 kV buses can be co-located at 30% penetration

### Expansion Sensitivity

The sensitivity assumptions, based on the expansion of renewables based on subregional load ratio and resource mix in the generation queue, results in:

- A shift from a wind-heavy system to a more balanced wind-solar mix
- A shift in capacity from the North to the Central and South regions in MISO

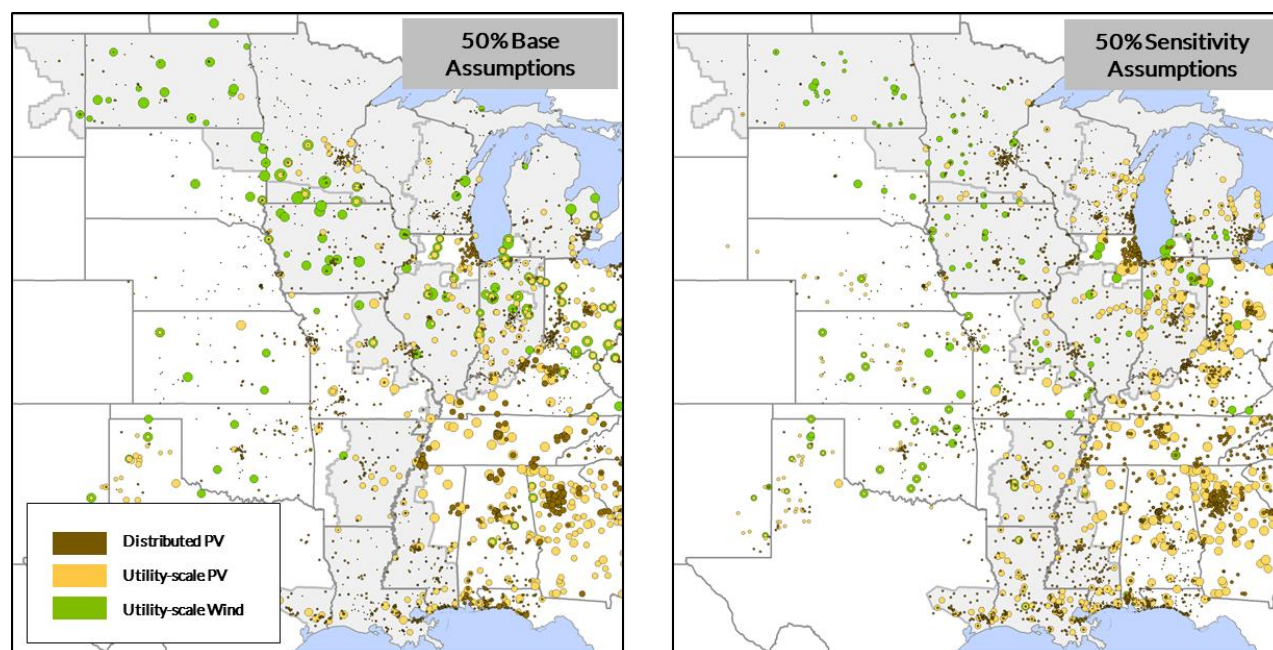
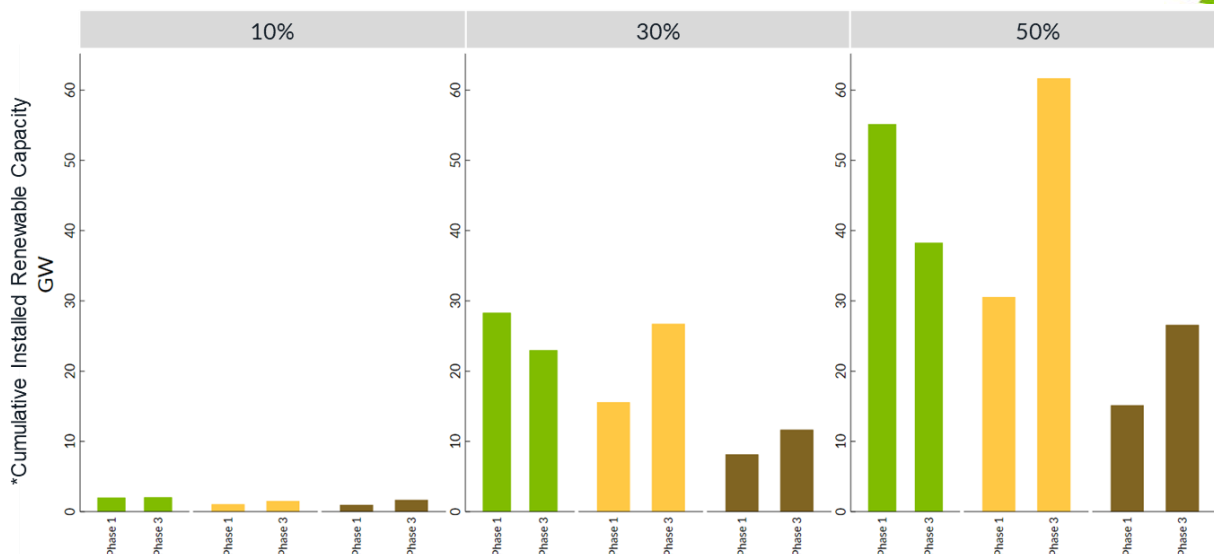


Figure TA-2: Geographic Distribution of Renewables Under Base and Sensitivity Assumptions

At the MISO level, the combined assumptions of a more regional distribution and recent queue trends for each subregion results in a shift from wind to solar compared to base assumptions (Figure TA-2 and Figure TA-3)



**Figure TA-3: Installed Renewable Capacity Per Milestone Under Base and Sensitivity Assumptions**

Furthermore, the expansion of renewable generation based on load ratio results in a shift of capacity from the North region to the Central and South regions (Figure TA-4).



**Figure TA-4: Installed Renewable Capacity Per Subregion Per Milestone**

Similar to the base assumptions, the capacity expansion used four steps, albeit with different approaches at each step.

Step 1: Determine the energy demand (GWh) in each region

As opposed to the base assumptions, the energy required from renewables was determined for each subregion in the footprint; for MISO, Local Resource Zones were used (Table TA-11 and Table TA-12).



	10%	20%	30%	40%	50%	60%	70%	80%	90%	100%
<b>MISO</b>										
LRZ 1	1.4	11.0	20.7	30.3	39.9	49.6	59.2	68.9	78.5	88.1
LRZ 10	0.3	2.7	5.2	7.6	10.0	12.4	14.8	17.2	19.6	22.0
LRZ 2	0.9	7.4	13.9	20.4	26.9	33.3	39.8	46.3	52.8	59.2
LRZ 3	0.7	5.6	10.5	15.4	20.3	25.2	30.1	35.0	40.0	44.9
LRZ 4	0.7	5.6	10.5	15.4	20.3	25.2	30.1	35.0	39.9	44.9
LRZ 5	0.5	4.3	8.0	11.8	15.5	19.2	23.0	26.7	30.5	34.2
LRZ 6	1.4	10.7	20.1	29.5	38.8	48.2	57.6	66.9	76.3	85.7
LRZ 7	1.4	11.3	21.2	31.1	40.9	50.8	60.7	70.6	80.5	90.3
LRZ 8	0.6	4.7	8.8	12.9	16.9	21.0	25.1	29.2	33.3	37.4
LRZ 9	1.8	13.8	25.8	37.9	49.9	62.0	74.0	86.1	98.1	110.2

**Table TA-11: MISO Subregional Incremental Renewable Energy**

Subregion	10%	20%	30%	40%	50%	60%	70%	80%	90%	100%
<b>SPP</b>										
SPP - Central	0.0	0.0	10.6	23.7	36.8	49.9	63.1	76.2	89.3	102.4
SPP - NBDK	0.0	0.0	5.3	12.0	18.6	25.2	31.8	38.4	45.1	51.7
SPP - KSMO	0.0	0.0	6.0	13.5	20.9	28.4	35.8	43.3	50.7	58.2
<b>TVA</b>										
TVA	14.5	31.1	47.7	64.3	81.0	97.6	114.2	130.9	147.5	164.1
TVA-Other	5.0	10.7	16.5	22.2	27.9	33.7	39.4	45.1	50.9	56.6
<b>SERC</b>										
AL	7.9	16.6	25.3	34.0	42.6	51.3	60.0	68.7	77.3	86.0
GA	13.3	27.9	42.5	57.1	71.6	86.2	100.8	115.4	130.0	144.5
MS	1.3	2.7	4.1	5.5	6.9	8.3	9.7	11.1	12.5	13.9
NC	15.6	32.7	49.8	66.9	84.1	101.2	118.3	135.4	152.5	169.6
SC	5.3	11.0	16.8	22.6	28.3	34.1	39.9	45.7	51.4	57.2
<b>PJM</b>										
AEP-ATSI	14.1	35.1	56.1	77.1	98.1	119.2	140.2	161.2	182.2	203.2
PJM-W	8.4	21.0	33.5	46.0	58.6	71.1	83.7	96.2	108.8	121.3
COMED	7.0	17.4	27.7	38.1	48.5	58.9	69.3	79.7	90.1	100.4
MidAtl-E	6.8	17.0	27.1	37.3	47.4	57.6	67.7	77.9	88.0	98.2
MidAtl-PA	8.3	20.8	33.2	45.7	58.1	70.6	83.0	95.5	107.9	120.4
PJM-S	11.3	28.3	45.2	62.1	79.0	95.9	112.9	129.8	146.7	163.6
<b>NY</b>										
NY	10.4	26.7	43.0	59.3	75.6	91.8	108.1	124.4	140.7	156.9

**Table TA-12: EI Subregional Incremental Renewable Energy**

Step 2: Assign the wind and solar energy mix for each region



The Generation interconnection queues as of March 2019 for each region in the were used to determine the mix of wind and solar. Specifically, the subregional (LRZ) mix was used (Table TA-13 & 14). The current mix of installed renewables was used 10% penetration milestone. The furthest queue projections were used for the 50% penetration and above. The mix for milestones 20-40% were interpolated.

Subregion	10%	20%	30%	40%	50%	60%	70%	80%	90%	100%
<b>MISO</b>										
LRZ 1	0.95	0.90	0.90	0.85	0.85	0.85	0.85	0.85	0.85	0.85
LRZ 10	0.00	0.10	0.15	0.20	0.25	0.25	0.25	0.25	0.25	0.25
LRZ 2	0.95	0.70	0.60	0.50	0.35	0.35	0.35	0.35	0.35	0.35
LRZ 3	0.95	0.95	0.90	0.90	0.90	0.90	0.90	0.90	0.90	0.90
LRZ 4	0.90	0.80	0.75	0.70	0.60	0.60	0.60	0.60	0.60	0.60
LRZ 5	0.95	0.85	0.80	0.75	0.70	0.70	0.70	0.70	0.70	0.70
LRZ 6	0.90	0.70	0.60	0.50	0.45	0.45	0.45	0.45	0.45	0.45
LRZ 7	0.95	0.85	0.75	0.70	0.65	0.65	0.65	0.65	0.65	0.65
LRZ 8	0.00	0.10	0.15	0.15	0.20	0.20	0.20	0.20	0.20	0.20
LRZ 9	0.00	0.05	0.05	0.05	0.05	0.05	0.05	0.05	0.05	0.05

Table TA-13: MISO Percentage of wind per subregion

Subregion	10%	20%	30%	40%	50%	60%	70%	80%	90%	100%
<b>SPP</b>										
SPP - Central	0.95	0.90	0.85	0.85	0.80	0.75	0.75	0.75	0.75	0.75
SPP - NBDK	0.95	0.95	0.95	0.90	0.90	0.85	0.85	0.85	0.85	0.85
SPP - KSMO	0.95	0.95	0.90	0.85	0.80	0.80	0.80	0.80	0.80	0.80
<b>TVA</b>										
TVA	0.15	0.10	0.10	0.05	0.05	0.05	0.05	0.05	0.05	0.05
TVA-Other	0.00	0.15	0.30	0.45	0.50	0.65	0.65	0.65	0.65	0.65
<b>SERC</b>										
AL	0.15	0.15	0.10	0.10	0.05	0.05	0.05	0.05	0.05	0.05
GA	0.35	0.25	0.20	0.15	0.10	0.05	0.05	0.05	0.05	0.05
MS	0.15	0.15	0.10	0.10	0.05	0.05	0.05	0.05	0.05	0.05
NC	0.00	0.00	0.05	0.05	0.05	0.05	0.05	0.05	0.05	0.05
SC	0.15	0.15	0.10	0.10	0.05	0.05	0.05	0.05	0.05	0.05
<b>PJM</b>										
AEP-ATSI	0.95	0.85	0.75	0.60	0.50	0.45	0.45	0.45	0.45	0.45
PJM-W	0.95	0.80	0.65	0.50	0.35	0.20	0.20	0.20	0.20	0.20
COMED	0.95	0.95	0.90	0.85	0.80	0.75	0.75	0.75	0.75	0.75
MidAtl-E	0.10	0.10	0.10	0.05	0.05	0.05	0.05	0.05	0.05	0.05
MidAtl-PA	0.95	0.80	0.60	0.50	0.30	0.15	0.15	0.15	0.15	0.15
PJM-S	0.70	0.55	0.50	0.35	0.20	0.05	0.05	0.05	0.05	0.05
<b>NY</b>										
NY	0.95	0.90	0.80	0.70	0.60	0.50	0.50	0.50	0.50	0.50

Table TA-14: EI Percentage of wind per subregion

Step 3: Determine avg. capacity factors for wind and solar resources at each penetration milestone



To convert the energy requirements into capacity, capacity factors for each technology in each subregion were used (Table TA - 15 -18).

Subregion	10%	20%	30%	40%	50%	60%	70%	80%	90%	100%
MISO										
LRZ 1	43%	43%	43%	43%	43%	43%	43%	43%	43%	43%
LRZ 10	36%	36%	36%	36%	36%	36%	36%	36%	36%	36%
LRZ 2	46%	45%	45%	45%	45%	45%	45%	45%	45%	45%
LRZ 3	46%	45%	45%	45%	45%	45%	45%	45%	45%	45%
LRZ 4	43%	45%	44%	44%	44%	44%	44%	44%	44%	44%
LRZ 5	43%	43%	44%	44%	44%	44%	44%	44%	44%	44%
LRZ 6	43%	42%	42%	42%	42%	42%	42%	42%	42%	42%
LRZ 7	42%	43%	43%	43%	43%	43%	43%	43%	43%	43%
LRZ 8	43%	43%	43%	43%	43%	43%	43%	43%	43%	43%
LRZ 9	34%	34%	34%	34%	34%	34%	34%	34%	34%	34%

**Table TA-15: MISO Wind Capacity Factors by subregion**

Subregion	10%	20%	30%	40%	50%	60%	70%	80%	90%	100%
<b>SPP</b>										
SPP - Central	45%	45%	46%	45%	45%	45%	45%	45%	45%	45%
SPP - NBDK	43%	43%	43%	43%	43%	43%	43%	43%	43%	43%
SPP - KSMO	48%	48%	48%	48%	48%	48%	48%	48%	48%	48%
<b>TVA</b>										
TVA	38%	38%	38%	38%	38%	38%	38%	38%	38%	38%
TVA-Other	45%	47%	44%	44%	45%	45%	45%	45%	45%	45%
<b>SERC</b>										
AL	33%	33%	33%	33%	33%	33%	33%	33%	33%	33%
GA	31%	32%	32%	32%	32%	32%	32%	31%	31%	31%
MS	32%	32%	32%	32%	32%	32%	32%	32%	32%	32%
NC	38%	38%	38%	37%	38%	38%	38%	38%	38%	38%
SC	38%	37%	37%	37%	38%	38%	38%	38%	38%	38%
<b>PJM</b>										
AEP-ATSI	41%	41%	41%	41%	41%	41%	41%	41%	41%	41%
PJM-W	38%	38%	38%	38%	38%	38%	38%	38%	38%	38%
COMED	43%	43%	43%	43%	43%	43%	43%	43%	43%	43%
MidAtl-E	38%	39%	39%	39%	39%	39%	39%	38%	38%	38%
MidAtl-PA	44%	44%	44%	44%	44%	44%	44%	44%	44%	44%
PJM-S	37%	37%	37%	37%	37%	37%	37%	37%	37%	37%
<b>NY</b>										
NY	44%	43%	43%	43%	43%	43%	43%	43%	43%	43%

**Table TA-16: EI Wind Capacity Factors by subregion**



Subregion	UPV	DPV	Weighted
MISO			
LRZ 1	18%	15%	17%
LRZ 2	18%	15%	17%
LRZ 3	19%	15%	18%
LRZ 4	19%	16%	18%
LRZ 5	19%	16%	18%
LRZ 6	18%	16%	18%
LRZ 7	17%	15%	17%
LRZ 8	19%	17%	19%
LRZ 9	19%	16%	18%
LRZ 10	19%	16%	18%

Table TA-17: MISO Solar-PV Capacity Factors by subregion

Subregion	UPV	DPV	Weighted
SPP			
SPP - Central	23%	17%	21%
SPP - NBDK	21%	17%	20%
SPP - KSMO	20%	16%	19%
TVA			
TVA	19%	16%	18%
TVA-Other	19%	16%	18%
SERC			
AL	19%	16%	18%
GA	19%	16%	18%
MS	19%	16%	18%
NC	18%	16%	18%
SC	19%	16%	18%
PJM			
AEP-ATSI	18%	15%	17%
COMED	18%	16%	17%
MidAtl-E	17%	15%	17%
MidAtl-PA	17%	14%	16%
PJM-S	18%	16%	17%
PJM-W	18%	15%	17%
NY			
NY	16%	14%	15%

Table TA-18: EI Solar-PV Capacity Factors by subregion



Step 4: Determine the expansion capacity for new wind and solar\* generation using the capacity factor and renewable energy target (Table TA – 19 – 26). Similar to the base RIIA assumptions, the installed capacity for the solar PV generation is split into 70% utility scale (UPV) and 30%.

Region	10%	20%	30%	40%	50%	60%	70%	80%	90%	100%
MISO	2.7	16.5	27.2	31.5	37.2	46.4	53.4	59.2	68.8	73.8
NY	2.8	6.8	9.5	11.3	12.2	12.2	14.6	16.6	19.2	21.5
PJM	13.0	28.3	39.6	43.7	48.2	50.3	56.4	60.1	64.5	69.8
SERC	2.9	4.7	5.8	6.8	6.8	6.8	7.0	7.3	7.5	8.0
SPP	-	-	5.1	10.9	15.9	20.5	26.3	31.1	36.2	41.6
TVA	0.8	1.7	3.0	4.5	5.9	8.4	10.1	11.0	12.3	13.9

**Table TA-19: Wind expansion by region**

Region	10%	20%	30%	40%	50%	60%	70%	80%	90%	100%
MISO	1.5	11.3	26.7	42.9	61.7	83.7	100.1	112.7	128.9	146.6
NY	0.4	1.7	4.9	9.5	16.1	24.4	28.2	31.9	36.1	40.2
PJM	6.3	20.5	42.2	73.2	114.0	156.7	184.5	213.2	237.6	267.3
SERC	16.8	35.2	55.4	77.9	99.4	120.9	138.3	156.6	174.0	194.1
SPP	-	-	1.2	2.8	5.2	9.3	11.5	23.0	23.0	23.0
TVA	8.2	17.7	23.4	32.3	39.8	47.0	53.5	61.7	68.3	77.4

**Table TA-20: UPV expansion by region**

Row Labels	10%	20%	30%	40%	50%	60%	70%	80%	90%	100%
MISO	1.7	5.6	11.7	18.8	26.6	35.2	41.7	47.9	54.2	60.4
NY	0.2	0.7	2.0	4.1	6.9	10.4	12.1	13.5	14.8	16.1
PJM	2.4	8.4	17.3	30.1	46.8	66.1	75.3	82.6	88.5	94.3
SERC	7.6	16.1	24.5	33.0	42.4	51.5	58.2	62.5	66.9	71.6
SPP	-	-	0.7	1.3	2.5	3.9	4.8	5.7	6.7	7.6
TVA	2.8	5.6	8.4	11.6	14.7	17.2	20.4	23.4	25.1	26.7

**Table TA-21: DPV expansion by region**



Subregion	10%	20%	30%	40%	50%	60%	70%	80%	90%	100%
<b>MISO</b>										
LRZ 1	1.8	5.6	8.4	8.4	8.9	11.4	12.0	12.6	13.8	14.4
LRZ 10	-	0.7	1.1	1.1	1.1	1.4	1.4	1.4	1.4	1.4
LRZ 2	0.2	1.8	2.7	2.7	3.2	3.6	4.1	4.5	5.4	5.9
LRZ 3	0.1	3.2	4.8	4.8	5.5	6.4	7.2	8.0	9.6	10.4
LRZ 4	0.1	1.6	3.3	3.3	3.9	4.4	5.0	5.5	6.6	7.2
LRZ 5	0.1	0.6	2.1	3.0	3.5	4.0	4.5	5.0	6.0	6.5
LRZ 6	0.2	1.1	1.7	4.5	5.2	6.0	6.7	7.3	8.6	9.3
LRZ 7	0.2	1.4	2.4	3.0	4.9	7.6	9.9	11.0	13.2	14.3
LRZ 8	-	0.3	0.4	0.4	0.8	0.8	1.8	2.0	2.2	2.4
LRZ 9	-	0.3	0.4	0.4	0.4	0.8	0.9	1.9	2.1	2.2

Table TA-22: MISO wind expansion by subregion

Subregion	10%	20%	30%	40%	50%	60%	70%	80%	90%	100%
<b>NY</b>										
NY	2.8	6.8	9.5	11.3	12.2	12.2	14.6	16.6	19.2	21.5
<b>PJM</b>										
PJM-S	1.5	3.0	4.1	4.5	5.0	5.1	5.7	6.0	8.8	11.0
AEP-ATSI	5.3	11.6	16.8	18.7	20.9	21.8	24.3	25.2	25.2	26.9
COMED	1.3	2.8	4.0	4.3	4.5	4.8	5.5	5.8	5.8	6.3
MidAtl-PA	2.8	5.3	6.7	7.6	8.4	8.9	9.7	10.3	11.5	11.7
PJM-W	1.8	4.9	7.0	7.5	8.0	8.4	9.6	11.2	11.4	12.0
MidAtl-E	0.5	0.9	1.1	1.3	1.5	1.5	1.6	1.7	2.0	2.0
<b>SERC</b>										
NC	0.8	1.4	2.2	2.6	2.6	2.6	2.6	2.6	2.6	2.6
AL	0.5	0.8	0.8	1.0	1.0	1.0	1.3	1.5	1.8	1.8
GA	0.9	1.5	1.8	2.0	2.0	2.0	2.0	2.0	2.0	2.2
SC	0.6	0.8	0.8	1.0	1.0	1.0	1.0	1.0	1.0	1.0
MS	0.2	0.2	0.2	0.3	0.3	0.3	0.3	0.3	0.3	0.5
<b>SPP</b>										
SPP - Central	-	-	2.4	4.7	7.0	9.4	12.0	14.3	17.1	19.4
SPP - KSMO	-	-	1.4	1.6	3.1	5.3	6.7	7.6	8.8	10.1
SPP - NBDK	-	-	1.4	4.6	5.8	5.8	7.6	9.2	10.3	11.4
<b>TVA</b>										
TVA	0.8	1.2	1.6	1.7	1.9	2.4	2.9	3.2	3.5	3.9
TVA-Other	-	0.5	1.4	2.8	4.0	6.0	7.2	7.8	8.9	10.1

Table TA-23: EI wind expansion by subregion



Subregion	10%	20%	30%	40%	50%	60%	70%	80%	90%	100%
<b>MISO</b>										
LRZ 1	0.1	0.6	1.1	1.6	3.2	4.7	5.4	5.9	6.9	7.8
LRZ 10	0.1	0.7	2.1	3.1	4.1	4.9	6.0	6.7	7.3	8.1
LRZ 2	0.1	0.6	2.2	4.8	7.4	10.8	13.0	14.9	17.6	20.3
LRZ 3	0.1	0.5	0.8	1.3	1.8	2.7	3.0	3.3	3.9	4.5
LRZ 4	0.1	0.6	1.6	2.3	3.5	5.4	6.5	7.2	8.5	9.8
LRZ 5	0.1	0.5	0.8	1.5	2.1	3.2	3.5	3.9	4.6	5.3
LRZ 6	0.1	0.7	2.7	5.3	8.5	12.8	15.2	17.8	20.8	23.7
LRZ 7	0.1	0.8	2.4	3.8	6.7	9.5	11.5	13.2	15.6	18.0
LRZ 8	0.3	2.0	3.4	5.6	6.1	7.6	8.8	9.7	10.6	12.1
LRZ 9	0.7	4.5	9.7	13.9	18.5	22.3	27.4	30.3	33.4	37.2

Table TA-24: MISO UPV expansion by subregion

Subregion	10%	20%	30%	40%	50%	60%	70%	80%	90%	100%
<b>NY</b>										
NY	0.4	1.7	4.9	9.5	16.1	24.4	28.2	31.9	36.1	40.2
<b>PJM</b>										
AEP-ATSI	0.8	3.3	7.2	15.5	25.5	33.5	38.5	44.0	48.9	55.5
COMED	0.5	1.1	2.4	4.4	7.5	9.9	13.0	14.8	14.4	16.3
MidAtl-E	2.0	3.9	6.3	9.1	11.5	12.8	14.6	16.9	18.5	19.9
MidAtl-PA	0.5	2.9	7.4	12.7	21.0	30.8	36.9	42.8	48.2	54.2
PJM-S	2.0	6.5	12.6	20.0	30.0	42.5	49.7	57.2	65.3	73.4
PJM-W	0.5	2.8	6.4	11.6	18.6	27.3	32.0	37.6	42.5	48.2
<b>SERC</b>										
AL	3.0	6.5	10.6	14.7	18.9	22.5	26.3	29.8	34.0	37.7
GA	3.9	9.4	15.0	21.3	28.2	36.4	42.4	47.8	53.8	60.7
MS	0.8	1.5	2.3	3.2	4.0	4.8	5.3	6.0	6.5	7.2
NC	7.1	13.4	20.6	28.4	35.6	42.3	46.9	53.1	57.7	63.9
SC	2.1	4.4	6.9	10.4	12.7	15.0	17.5	20.0	22.1	24.7
<b>SPP</b>										
SPP - Central	-	-	0.7	1.3	2.7	4.6	5.9	11.8	11.8	11.8
SPP - KSMO	-	-	0.3	0.9	1.7	3.0	3.4	6.8	6.8	6.8
SPP - NBDK	-	-	0.2	0.6	0.9	1.8	2.2	4.4	4.4	4.4
<b>TVA</b>										
TVA	5.6	12.0	15.8	22.0	24.8	29.3	33.3	38.5	41.5	47.8
TVA-Other	2.4	5.4	7.2	9.6	10.2	12.0	13.8	15.6	18.5	20.4

Table TA-25: EI UPV expansion by subregion



Row Labels	10%	20%	30%	40%	50%	60%	70%	80%	90%	100%
<u>MISO</u>										
LRZ 1	0.3	0.8	1.7	2.6	3.8	5.1	5.9	6.8	7.7	8.6
LRZ 10	0.1	0.3	0.6	0.9	1.4	1.7	2.1	2.4	2.7	3.0
LRZ 2	0.3	0.6	1.2	1.9	2.7	3.6	4.2	4.8	5.5	6.2
LRZ 3	0.2	0.4	0.9	1.4	1.9	2.5	3.0	3.4	3.9	4.4
LRZ 4	0.1	0.3	0.7	1.1	1.6	2.1	2.5	2.9	3.3	3.6
LRZ 5	0.1	0.3	0.7	1.0	1.5	2.0	2.4	2.8	3.2	3.6
LRZ 6	0.2	0.7	1.4	2.2	3.2	4.1	5.0	5.8	6.5	7.3
LRZ 7	0.2	0.9	1.8	2.9	4.2	5.5	6.6	7.3	8.1	8.9
LRZ 8	0.1	0.3	0.7	1.1	1.6	2.1	2.5	2.9	3.3	3.5
LRZ 9	0.2	1.0	2.0	3.3	4.6	6.2	7.3	8.5	9.6	10.7

Table TA-26: MISO DPV expansion by subregion



## Focus Area Outlines

This section describes the models, processes and assumptions used for RIIA’s three focus areas.

### Summary of Tools Used for Analysis

Table TA-27 gives a brief introduction to the models used, before in depth discussions in the subsequent sections.

	Tools	Vintage	Criteria to meet
<b>Resource Adequacy</b>	PLEXOS	MTEP17 model; uses MTEP16 Powerflow model at 10-year out transmission	LOLE per BAL-502-RFC-02; ELCC
<b>Energy Adequacy – Planning Focus area</b>	PLEXOS	MTEP17 model; uses MTEP16 Powerflow model at 10-year out transmission	Renewable targets energy adequacy; ramping adequacy;
<b>Energy Adequacy – Markets and Operation Focus Area</b>	(a) MISO production engines for commitment, clearing, dispatch and pricing, (b) KERMIT (Regulating reserves simulation tool); and (c) other simplified commitment and clearing engine models	current MISO production data and models, as well as future renewable portfolios developed in RIIA,	Generation’s ability to meet load; ramping adequacy; price volatility
<b>Operating Reliability</b>	PSSE, TARA, TSAT, VSAT	MTEP17 Series 5-year out models	BAL-003; TPL-001; small-signal stability; critical-clearing time (CCT); weak grid short-circuit ratio (SCR)

**Table TA-27: RIIA focus area tools and models**

## Resource Adequacy Focus Area

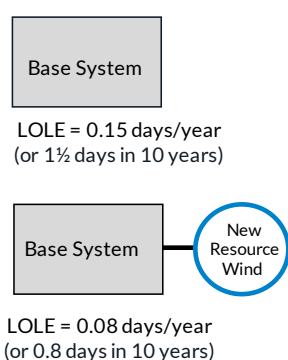
A key component of MISO’s transmission planning process is the resource adequacy analysis, as required by the North American Electric Reliability Council (NERC) Standard BAL-502-RFC-02. The standard requires Planning Coordinators to perform and document a resource adequacy study every year. The metric used to calculate the planning reserve margin (PRM) is the “ 1-day in 10-years “ metric, also known as the loss of load expectation (LOLE). The LOLE takes into account the forced and unforced outages and provides a probabilistic assessment of a given system.

The integration of higher levels of renewable resources into the MISO market has driven the need to quantify the effect of wind resources on the LOLE target. MISO has adopted the effective load carrying capability (ELCC), which

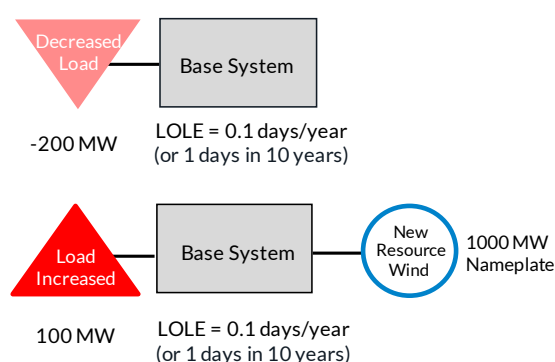


uses an LOLE-type study to quantify the capacity value of wind during MISO's peak. A two-stage process (as shown in Figure TA-5) is used to calculate the capacity contribution of wind generation<sup>31</sup>. Using the ELCC technique, the load is adjusted to balance the LOLE to a common reliability level of 1-day in 10-years (or 0.1 d/yr.), both in the case before the renewable resource being studied is added and after the renewable resource is added. The simple difference in these load adjustments is the ELCC of the resource. Dividing this number by the installed capacity of the resource added yields the ELCC as a percentage. For this analysis, the ELCC was measured for: each 10% renewable penetration milestone; each renewable technology being studied: wind, utility-scale PV (UPV) and distributed solar PV (DPV); the isolated collective solar technologies and the combination of all renewable technologies; and each of six different profile years being studied (2007-2012). Including the reference case for each year with no renewables and the base case with current levels of existing wind and UPV solar (~8% penetration) leaves a grand total of 324 different ELCC cases being analyzed.

#### Example System "With" & "Without" New Resource



#### ELCC Example System at the same LOLE



**ELCC:** the amount of incremental load a resource can dependably and reliably serve, while considering the probabilistic nature of generation shortfalls and random forced outages as driving factors to load not being served

**Figure TA-5: Example ELCC Calculation**

### Tool and Model Data Background

To calculate ELCC and measure the capacity contribution of renewables, a commonly used power system analysis tool was chosen: PLEXOS by Energy Exemplar. This program is used by many energy markets and system planning engineers throughout the industry. Most importantly, it has the functionality to compute LOLE using the convolution method and can be set up to perform sequential Monte Carlo simulations. In order to capture the inter-annual variability of weather-related patterns, synchronized load, wind and solar hourly datasets were used for the study. A description of each dataset is included next.

### Existing generation fleet

This model uses generation included in MISO's business-as-usual planning models with a signed Generator Interconnection Agreement (GIA) and an in-service date before 12/31/2017. Units scheduled to come on line and retirements scheduled to take place during the 2017 year are pushed to 1/1/2017 to produce a study year with no

<sup>31</sup> MISO, "Planning Year 2017-2018 Wind Capacity Credit", Report, December 2016. Available online: <https://www.misoenergy.org/Library/Repository/Report/2015%20Wind%20Capacity%20Report.pdf>



generation changes. Forced outages occur randomly within the simulation and maintenance outages are scheduled during periods of high capacity reserves using the PLEXOS software.

### Load profiles

Historical load profiles from 2007-2012 were gathered from MISO's market operations database. In order to keep the same peak load assumption, all hourly shapes are adjusted in magnitude to reflect the 2017 peak load of 126,465 MW. More details about load profile development can be found in page 173.

### Wind and solar profiles

Hourly wind profiles were gathered from NREL's Wind Integration National Dataset (WIND) Toolkit. Solar data was sourced from NREL's Solar Integration National Dataset (SIND) Toolkit. Each wind and solar resource was assigned specific profiles based on their location, one profile for each of the six years (2007-2012) studied in the Resource Adequacy focus area. Sensitivity analysis for the Resource Adequacy focus area was conducted with additional data supplied by Vibrant Clean Energy for the years 2013-2018. More details about these data resources can be found in page 175.

### Capacity Calculation Methods

Four methods were initially considered for the analysis. First deterministic methods were explored. Two options were studied, "Top n peak load hours", and second "top n peak net load hours". Second probabilistic methods were explored. Two options were studied, "sequential monte Carlo" and second "convolution".

The sequential Monte Carlo method for calculating LOLE was first considered for the ELCC analysis part of this research, as it is one of the most robust methods of determining LOLE. Accuracy can be easily controlled by selecting the number of random outage samples to simulate and by calculating the resulting statistical error. One downside to using the sequential Monte Carlo method is the run time associated with it due to computational intensity, especially for a system the size of MISO with more than a thousand generating units. With simulation times taking longer than a day for a sequential Monte Carlo run with 5,000 samples, and considering the number of runs it would take to adjust the LOLE to the targeted value as well as the number of cases and years that would need to be investigated for this research, it would have been extremely difficult to accomplish the goals of this study in a timely manner. Thus, a faster calculation method was sought after.

The second method tested for calculating LOLE was the convolution method as shown in Figure TA-6. This method proved to be much faster, taking only a few minutes. This technique, also known as the "Effective Load Approach", iterates through all units accumulating the unit outage patterns, calculating their respective probabilities and formulating a capacity outage probability table. The table is compared to a load duration curve and the installed capacity to calculate the Loss-of-Load Probability (LOLP) that, in turn, is used to determine the daily LOLE. An LOLE benchmark was performed between the 5,000-sample sequential Monte Carlo approach and the convolution approach to approximate the amount of any additional inaccuracy in the ELCC value by using the faster convolution technique. Given the size of the system and number of study cases, it was concluded that the convolution method is acceptable for use in this assessment and the amount of error it introduces in the ELCC value is within the uncertainties of other modeling and data assumptions<sup>32</sup>

---

32 B. Heath and A. L. Figueroa-Acevedo, "Potential Capacity Contribution of Renewables at Higher Penetration Levels on MISO System," *2018 IEEE International Conference on Probabilistic Methods Applied to Power Systems (PMAPS)*, Boise, ID, 2018, pp. 1-6.

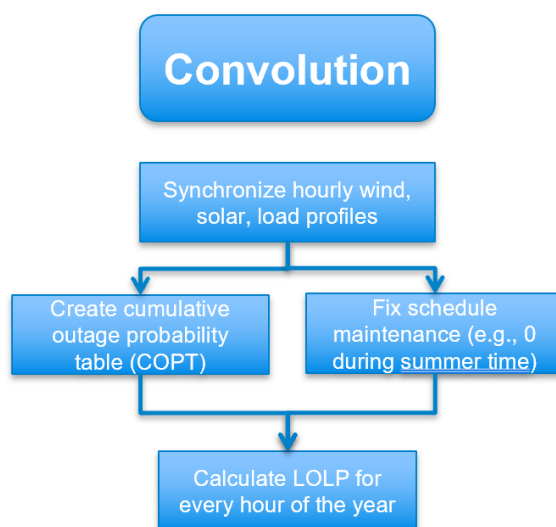
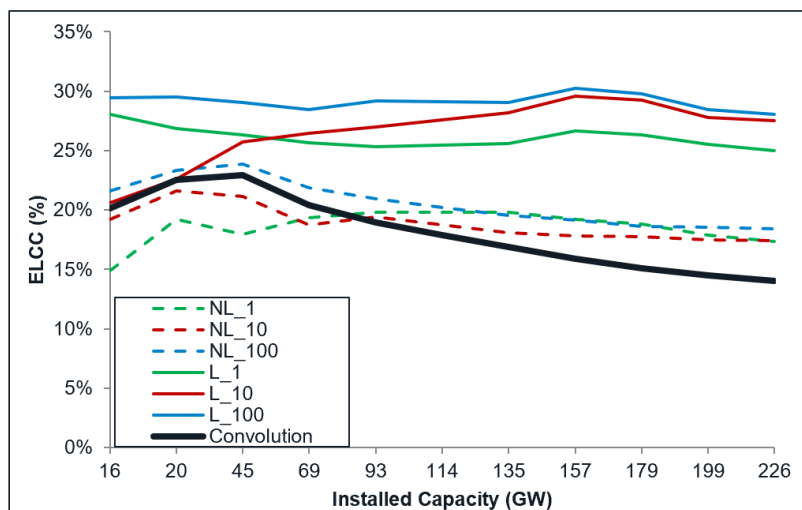


**Figure TA-6: Process to conduct Convolution**

Comparisons were conducted for each of the four methods to determine which one was the best fit for the scope of RIIA. As demonstrated by Figure TA-7, Figure TA-8 and Table TA-28 the convolution approach is within a reasonable error tolerance and is more computationally tractable. The majority of the Resource Adequacy analysis in RIIA was done using convolution for this reason.

Approach	Modeling Features				Simulation time
	Number of hours	Forced outage rates (FOR)	Scheduled maintenance	Renewables modeling	
Deterministic using gross load	1, 10, etc.	Not Included	Not Included	Availability at peak	None
Deterministic using net load	1, 10, etc.	Not Included	Not Included	Availability at net load peak	None
Probabilistic using Convolution	8760	Average	Optimized	Hourly generation	~5min/case
Probabilistic using Sequential Monte Carlo	8760	Random	Optimized	Hourly generation	~80hrs/case

**Table TA-28: Comparison of Resource Adequacy modeling approaches**



Deterministic Methods	Total number of samples averaged across all years
Peak Load (L_1)	Top 1 (peak load)
Peak Net Load (NL_1)	Top 1 (net peak load)
Peak Load (L_10)	Top 10 (peak load)
Peak Net Load (NL_10)	Top 10 (net peak load)
Peak Load (L_100)	Top 100 (peak load)
Peak Net Load (NL_100)	Top 100 (net peak load)

Figure TA-7: Deterministic and probabilistic approaches produce largely different results

- All Renewables ELCC at 100% penetration

Approach	ELCC
Top 100 Deterministic (Gross load)	28.00%
Top 100 Deterministic (Net load)	18.40%
Convolution	14.00%
Sequential MC	13.95%

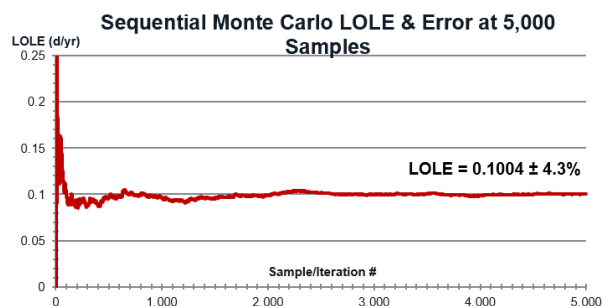


Figure TA-8: ELCC Comparison of Resource Adequacy approaches

A data comparison was conducted between two different datasets MISO uses. The first is the Generator Availability Data System (GADS), which contains actual generator level performance information, and the second is the MISO Transmission Expansion Plan (MTEP) dataset, which contains class average generator performance information. The difference between these datasets on the ELCC of wind and solar is shown in Figure TA-9. For the purpose of system level studies, the error introduced by using class average data is negligible.

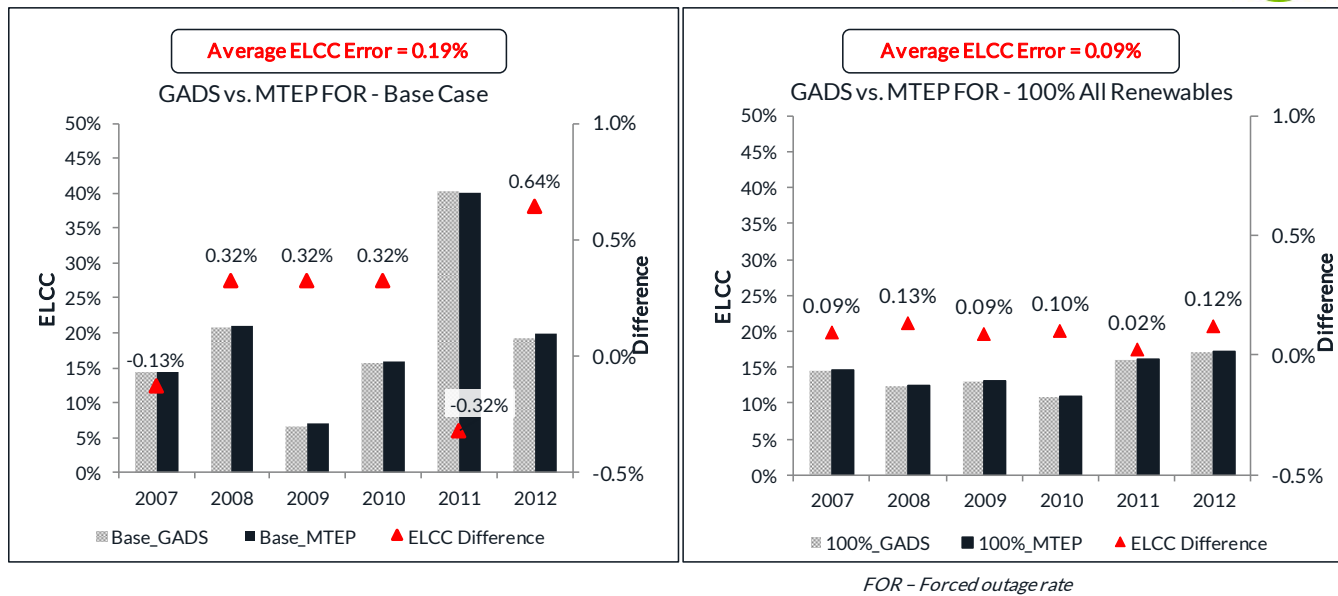


Figure TA-9: GADS vs. MTEP for current system and high renewable system

Another test was done to understand the impact of using a load adjustment versus a generation adjustment to calculate ELCC. The process is demonstrated in Figure TA-10.

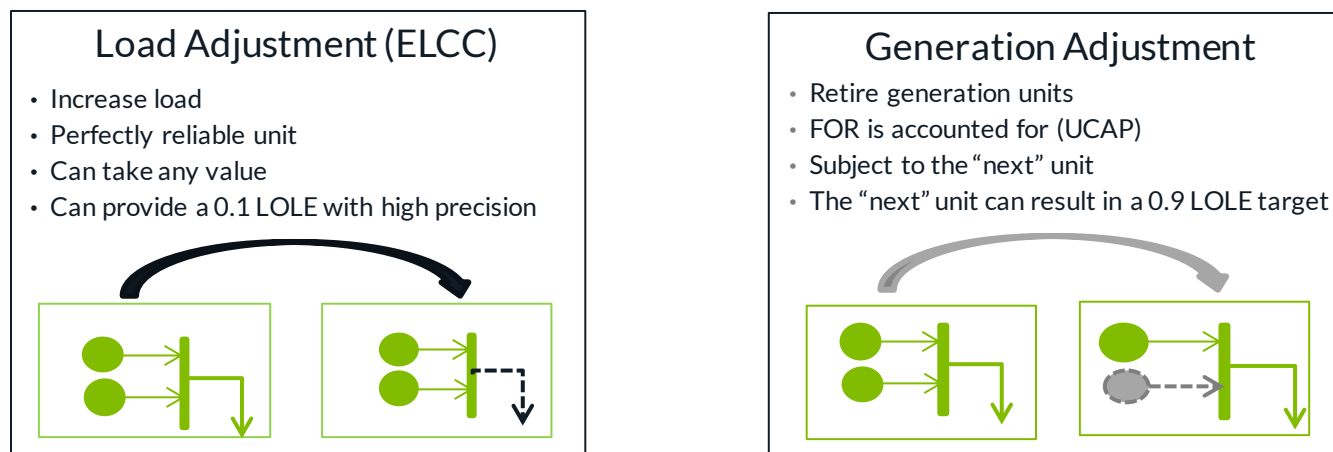


Figure TA-10: Load and generation adjust process

The results of the test show that either method produces very similar results. Table TA-29 shows a consistent negligible difference between these methods for the purpose of understanding trends in ELCC as the penetration of wind and solar changes in the footprint. It is worth noting that the load adjustment initially produces a higher ELCC value and then switches as the penetration of renewables increases.



Capacity Value (%) comparison				
Method	Base	10%	50%	100%
Generation Adjustment	19.66%	21.50%	19.88%	16.03%
Load Adjustment	20.12%	22.54%	17.87%	14.04%
Difference	-0.46%	-1.03%	2.01%	1.99%

Table TA-29: ELCC comparison by adjustment method

### Capacity Contribution of Renewables

Other industry work has been conducted on the ELCC of wind and solar both inside and outside of MISO. Figure TA-11 and Figure TA-12 show the results of this work. The general conclusions shown here are directionally consistent with the findings in RIIA.

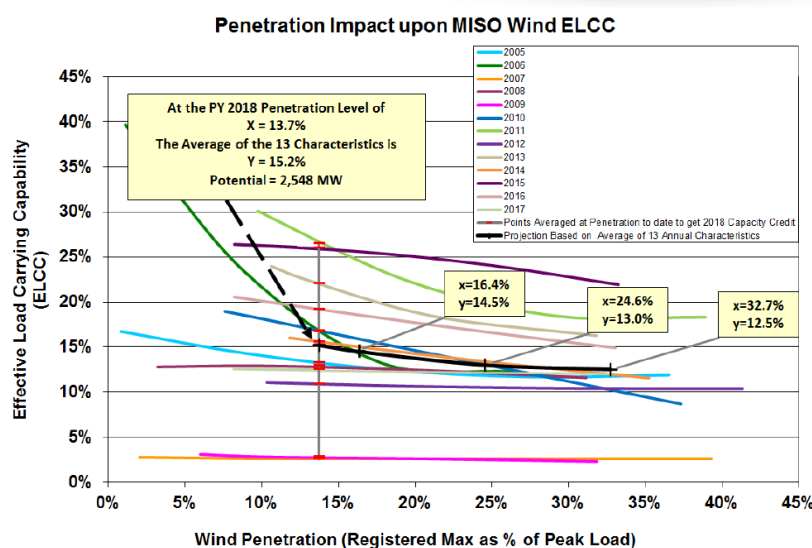
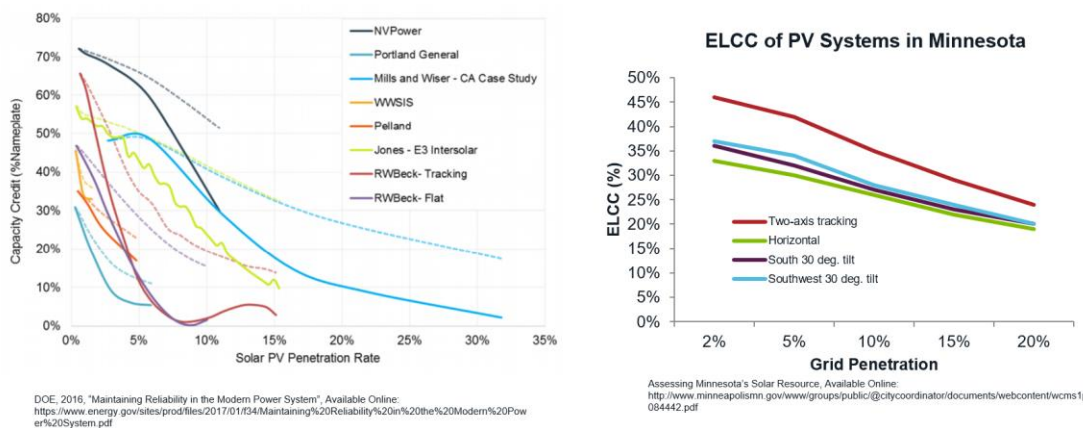
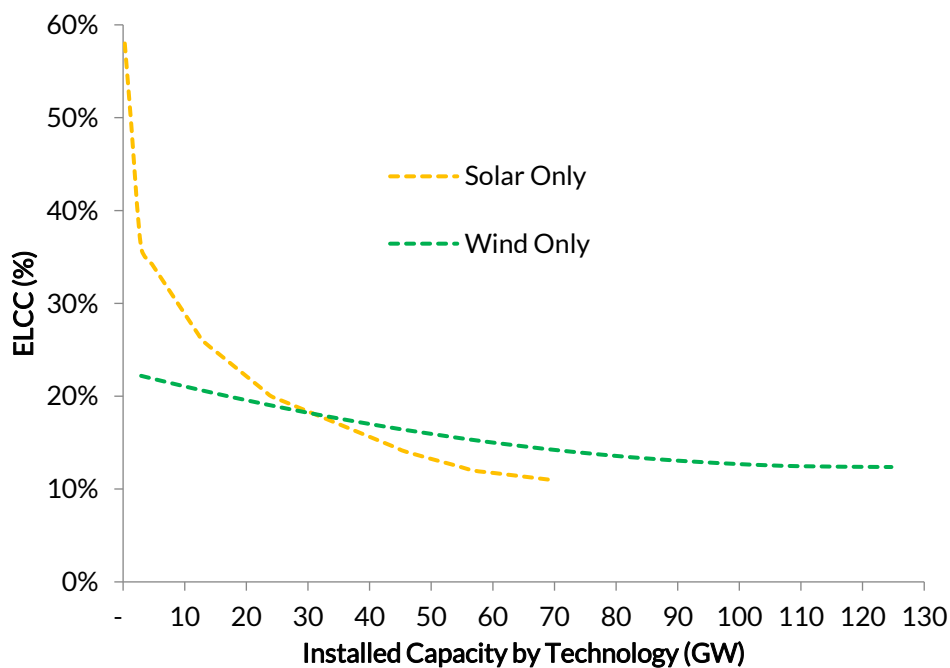


Figure TA-11: Previous MISO Studies have shown a decrease in wind ELCC as penetration increases



**Figure TA-12: Previous industry work on ELCC of solar has shown a rapid decrease as penetration increases**

An ELCC function was developed for each renewable technology to inform retirement decisions. The ELCC curve of each technology was characterized using the results from each milestone and a polynomial fitting (Figure TA-13).



**Figure TA-13: Wind and solar ELCC curves as a function of installed capacity**

These graphs were approximated by the *siting- and fuel-mix specific* functions in Equation 1, where UCAP is unforced capacity and ICAP is installed capacity, in units of GW.

Equation 1: Approximate ELCC functions for wind and solar

$$\text{Wind UCAP} = 100 * (-0.03 \ln(\text{ICAP}) + 0.26), \text{ in percentage}$$

$$\text{Solar UCAP} = 100 * (-0.07 \ln(\text{ICAP}) + 0.42), \text{ in percentage}$$



These functions were evaluated for each milestone for each region to determine the appropriate amount of retirements to select.

## Retirements

Retirements are incorporated into each milestone to accommodate the new generation. Candidates for retirements will ultimately include all non-renewable fuel types, although some are not initially considered. In the lower-end milestones, nuclear, hydro and combustion turbine (CT) and steam turbine (ST) and internal combustion (IC) renewable units are not considered candidates for retirements. The retirement process involves assessing a unit's viability using costs and revenues, and it is difficult to obtain decommission costs for nuclear units. MISO recognizes that not initially retiring nuclear units is counter to current trends, but it is necessary to work with the available data. MISO will continue to research nuclear retirements to ultimately work them in to later milestones. Hydro units are not initially retired due to lack of precedence. CT/ST and IC renewable units are not retired because they represent a small percentage of total system capacity. These assumptions are consistent with those in MTEP18 but may change as milestones progress.

1. *Determine the capacity contribution of all generators, both current and future.*

For retirement-eligible conventional generation, a unit's contribution to the reserve margin is equal to its maximum capacity multiplied by (1-Forced Outage Rate). For renewable units, the capacity credits developed in the Resource Adequacy focus area are evaluated for the given technology at the given penetration level.

2. *For each milestone, determine the net revenue of each generator using preliminary model results.*

One feature PLEXOS offers is its Medium-Term Scheduling, discussed in page 166. This feature solves the optimization problem by creating regional load duration curves (LDCs) for each user-defined interval then slicing those curves into blocks using a weighted least-squares fit methodology. This method enables accurate results in a shorter period of time. An output of this feature is the net revenue of each unit. Net revenue is calculated using the difference between a unit's revenue (the LMP multiplied by generation) and its variable and fixed O&M costs.

3. *For each milestone, determine the net present value (NPV) of each unit's revenue based on its simulated net revenue and remaining useful life. Rank units by these values.*

For each renewable milestone, a unit's "lifetime" revenue is calculated by assuming that the annual revenue determined at that milestone will persist for the remainder of the unit's useful life. A unit's remaining useful life is taken from Powerbase data (if the date is public) or fuel type specific useful life assumptions (if the date is not public). These assumptions are consistent with MTEP18.



Unit Type	Useful Life (years)
CC	55
CT Gas/IC Gas	50
CT Oil & Other	55
IC Oil/Other	50
IGCC	75
ST Coal	65
ST Gas & Oil	55
ST Other	60

**Table TA-30: Generator useful life by fuel type**

4. For each region, retire units until the capacity contribution removed is equivalent to the capacity contribution added by renewables.

Within the ranked list, retirements begin with units that were not economically selected to run within the preliminary simulation, thus have a 0% capacity factor. When those units have been exhausted, units are chosen based solely on their net revenue ranking. MISO will also consider candidates for retirements identified in MTEP and other MISO processes. The amount of retirements is based on the capacity contribution added by renewables as discussed in page 156.

5. Add the chosen retirements into the model of the current milestone and the subsequent milestone.

Retirements chosen in one milestone will section persist for the remaining milestones. Retirements are incorporated into the model for each focus area. Issues associated with retirement choices will be identified and remedied as necessary. This process is, by design, adaptive, and if retirements are causing irreparable issues, one solution may be to reevaluate retirement choices.

Table TA-31 details the retirements derived by this process for each region and milestone.

	10%	20%	30%	40%	50%	60%	70%	80%	90%	100%
MISO	1,206	6,615	10,599	14,673	17,018					
SPP	-	-	1,885	3,829	5,241					
TVA	-	-	-	-	-					
SERC	6,174	10,664	12,846	14,882	16,326					
PJM	4,662	10,527	15,164	19,708	21,351					
NYISO	1,115	2,747	4,022	5,480	6,590					

**Table TA-31: Cumulative retirements by region and milestone**



## Energy Adequacy – Planning Focus Area

The Energy Adequacy focus area is studied in Energy Exemplar's PLEXOS software. PLEXOS offers several interdependent phases for production cost simulations, three of which are used here: PASA, MT Schedule and ST Schedule, each described below.

### PLEXOS Modeling Phases

- PASA (Projected Assessment of System Adequacy)
  - *Model or Algorithm:* Linear program (LP)/Simplex
  - *Functions:* The objective is to produce randomly generated maintenance events for all generation resources. PASA schedules maintenance based on availability of reserves. The maintenance schedules are then passed to the MT Schedule and ST Schedule phases for production cost simulations.
  - *Main assumptions:* Maintenance is not scheduled for the summer months of June, July and August (maintenance during periods of higher load is historically infrequent); maintenance is not scheduled for nuclear generators (nuclear maintenance schedules are part of the Powerbase dataset and provided by the Nuclear Regulatory Commission)
- *Relevant outputs:* Maintenance schedules for non-nuclear generators  
MT Schedule (Medium-term Schedule)
  - *Model or Algorithm:* Linear program (LP)/Simplex
  - *Functions:* The objective is to solve the optimization problem using a computationally tractable approach. The MT Schedule simulates typical operating conditions (e.g., load/net load duration curves) and solves a simplified production cost model. MT Schedule also decomposes system constraints that span time periods longer than those used in subsequent phases.
  - *Main assumptions:* Regional transmission representation; non-chronological solve
  - *Relevant outputs:* Generator-specific net revenue used in retirement decisions; dispatch of energy-limited resources (e.g. hydro)
- ST Schedule (Short-term Schedule)
  - *Model or Algorithm:* Mixed-integer linear program (MIP)/Branch and bound
  - *Functions:* The objective is to provide an optimal, chronological dispatch with user-defined time steps over a given period of time. This phase simulates conditions most similar to actual market operations.
  - *Main assumptions:* Chronological dispatch
  - *Relevant outputs:* The majority of outputs in this assessment come from the ST Schedule. The outputs include, but are not limited to, generator properties (output, capacity factor, ramping, and LMPs), load properties (unserved energy, LMPs) and transmission properties (congestion, congestion costs).



- Interleaved Run Mode

- *Model or Algorithm:*

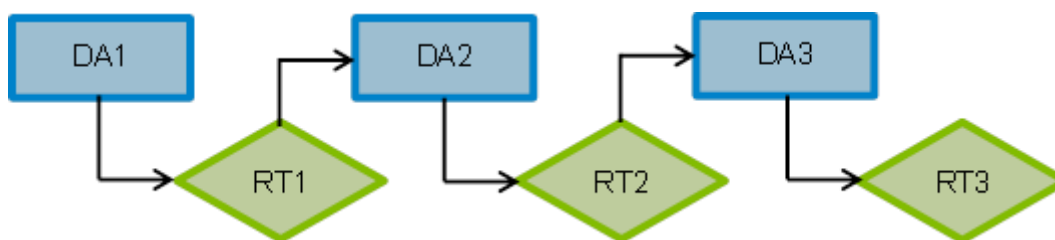


**Figure TA-14: PLEXOS' interleave feature**

- *Functions:* The objective of the interleave mode as seen in Figure TA-14 is to enable the passing of data between models so that they are solved “in step”. MISO is using this feature to model both a day-ahead and a real-time market. The day-ahead market uses an MT Schedule and an ST Schedule, while the real-time market uses only the ST Schedule. Operating conditions are passed by the model from day-ahead to real-time at the end of each day, and vice versa.
  - *Main assumptions:* Unit commitment decisions are passed from day-ahead to real-time, while economic dispatch can change in the real-time model (except for units with fixed generation profiles)<sup>33</sup>; random forced outages occur in the real-time model and are only passed to day-ahead if they occur over the span of multiple days
  - *Relevant outputs:* ST Schedule results for both day-ahead and real-time simulations

These phases can be run separately or together. PLEXOS production cost modeling is two-pronged: hourly modeling and sub-hourly modeling. For hourly Energy Adequacy modeling, MISO uses the MT and ST schedules. PLEXOS also offers an interleave feature, which allows the user to simulate both a day-ahead and real-time market. MISO will use this feature for 5-minute Energy Adequacy modeling.

### Analysis and Solution Development

Put more broadly, the Energy Adequacy production cost model uses the inputs and outputs listed in Figure TA-15.

---

<sup>33</sup> Units with fixed generation profiles include qualifying facilities, some conventional hydro and other energy-limited resources.

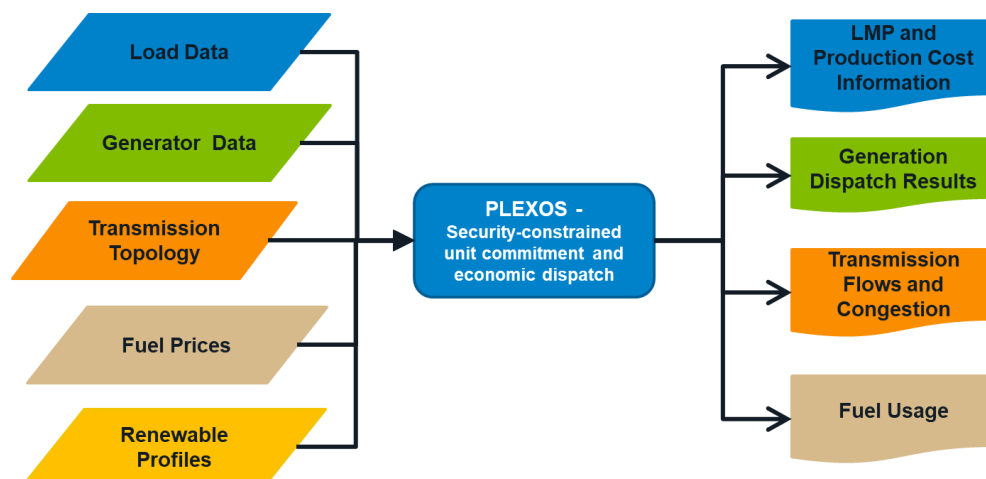


**Figure TA-15: Inputs and outputs to the Energy Adequacy model**

The input base model for the Energy Adequacy portion of RIIA is taken from MTEP17. Although this assessment aims to remain “year agnostic”, for modeling reasons it is necessary to choose a specific year to simulate and this study uses 2017 as a proxy year. The model includes a 15-year out transmission topology, including the remaining Multi-Value Projects (MVPs) and Appendix A transmission. Each milestone’s model includes the expansions and retirements discussed in Sections 0 and 0. As these expansions and retirements significantly change dispatch, analysis is performed to determine which flowgates are necessary for monitoring at each milestone. Other detailed assumptions are described in Appendix A of this document.

For a given milestone, the Energy Adequacy output analysis first looks at the percent of load served by renewable energy to determine whether the milestone target has been met. If this metric is within 5% of the target, the milestone is deemed met. If, due to curtailment or other factors, the milestone is not met, more analysis is necessary to develop solutions that enable the appropriate level of renewable energy penetration. Other metrics of note in output analysis are LMPs, capacity factors, reserve shortages, interchange, ramping behavior and transmission congestion. If any of these metrics indicate an inoperable/inadequate system, development of solutions is necessary.

Solution development in Energy Adequacy can take two forms: an optimized transmission build-out or a non-transmission solution. The transmission build-out uses a computer optimization program to identify system needs and design a conceptual transmission design to facilitate the delivery of renewable energy. The objective is to minimize total generation production cost and transmission build cost, subject to defined system constraints. With the input of a set of promising transmission candidates, the optimization program is able to select an economically effective combination of solutions to meet the objective and constraint, and to provide detailed information for engineers to design transmission. The non-transmission solutions could include re-siting renewable resources, changing retirement assumptions, increased reserves, energy storage or fast ramping generation.

### Base Dataset

For this assessment, the MTEP17 model is used. This model includes all Appendix A transmission current as of MTEP16 to ensure the assessment will not develop solutions for problems that may be fixed by currently planned transmission infrastructure. This model also includes generation included in MTEP17 with a signed Generator Interconnection Agreement (GIA) with an in-service date before 12/31/2017. Units scheduled to come online and retirements scheduled to take place during the 2017 year are pushed to 1/1/2017 to produce a study year with no



generation changes. This document provides assumptions used in this study that differ from those used in the MTEP process. Readers can access information about MTEP17 assumptions in the MTEP17 report.<sup>34</sup>

## Study Areas

The Renewable Integration Impact Assessment (RIIA) model comprises the following six areas the combination of which is seen in Figure TA-16:

- Midcontinent Independent System Operator (MISO)
- New York Independent System Operator (NYISO)
- PJM Interconnection (PJM)
- SERC Reliability Corporation (SERC)
- Southwest Power Pool (SPP)
- Tennessee Valley Authority (TVA)

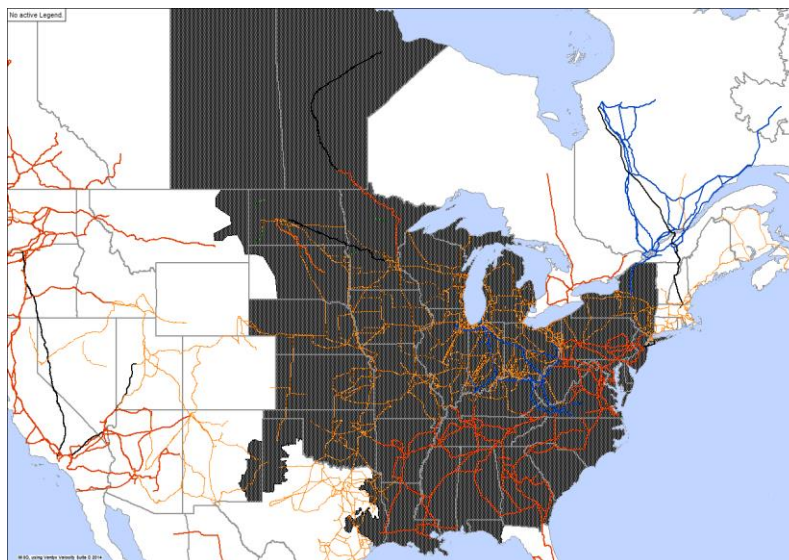


**Figure TA-16: RIIA study footprint**

## Resource Mixes

Each planning region within the Eastern Interconnection is made up of a diverse mix of capacity resources. The base RIIA model's fuel mix is captured in the table below. Results of resource expansions and retirements performed as part of MTEP17 are not included in the RIIA model. Each region is assumed to meet its Planning Reserve Margin Requirement (PRMR) with these fuel mixes.

<sup>34</sup> <https://www.misoenergy.org/Library/Repository/Study/MTEP/MTEP17/MTEP17%20Full%20Report.pdf>



	Coal	Gas	Nuclear	Wind	Solar	Hydro	Pumped Storage Hydro	Oil	Other
MISO	63,845	71,954	13,317	18,618	274	2,331	2,447	3,534	1,253
MHEB	97	274	0	258	0	4,476	0	0	0
NYISO	1,379	21,018	5,304	2,237	0	4,938	1,409	3,621	806
PJM	61,989	74,139	34,575	9,018	487	2,970	5,590	9,047	2,002
SERC	32,982	51,175	17,773	250	1,086	6,631	4,626	2,161	745
SPP	25,343	28,988	1,971	16,004	50	4,973	474	1,332	172
TVA	11,747	14,730	8,077	29	381	5,233	1,825	7	50
TVA - Other	8,088	6,599	0	308	0	147	31	69	0

Table TA-32: Base RIIA resource mix by region (MW)

### Generator Characteristics

Table TA-33 contains the average values for the generator characteristics used in the model. These assumptions are taken directly from Ventyx (Hitachi ABB) unless otherwise noted.

	Coal	Gas	Nuclear	Hydro	Pump. Hydro	Oil	Other
Min Gen Level (% of Max Cap)	40.2	CC: 50.1 CT: 25.2 ST: 30.7	100	24.5		25.0	35.6
Min Up Time (hours)	15.8	CC: 5.7 CT: 1.8 ST: 22.2	122.8	1		1.8	4.5
Min Down Time (hours)	9.8	CC: 6.6 CT: 2.2 ST: 10.1	122.8	1.6		1.8	5.2
Variable O&M (\$/MWh)	1.31	CC: 1.48 CT: 0.80 ST: 1.40	2.52	0	0	0.74	1.71
Forced Outage Rates (% of year)	10	CC: 5.8 CT: 5.8 ST: 9.1	4.8	5.2	NA	6.8	8.8
Maintenance Rates (% of year)	7	CC: 7.4 CT: 3.4 ST: 8.2	Sched. Maint.	6.1	7.7	3.5	3.6

Table TA-33: Generator characteristics by fuel type

Forced outages occur randomly within the simulation and maintenance outages are scheduled using PASA and remain constant throughout the study (see page 166).



## Ramp Rates and Start-Up Costs

One major aspect of renewable integration is generation variability. This assessment incorporates a sub-hourly real-time simulation phase with five-minute step sizes, thus there is need for special consideration of unit start-up and ramping assumptions. Typically, MISO production cost models use one-hour simulation step sizes where ramping and unit start-up modeling data provided by ABB is sufficient. Here, the assumptions are reviewed against other industry studies and updated to capture a unit's physical ability to ramp in a five-minute simulation.

NREL's Eastern Renewable Generation Integration Study (ERGIS)<sup>35</sup> is a helpful reference source for review of these assumptions and thus is the basis for the updates to MISO's typically used ABB data.

### Ramp Rates

*Ramp rate* is a unit's rate of change (MW/min) when the output is between the unit's minimum stable level and max capacity. *Run rate* is a unit's rate of change (MW/min) when the output is between zero and the minimum stable output level, or the start-up and shut-down rates. For this assessment, the source for the updates to ramp and run rates is the Black and Veatch<sup>36</sup> study performed for NREL, an analysis that yielded ramp rate data by various unit classes. Spin ramp rate and quick start ramp rate are listed as a percent of max capacity per minute. Spin ramp rate in the B&V study is used as the ramp rate in RIIA. Quick start ramp rate in the B&V study is used for the run rate in RIIA.

Category	Ramp Up & Down Rate (% Max Cap/Min)	Run Up & Down Rate (% Max Cap/Min)
CC	5	2.5
CT Gas/Oil	8.33	22.2
Nuclear	5	5
ST Coal	2	2
ST Gas & Oil	4	4

**Table TA-34: Ramp and run rates by fuel type. Unit types not listed use ramp and run rates consistent with ABB's assumptions.**

### Start-Up Costs

The Power Plant Cycling Costs Report<sup>37</sup>, also prepared for NREL use in the ERGIS study, is a useful reference source for updating the unit start-up assumptions for different thermal unit classes. It includes the cost estimates (\$/Max Cap) for hot, warm and cold start-ups, as well as the duration (in hours) of hot, warm or cold starts.

---

<sup>35</sup>NREL Eastern Renewable Generation Integration Study: <https://www.nrel.gov/grid/ergis.html>

<sup>36</sup>Black and Veatch. (2012). "Cost and Performance Data for Power Generation Technologies." Prepared for the National Renewable Energy Laboratory. <http://bv.com/docs/reports-studies/nrel-cost-report.pdf>

<sup>37</sup>Kumar et al. (2012). "Power Plant Cycling Costs." Prepared for the National Renewable Energy Laboratory. <https://www.nrel.gov/docs/fy12osti/55433.pdf>



	Small Coal (<300 MW)	Large Coal (>=300 MW)	Combined Cycle	Large CT (>=40 MW)	Small CT (<40 MW)	ST Gas
Hot Start Time (h)	<4	<12	<5	<2	0	<4
Warm Start Time (h)	4 to 24	12 to 48	5 to 40	2 to 3	0 to 1	4 to 48
Cold Start Time (h)	>24	>48	>40	>3	>1	>48
Hot Start Cost (\$/MW cap.)	94	59	35	32	19	36
Warm Start Cost (\$/MW cap.)	157	65	55	126	24	58
Cold Start Cost (\$/MW cap.)	147	105	79	103	32	75

**Table TA-35: Start-up costs by fuel type**

### Fuel Prices

Fuel price assumptions are also taken from MTEP17 futures and are discussed in the following sections.

### Natural Gas Prices

The Henry Hub natural gas price as shown in Figure TA-17 is the base price input to the model, with location-specific adders used to represent more granular prices. This natural gas price is the verbatim NYMEX forecast, as discussed in stakeholder forums during MTEP futures development.

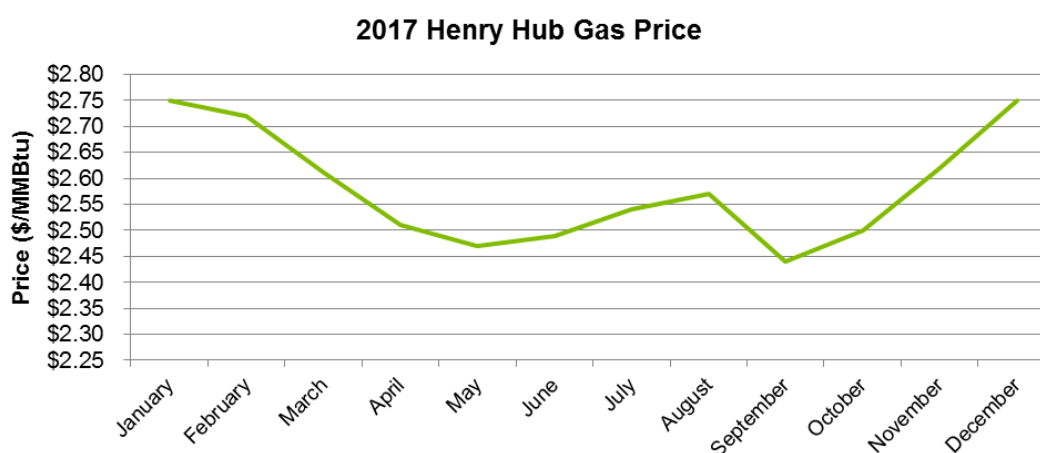


**Figure TA-17: Monthly natural gas prices**



## Other Fuel Prices

The remaining fuel prices are listed in the Table TA- 36: Fuel prices. Several other fuel types also use location-specific prices. In those cases, the values are average values.

Fuel	Fuel Price (\$/MBtu)
Coal	2.52
Kerosene	11.71
Oil-H	7.73
Oil-L	11.41
Uranium	1.11
Other	1.74

Table TA- 36: Fuel prices

## Load Profiles

MISO's local balancing authority (LBA)<sup>38</sup> five-minute load profiles are obtained for 2012 from historical market data. Hourly load profiles are obtained for areas outside of MISO from PROMOD (Ventyx [Hitachi ABB]), and then adjusted to create five-minute load profiles. This process is necessary due to the lack of publicly available five-minute load data. It is described in detail in the following sections.

### Hourly and Sub-Hourly Load Profiles

To create hourly load shapes for MISO LBAs, five-minute load values are averaged across each hour (e.g. 12:00-12:55). The load profile is scaled within the PLEXOS simulation from 2012 to 2017 using the ratio of each LBA's peak in MTEP17 and each LBA's 2012 hourly peak obtained by the averaging method.

Hourly profiles for areas outside of MISO for 2012 are obtained from Ventyx (Hitachi ABB). Using these 2012 profiles and data gleaned from MISO's five-minute load profiles, five-minute load shapes are developed for non-MISO areas. The process involves identifying patterns in five-minute load changes in MISO data and applying those patterns to the non-MISO hourly data. This creates load shapes that capture realistic variation that would not be present through simple interpolation, which is essential for the five-minute simulations used in this assessment. For a detailed explanation of this process, see Hourly and Sub-Hourly Load Profiles.

## Data Processing

Within the 2012 five-minute load data, several LBAs have irregular dips and spikes in their load shapes. While a certain level of volatility is anticipated, extreme dips/spikes can often be attributed to metering errors. For this study, dips/spikes with a percent change from annual peak greater than 3-5% (depending on the size of the area) lasting 5-10 minutes are removed. As an example, Utility A had three such errors (dips) (left, Figure TA-18). By taking the load values from either side of the event and averaging their difference across the low (or high) period(s), these events are erased to obtain a smoother load shape (right, Figure TA-18). Dips/spikes below the 3-5% threshold is considered regular occurrences and assumed to represent expected levels of variation.

---

<sup>38</sup> An operational entity or a Joint Registration Organization which is (i) responsible for compliance with the subset of NERC Balancing Authority Reliability Standards defined in the Balancing Authority Agreement for their local area within the MISO Balancing Authority Area, (ii) a Party to Balancing Authority Agreement, excluding MISO, and (iii) shown in Appendix A to the Balancing Authority Agreement.

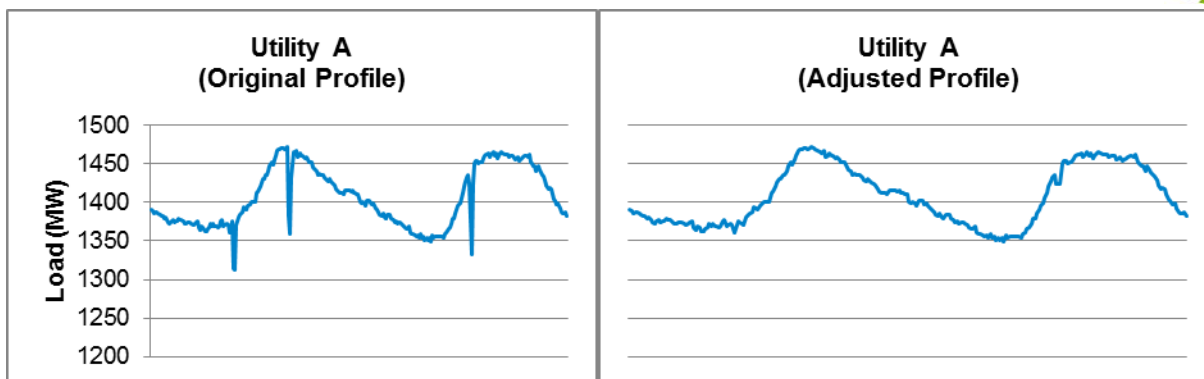


Figure TA-18: Utility A's load profile before and after data processing

### Forecast Error

For this assessment, the PLEXOS interleave feature was planned to be used to simulate both the real-time and day-ahead markets. Because the hourly load shapes (for use in the day-ahead simulation) are calculated from the five-minute load shapes (for use in the real-time simulation), there is not a significant amount of error between the day-ahead forecast and real-time load. Some amount of error is expected to more accurately represent the relationship between day-ahead and real-time load. Due to complication in analysis, the interleave function was not used in the final analysis, but the data was used to understand the change in risk due to forecast error as seen in Energy Adequacy – Uncertainty and Variability Trends.

The historical market data used also provides hourly real-time load and hourly day-ahead load forecasts for MISO as a whole for 2009-2016. Loads are not forecasted at the LBA level. The error between the actual load and forecasted load is calculated for all years. The error from 2012 was applied to each of the MISO LBAs' day-ahead forecasts, and the errors from the remaining years are applied to external regions (e.g. apply 2007 error to PJM, 2008 error to SPP, etc.). Using different years for different regions provides error values that are in the range of historically accurate values and unique for each region in the model. The forecast error of MISO's footprint for a sample week shown in Figure TA-19.

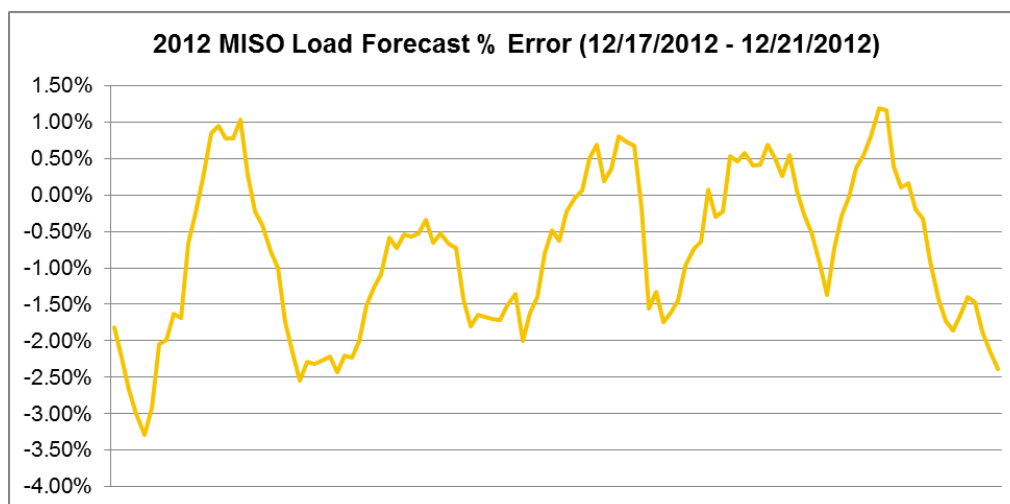


Figure TA-19: MISO's load forecast error



## Renewable Profiles

The ongoing seams study performed by the National Renewable Energy Study (NREL) concluded that 2012 represents the year with the most typical meteorological conditions of wind, solar and hydro generation. MISO has historically used 2006 renewable and load profiles, but beginning with MTEP18, MISO will use a 2012 profile year. NREL's data is used to provide these 2012 profiles, the details of which are described below.

### Wind Profile Source

Wind profiles source from NREL's Wind Integration National Dataset (WIND) Toolkit<sup>39</sup>. Meteorological conditions are captured at 5-minute intervals for 126,000 2-km x 2-km sites in the continental United States for years 2007-2013. Power output provided by NREL is estimated from the wind data by assuming a 100-m hub height. In addition, hourly forecast data is also available for every site at 1-hour, 4-hour, 6-hour, and 24-hour horizons.

Existing and expansion wind sites in the PLEXOS model are assigned a profile based on the closest NREL site to the modeled sites' latitude and longitude. Existing sites (with few exceptions) are assigned 80-m hub height profiles and expansion sites are assigned 100-m hub height profiles. The 80-m hub height profiles are obtained by scaling the 100-m profiles<sup>40</sup>. Both sub-hourly generation profiles for real-time modeling and hourly 24-hour forecast generation profiles for day-ahead modeling are used in the RIIA model.

### Solar Profile Source

Solar profiles source from NREL's Solar Integration National Dataset (SIND) Toolkit<sup>41</sup>. In the latest toolkit available at time of study, meteorological conditions are captured at 30-minute intervals for more than 154,000 4-km x 4-km sites in the United States for years 2007-2012. Power output provided by NREL is estimated from the solar data and categorized based on solar technology type: single-axis tracking, fixed axis, or rooftop. Forecast data is not available at time of the study.

Existing and expansion solar sites in the PLEXOS model are assigned a profile based on the closest NREL site to the modeled sites' latitudes and longitudes. For the real-time model, the sub-hourly single-axis tracking generation profiles are interpolated via PLEXOS for utility scale solar while distributed generation is assigned interpolated sub-hourly rooftop profiles. Since solar forecast data is in development, MISO uses an hourly aggregation of the sub-hourly solar data as a proxy in the day-ahead model.

### Wind and Solar Profile Source for Sensitivity Analysis

Additional data was sourced from Vibrant Clean Energy (VCE) for the purpose of robustness testing in the RIIA sensitivity analysis.

VCE provides a normalized power dataset for both wind and solar technologies for various weather years based on the National Oceanic and Atmospheric Administration's (NOAA) High Resolution Rapid Refresh (HRRR) weather forecast model. The power dataset is the best available estimate of what the synchronous wind and solar power profiles looked like across the contiguous United States (CONUS). These are provided on a calendar year basis, gridded spatially at 3km and temporally at five minutes. The calendar years originally provided to MISO were for

---

<sup>39</sup><https://www.nrel.gov/grid/wind-toolkit.html>

<sup>40</sup> Factors used to scale 100-m profiles to 80-m profiles are calculated using MISO market historic output energy from specific units, compared to the output energy from the 100-m profiles. When unit-specific data is not available, the scaling factor is developed by comparing 80-m and 100-m NREL profiles from years where both heights are available.

<sup>41</sup><https://www.nrel.gov/grid/sind-toolkit.html>



2014 through 2018. The input weather data is obtained from the NOAA HRRR weather forecast model, which is a specially configured version of Advanced Research WRF (ARW) model. The HRRR is a run hourly on a 3-km grid resolution and its domain covers the continental United States as well as portions of Canada and Mexico. Since its inception, the HRRR has undergone rapid and continuous improvement to its physical parameterization schemes, many of which have specifically targeted improved forecasts for the renewable energy sector. Through collaborative research efforts between Department of Energy (DOE) and NOAA, projects such as the Solar Forecast Improvement Project (James et al. 2015, Benjamin et al. 2016), the Wind Forecast Improvement Projects I and II (Wilczak et al. 2015, Shaw et al. 2019) were conducted to improve forecasts of meteorological quantities important for wind and solar energy forecasting.

### Creating non-MISO Load Shapes

1. Create a matrix  $MI_h$  containing the change in MISO LBA load  $ML_h$  from the beginning of one hour,  $h$ , to the beginning of the next hour,  $h+1$ , over all hours for each MISO LBA. Create a matrix  $MR_h$  with the hourly percent change using these values.

$$MI_h = [(ML_{h+1} - ML_h) \quad \dots \quad (ML_{h+8783} - ML_{h+8782})]$$

$$MR_h = \left[ \frac{ML_{h+1} - ML_h}{ML_h} \quad \dots \quad \frac{ML_{h+8783} - ML_{h+8782}}{ML_{h+8782}} \right]$$

2. If the absolute value of the percent change between two hours  $MR_h$  is greater than 0.25%, calculate the ratio of *the difference between each 5-minute interval  $i$  in an hour and the first interval of that hour and the MW difference between the two hours*  $MI_h$ .

$$MP_{h,i} = \left[ \frac{ML_{h,i+1} - ML_{h,i}}{MI_h} \quad \dots \quad \frac{ML_{h,11} - ML_{h,0}}{MI_h} \right]$$

If the value of a given of  $MP_{h,i}$  is greater than 300% or if the percent change between two hours  $MR_h$  is less than 0.25%, consistent growth is assumed, thus  $MP_{h,i} = i/12$ .

The bounds of 0.25% and 300% were chosen using engineering judgment to prevent the passing of atypical data from MISO load data to non-MISO load data.

3. Calculate an average percent change per interval across all MISO LBAs for the entire year.

$$MA_{h,i} = \left[ \begin{array}{ccc} \text{avg}(|MP_{h,i}|) & \dots & \text{avg}(|MP_{h,i+11}|) \\ \vdots & \ddots & \vdots \\ \text{avg}(|MP_{h+8783,i}|) & \dots & \text{avg}(|MP_{h+8783,i+11}|) \end{array} \right]$$

4. Create a matrix  $NL_h$  containing the hourly load values for non-MISO LBAs. Create a matrix  $NI_h$  containing the change in non-MISO LBA load  $NL_h$  from the beginning of one hour,  $h$ , to the beginning of the next hour,  $h+1$ , over all hours for each non-MISO LBA.

$$NL_h = [NL_h \quad \dots \quad NL_{h+8783}]$$

$$NI_h = [(NL_{h+1} - NL_h) \quad \dots \quad (NL_{h+8783} - NL_{h+8782})]$$

5. Finally, calculate the load values for each 5-minute interval  $i$  in matrix  $NL_{h,i}$  using values from  $NL_h$ ,  $NI_h$  and  $MA_{h,i}$ .

$$NL_{h,i} = NL_h + NI_h * MA_{h,i}$$



## Energy Adequacy – Market and Operation Focus Area

### Methodology

The Energy Adequacy – Market and Operation Focus Area, also referred to as the Portfolio Evolution Study (PES) navigates different timescales to simulate detailed operational and market outcomes. The general methodology is shown in Figure TA-20. PES utilizes both current MISO production data and models, as well as future renewable portfolios developed in RIIA, as inputs to the models. The modeling tools then feed longer-term forward-looking solutions into the shorter-term finer granularity processes.

The tools used in study include (a) MISO production engines for commitment, clearing, dispatch and pricing, (b) KERMIT (Regulating reserves simulation tool); and (c) other simplified commitment and clearing engine models.

This method allows us to examine the evolution of portfolios and its associated uncertainty from the day-ahead market down to the real-time market. In particular, PES investigates the impact to the market due to the potential future changes in portfolio, including:

- Renewable penetrations of up to 40% of system-wide load level
- Load Modifying Resources up to additional 5 GW (on top of current portfolio)
- Battery storage up to 200 MW-capacity and 800 MWh energy storage capability (currently in Automatic Generation Control [AGC] study only)

The PES also includes the following modeling features in market and operation, including:

- Use as-is Net Scheduled Interchange (NSI) without modification.
- The virtual offers and bids are unchanged from the current Day Ahead market levels.
- “Must-run” units from the current Day Ahead market are preserved as in the original production data.
- To model the 40% renewable penetration level, a high level of solar production is assumed for exploring the impact on potential operational needs.
- A total of four weeks of data from 2017-2018 with each representative week selected from a different season. Note that three of the weeks had experienced Max-Gen events.
- Use as-is transmission system, i.e., no rebuild of transmission.
- The solar resources are spread out on the market footprint to avoid congestion focus.
- Wind and solar resource energy offers were offered at a flat 0 \$/MWh.

### Methodology

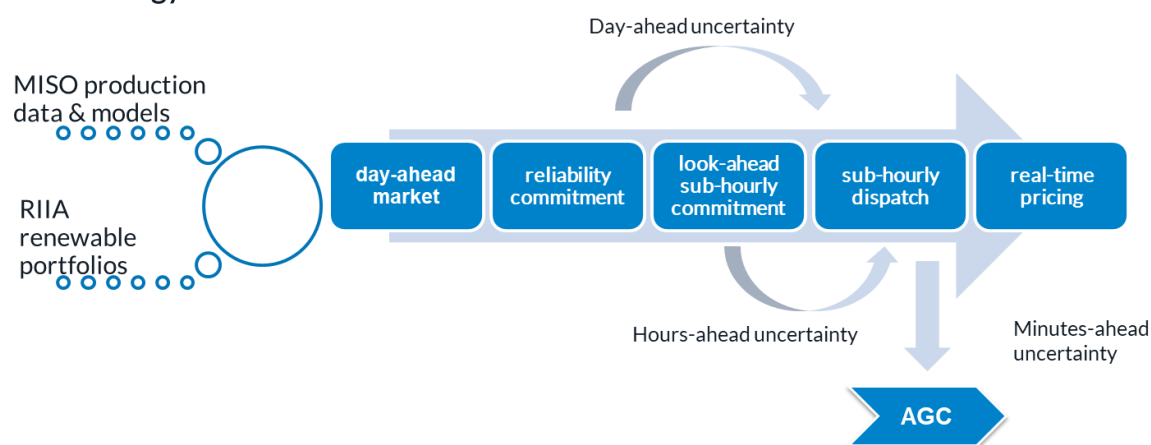
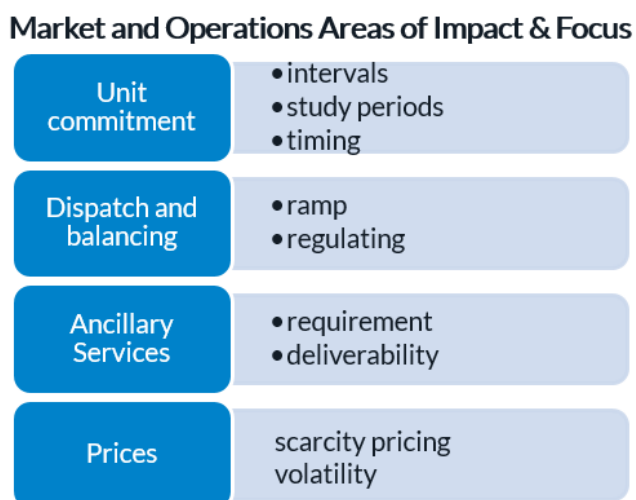


Figure TA-20: Day-Ahead and Real-Time Market Operations Analyses



Figure TA-21 is an itemization of the key metrics in the PES. In terms of Unit Commitment, the impact of additional time granularity on commitment is investigated as well as the timing. For dispatch and balancing, ramp rates and regulation are analyzed for the future portfolios. Deliverability is also being considered for studying whether and how ancillary service requirements could be met during times of congestion in the future scenarios, and how the requirements may have to be evolved. Finally, the impact to prices in terms of scarcity, as well as price volatility, are studied.



**Figure TA-21: Market areas of impact and focus**

## Operating Reliability – Steady State Focus Area

The Operating Reliability focus area is divided into two categories: steady-state analysis and dynamics analysis. Per the process map (Figure TA-1), models are created first for steady-state analysis then passed and transformed for dynamics analysis.

### Tool and Model Data Background

Steady-state analysis is performed using Siemens' PSSE powerflow simulation software and PowerGem's TARA. PSSE and TARA's AC contingency analysis allows for the identification of voltage and thermal reliability issues as a result of generation and transmission contingency events.

Steady-state models will be based on the MTEP17-5-year out models. This series was chosen for consistency between steady-state and dynamics models. The closest MTEP17 model to the given study scenario were chosen as a starting point (e.g. to build a low load-high renewables RIIA model the MTEP17 2022 Light Load case will be the starting point).

Three power-flow models are required for each renewable level (like 40% and 50%) – one for each snapshot of load and generation chosen. The topology of all three models were made consistent to represent consistent electrical topology. The primary benefit of this practice is all the mitigations identified in RIIA study are deemed due to RIIA, instead of being possibly due to a missing MTEP project or other facility.

### Grid-Scale Generation Modeling

Modeling of wind and grid-scale solar in the powerflow model included a generator step-up transformer topology. Renewable siting was split into segments of no more than 300 MW, with each generator possessing its own



Generator Step-Up (GSU) and Point-of-Interconnection (POI) transformer. All generators (both wind and grid-scale solar) were modeled with a PSSE Reactive Power Control Mode of 2, which means that Q limits are based on a Power Factor of  $\pm 0.95$  applied to the unit's active power output. This represents a "triangular" reactive capability curve, as opposed to a "rectangular" curve in which the entirety of the  $\pm Q$  range is available at all active power output levels<sup>42</sup>. Wind units were given an Mbase of  $1.11 * P_{max}$  and an Xsource of 0.8. PV and Type-IV wind units were given an Mbase of  $1.11 * P_{max}$  and an Xsource of 999.

The renewable units were sited at a 0.69 kV bus, with a GSU transformer connecting it to a 34.5 kV bus. The GSU was modeled per WECC recommendations, with 6% impedance and an X/R ratio of 8. A POI transformer was connected to the 34.5 kV bus to the BES bus at which the generator is ultimately interconnected. Collector system impedance was ignored as it is specific to any wind or solar site, and generic assumption could not be made for such a large number of diverse siting. The POI transformer was modeled per WECC recommendations, with 8% impedance and an X/R ratio of 40. For example, Figure TA-22 shows the siting for 500 MW of grid-scale solar interconnected at a 230 kV bus. The siting is split into two segments: 300 MW and 200 MW. For more details on siting amounts and locations, refer to 144 of this document.

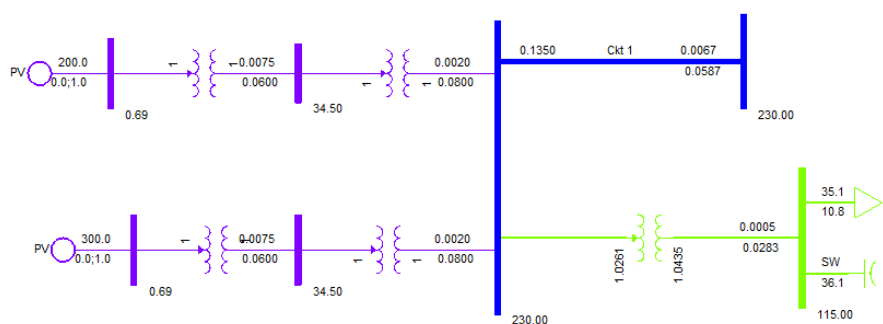


Figure TA-22: PSSE configuration for 500 MW of grid-scale solar

### Distributed Generation Modeling in Steady-State

Distributed solar generation were modeled as a Retail-Scale Distributed Energy Resource (R-DER). These are single-phase units and are used to offset customer loads. For the sake of simplicity, DG units will be modeled in both Operating Reliability analyses as constant-current negative loads sited directly on the BES load bus. DG units were assumed to not provide any reactive power support.

It is worth noting that at the time of commencement of RIIA study, the latest DER models such as DER\_A were still under development and could not be used in the study.

### Powerflow Model Dispatch

The PSSE Powerflow models was developed based on snapshots of "stressful" periods by examining the hourly output of the Energy Adequacy focus area. Following criteria was used to select candidates of these "stressful" dispatch scenarios, but are not limited to:

- Periods of peak system demand with high instantaneous renewable penetration
- Periods with the maximum non-synchronous generation online
- Periods with the highest percentage of total energy from non-synchronous generation

<sup>42</sup> Per FERC clarification on Order 827 (<https://www.ferc.gov/whats-new/comm-meet/2016/061616/E-1.pdf> paragraph 49)



- Periods of lowest system load with high instantaneous renewable penetration
- Periods with maximum transfers across existing (or new) monitored transmission interfaces

Dispatch scenario selection varied under different renewable milestones. RIIA focused on peak and off-peak load and peak renewable system conditions, providing samples representative of year-round grid operating patterns to bound the majority of system issues likely to occur under “stressful” operating bookends. The selection criteria below could be adjusted to better suit the needs of future studies under higher system renewable penetration level where the operating states may drastically change from today.

- 1 Peak load: highest renewable percentage hour among the top 20 highest loading hours
- 2 Off peak load/Light load: highest renewable percentage hour among the 20 lowest loading hours
- 3 Peak renewable: lowest load hour among the top 20 highest renewable generation hours

Figure TA-23 illustrates an example of MISO-wide renewable generation versus MISO-wide load for 8760 snapshots during a year-long PLEXOS simulation. The selection of the three study scenarios in Figure TA-23 ensures that nearly all possible operating conditions are accounted for i.e. the “problem is bounded”. Generally, the system inertia decreases as instantaneous penetration of renewables increases, which was one of the key considerations for selecting

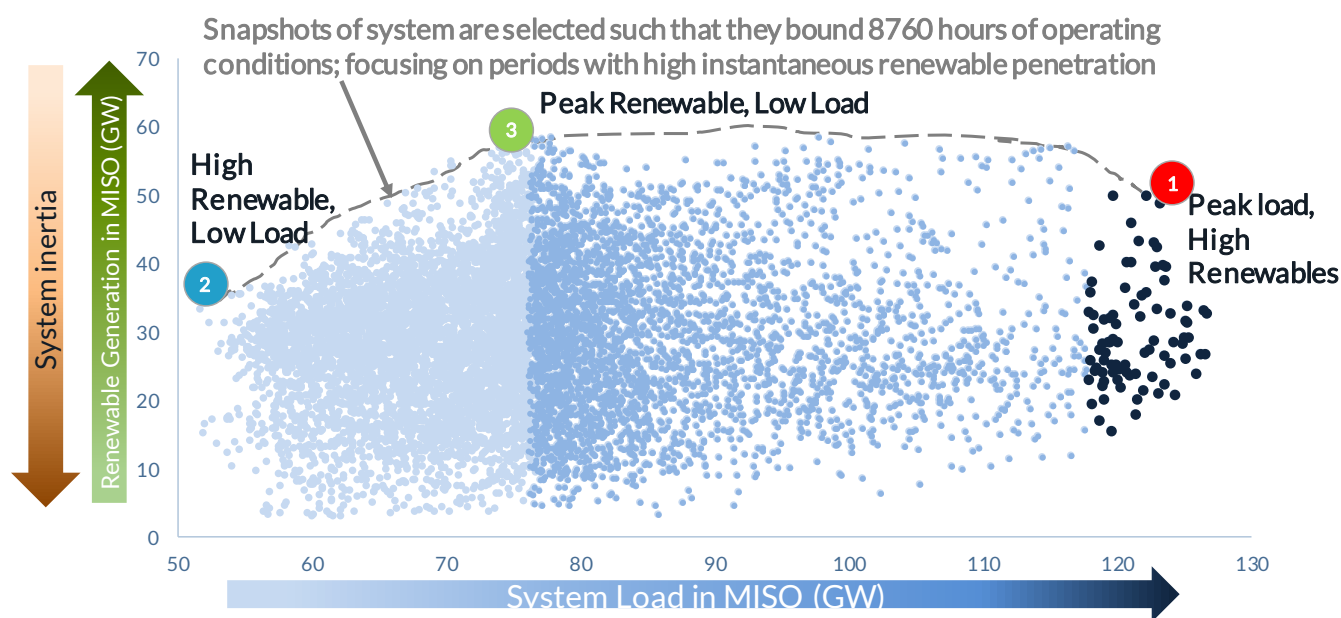


**Figure TA-23: MISO renewable generation vs. load in the 40% milestone**

The dispatch of wind and solar (distributed and grid-scale) and conventional generator from these snapshots in the PLEXOS model were applied to the PSSE model using a PLEXOS-to-PSSE unit mapping. Similarly, area loads in PSSE were scaled based on load levels in the PLEXOS model during each of these snapshots. For external areas, the dispatch of wind and solar was obtained from PLEXOS, however, conventional generation in each powerflow area were adjusted based on economic merit order to compensate for changes in load and renewable generation levels. A summary of models developed in Steady-state analysis is provided in Table TA-37.



RIIA Milestone	RIIA Snapshot Number	Total Renewable Output (GW)	Total Conventional Output (GW)	Renewable as % Output
Base	1	6.7	119.9	5%
	2	16.0	100.3	14%
	3	17.9	57.8	24%
20%	1	16.0	110.1	13%
	2	30.1	86.2	26%
	3	33.2	42.6	44%
30%	1	37.1	86.3	30%
	2	25.9	27.4	49%
	3	42.0	25.2	63%
40%	1	51.4	72.0	42%
	2	35.7	17.6	67%
	3	60.3	13.9	81%
50%	1	61.5	62.5	50%
	2	43.9	9.4	82%
	3	69.8	8.5	89%

**Table TA-37: Summary of steady state models developed for analysis**

### Powerflow solution criteria and input model quality

The power-flow models were solved with all adjustments enabled, except for Area Interchange; the maximum mismatch tolerance was 3.0 MW and Mvar. Generator terminal voltages generally need to be within an acceptable range. Voltage of other buses were monitored and ensured that they are within acceptable range ( $0.95 < \text{Voltage} < 1.05$  pu). Following process was used for monitor and update the terminal voltage of new renewable units through the application of MISO developed script.

- 1) Input powerflow models were screened to ensure voltage profile of new units is in the range  $0.95 < V < 1.05$  pu
- 2) A script developed to perform checks, correct the voltages of future renewable generator sites in following order
  - a) Update powerfactor value
  - b) Update power factor and remote bus control
  - c) Add switched shunt to POI if # a) and # b) is unsuccessful
  - d) Manually fix if #c) is unsuccessful, manually add switched shunt if needed at the Point of Interconnection or collector system bus (34.5kV)

Ensuring input models for steady-state and dynamic analyses have good voltage profile has two significant advantages: 1) it ensures that simulation is not noisy and real issues are easily identified, and b) more importantly, it uncovers the need for mitigations. For example, the script developed to perform checks on powerflow models to tune generator terminal voltages indicated 72 locations needed switched shunts in 30% milestone and 19 of the locations were converted to STATCOM during dynamic stability analysis. The exercise also indicated the 30% final steady-state models (which are input to 30% dynamic models) post screening for terminal voltage of renewable units



outside the bounds of 0.95 pu to 1.05pu, 30% snapshot 3 showed (Figure TA-24) 8.4 GVar difference in the net reactive power output after the improvement was implemented.

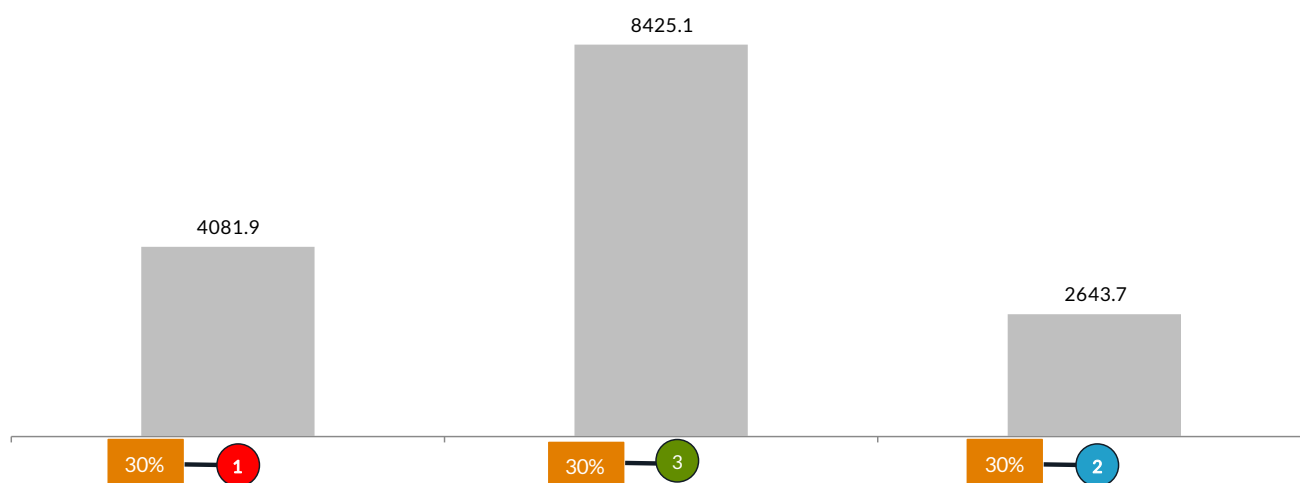


**Figure TA-24: Difference between total reactive power (Mvar) output in the input 30% steady state model and starting dynamic input powerflow model**

### Scope of Equipment to be Mitigated Under Steady-State Study

All transmission facilities 100 kV and above will be monitored for MISO and its first-tier neighbors, and a contingency analysis consisting of P1 events and 230 kV and above P2 events<sup>43</sup> were applied for MISO and its first-tier neighbors using MTEP 17 series base contingency files.

The analyses used the following Bulk-Electric System definition per NERC to determine facilities to be mitigated:

- 1) Transmission lines > 100 kV
- 2) Transformers with at least two windings > 100 kV
- 3) Generator step-up transformers for plants > 75 MVA and units > 20 MVA.

### Issue Fix Development in Steady-State

For identified system thermal overload and voltage violations, a screening process was performed to focus on the high-likelihood events that tend to cause severe reliability violations on MISO system (Table TA-38).

<sup>43</sup><https://www.nerc.com/pa/Stand/Reliability%20Standards%20Complete%20Set/RSCCompleteSet.pdf> pg. 1956



Violation Criteria	
Thermal Overload	Voltage Violation
<p>Criteria for Thermal Overload</p> <ul style="list-style-type: none"> <li>A line or branch was considered overloaded if it overloaded more than 103% of its emergency rating and more than 5 MVA above its applicable rating – normal rating or emergency rating. The 3% and 5 MVA adder was included to focus on more severe issues, and to isolate some of the issues arising from basecase models.</li> <li>Thermal violation that did not show up in base case or show up in base case but increased by at least 5MVA and 3% of circuit emergency MVA rating in current milestone.</li> <li>Erroneous contingencies were screened out or other non-actual issues (like overloads covered by op-guides).</li> <li>If a contingency did not solve in the basecase, the practice was to not attempt to solve it in the study Case (with added RIIA generation).</li> </ul>	<p>Criteria for Voltage Violation</p> <ul style="list-style-type: none"> <li>Voltage criteria per Local Planning criteria of MISO transmission operators was utilized to define voltage violations.</li> <li>Voltage violations that did not show up in base case or significantly more severe from the most severe scenario in base case (more than 5%).</li> <li>If a contingency did not solve in the basecase, the practice was to not attempt to solve it in the study Case (with added RIIA generation).</li> </ul>
Mitigation Criteria	
Thermal Overload	Voltage Violation
<ul style="list-style-type: none"> <li>Fix thermal overloads on BES (100kV above monitored) elements in MISO footprint</li> <li>Fix severe thermal overload issues in external system.</li> </ul>	<ul style="list-style-type: none"> <li>Mitigations were focused on low voltages issues, occurring in all three scenarios. If voltage violations are <math>\pm 5\%</math> across all the milestone, the equipment was upgraded. If a voltage violation was not observed in all 3 scenarios, 10% threshold was used</li> </ul>
Mitigation Technique	
<p>A step-by-step approach is being developed to reflect the band-aid system issue mitigation practice widely implemented in industry, instead of trying to find the optimal minimum cost solutions. The mitigations are shown in order of preference below.</p>	
Thermal Overload	Voltage Violation
<ul style="list-style-type: none"> <li>Re-build the line to a higher rating (per modified MIO's Competitive Transmission Administration's minimum design requirements)</li> <li>Re-build existing facility to a higher voltage class</li> <li>Build a new transmission project</li> <li>Other types of transmission or non-transmission fixes</li> </ul>	<ul style="list-style-type: none"> <li>Reactive support device (switched cap bank, switched inductor)</li> <li>Other types of transmission or non-transmission fixes</li> </ul>

**Table TA-38: Steady-state violation, mitigation criteria and mitigation technique**



## Operating Reliability – Dynamic Stability Focus Area

### Tool and Model Data Background

Operating Reliability’s dynamics analysis uses TSAT to look at the impact of high levels of renewable penetration on voltage stability, transient stability and MISO’s frequency response obligations. This focus area uses the models developed as part of the steady-state powerflow analysis (Table TA-37) and MTEP17 dynamic data as base-models, and mapping of TSAT models<sup>44</sup> (Table TA-39).

Milestone	RIIA Snapshot Number	TSAT Name
Base	1	RIIA_Base_Snapshot1_July_18_4 pm
	2	RIIA_Base_Snapshot3_March8_2am
	3	RIIA_Base_Snapshot2_June20_8pm
20%	1	RIIA_20p_Snapshot1_July_24_4pm
	2	RIIA_20p_Snapshot2_June20_3pm
	3	RIIA_20p_Snapshot3_March8_28_2pm
30%	1	RIIA_30p_Snapshot1_July26_3pm
	2	RIIA_30p_Snapshot2_April9_5am
	3	RIIA_30p_Snapshot3_Feb26_3pm
40%	1	RIIA_40p_Snapshot1_July26_3pm_VSC
	2	RIIA_40p_Snapshot2_April9_5am_VSC
	3	RIIA_40p_Snapshot3_Oct_2pm_VSC
50%	1	RIIA_50p_Snapshot1_July26_4pm_wSCs_PSS
	2	RIIA_50p_Snapshot2_April9_12pm_wSCs_PSS
	3	RIIA_50p_Snapshot3_Oct18_11am_wSCs_PSS
	2'	RIIA_50p_Snapshot2_April9_12pm_wSCs_PSS_wFreq_Batteries
	3'	RIIA_50p_Snapshot3_Oct18_11am_wSCs_PSS_wFrq_Batteries

**Table TA-39: Dynamic model names corresponding to Steady state models**

### Grid-Scale Renewable Generation Dynamic Parameters Modeling

Consistent with modeling practice of wind and grid-scale solar in the powerflow models, RIIA uses WECC 2<sup>nd</sup> generation models for dynamic representation. A standard set of dynamic models for newly sited wind and solar generation was compiled, with the assumptions that these resources do not observe momentary cessation phenomenon<sup>45</sup> (Table TA-43, Table TA-44, Table TA-45, Table TA-46, Table TA-47, and Table TA-48). Wind resources were equally represented by Type-3 and Type-4 technologies. Solar resources are considered large scale utility type

<sup>44</sup>MISO has posted RIIA TSAT models on its secured file transfer site per the name indicated in Table TA-39

<sup>45</sup>NERC report on Southern California 8/16/2016 Event involving momentary cession, available online : [https://www.nerc.com/pa/rrm/ea/1200\\_MW\\_Fault\\_Induced\\_Solar\\_Photovoltaic\\_Resource\\_/1200\\_MW\\_Fault\\_Induced\\_Solar\\_Photovoltaic\\_Resource\\_Interruption\\_Final.pdf](https://www.nerc.com/pa/rrm/ea/1200_MW_Fault_Induced_Solar_Photovoltaic_Resource_/1200_MW_Fault_Induced_Solar_Photovoltaic_Resource_Interruption_Final.pdf)



resources. Future renewable resources will be assumed to operate in modes shown in Table TA-40 and small test system was used to evaluate the dynamic response of a wind farm Figure TA-25.

Control Modes	Type 3 Wind Turbine	Type 4 Wind Turbine	Grid scale Solar plant	Grid Scale Battery
Reactive power Control Mode: Voltage Control at Point of Interconnection	Yes	Yes	Yes	Yes
Active power control (Primary frequency control)	Capability modelled, but headroom was assumed to be zero.			Capability modelled; assumed non-zero state of charge.
Certain control parameters were tuned and updated during the course of study				

**Table TA-40: Control modes for renewable plants**

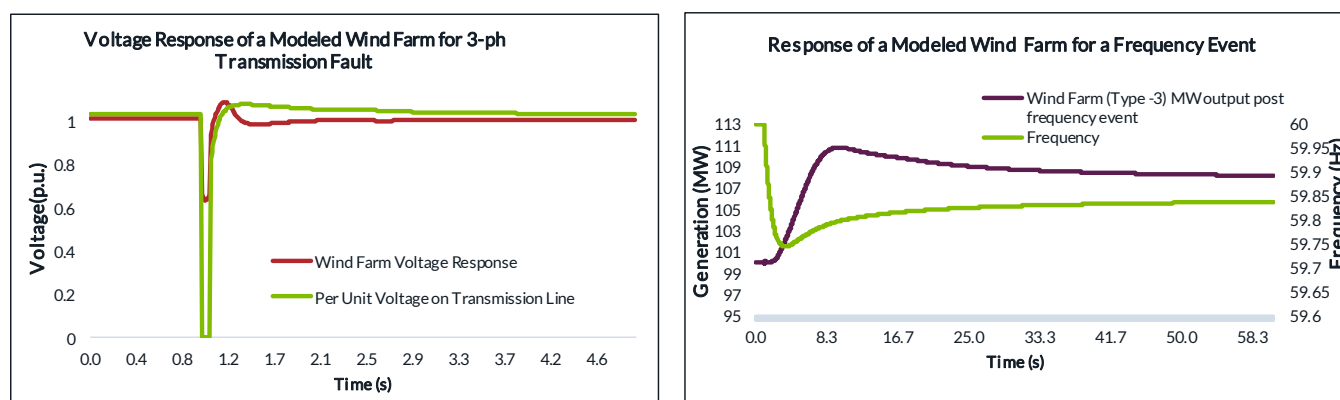


**Figure TA-25: Reasonable dynamic base model behavior was obtained for renewable resources**

### Generic Dynamic Parameters for Synchronous Condensers

PSSE library model GENROU representing Round Rotor Generator Model with Quadratic Saturation and IEEE Type ST4B exciter (PSSE model name ESST4B) were used to represent synchronous condensers. The inertia range for the synchronous condensers added for the 50%-renewable analyses is  $2.5 < H < 4$ ; the gain range assumed is  $2.0 < \text{gain} < 10.0$ , with both integral and proportional gains of each exciter for each machine held equal to each other. Gains and inertia are varied for added machines to avoid common modes of operation.

### Weak-area Study Process: Metrics and Modelling and Potential Solutions for Breached Threshold

Weak areas were identified by calculating SCR at each of the POI. A script was developed utilizing PSSE fault calculation (ASCC) module. Input to this script were steady-state models at each milestone for each snapshot, and MW injection at each milestone at selected bus (existing and new generating sites). The short circuit ratio (SCR) at